BRL-TR-3151

TECHNICAL REPORT BRL-TR-3151

BRL

A COMPARISON BETWEEN EXPERIMENT AND SIMULATION FOR CONCEPT VIC REGENERATIVE LIQUID PROPELLANT GUNS III. 155 MM

GLORIA P. WREN
TERENCE P. COFFEE
WALTER F. MORRISON

SEPTEMBER 1990

U.S. ARMY LABORATORY COMMAND

BALLISTIC RESEARCH LABORATORY
ABERDEEN PROVING GROUND, MARYLAND

NOTICES

Destroy this report when it is no longer needed. DO NOT return it to the originator.

Additional copies of this report may be obtained from the National Technical Information Service, U.S. Department of Commerce, 5285 Port Royal Road, Springfield, VA 22161.

The findings of this report are not to be construed as an official Department of the Army position, unless so designated by other authorized documents.

The use of trade names or manufacturers' names in this report does not constitute indorsement of any commercial product.

REPORT DOCUMENTATION PAGE

Form Approved
OMB No. 0704-0188

1. AGENCY USE ONLY (Leave blank)	2. REPORT DATE	3. REPORT TYPE AND DATES COVERED
	September 1990	Final June 1988 - June 1989

4. TITLE AND SUBTITLE

A Comparison Between Experiment and Simulation For Concept VIC Regenerative Liquid Propellant Guns III. 155 MM

5. FUNDING NUMBERS

1L263004D155

DA30 6709 444600

6. AUTHOR(S)

Gloria P. Wren, Terence P. Coffee, Walter F. Morrison

7. PERFORMING ORGANIZATION NAME(S) AND ADDRESS(ES)

8. PERFORMING ORGANIZATION REPORT NUMBER

9. SPONSORING/MONITORING AGENCY NAME(S) AND ADDRESS(ES)

US Army Ballistic Research Laboratory
ATTN: SLCBR-DD-T
Aberdeen Proving Ground, MD 21005-5066

10. SPONSORING/MONITORING AGENCY REPORT NUMBER

BRL-TR-3151

11. SUPPLEMENTARY NOTES

12a. DISTRIBUTION/AVAILABILITY STATEMENT

Approved for public release; distribution unlimited

12b. DISTRIBUTION CODE

13. ABSTRACT *(Maximum 200 words)*

Regenerative liquid propellant gun (RLPG) technology is sufficiently mature to allow the testing of the first 155 mm liquid propellant gun. In support of the development of this artillery weapon, test fixtures in 30 mm and 105 mm sizes have been built and fired. This report describes the analysis and modeling of the 155 mm gun fixture labeled Gun 1, an experimental fixture planned as the forerunner of the final design. Previous reports discussed the 30 mm and 105 mm gun fixtures.

In this report the 155 mm Concept VIC gun design is described together with a brief discussion of the 155 mm test program. Three charge sizes of 2 liter, 5 liter and 7 liter were tested with two igniters, a one-stage solid propellant igniter and a two-stage solid and liquid propellant igniter. The experimental data are analyzed, and the model is compared to experiment. The process of choosing input values for the gun code is discussed in detail. The result is in excellent agreement with all the experimental data.

14. SUBJECT TERMS

Liquid Monopropellant; Concept VIC; Regenerative Gun; Lumped Parameter Model; Liquid Propellants

15. NUMBER OF PAGES

123

16. PRICE CODE

17. SECURITY CLASSIFICATION OF REPORT	18. SECURITY CLASSIFICATION OF THIS PAGE	19. SECURITY CLASSIFICATION OF ABSTRACT	20. LIMITATION OF ABSTRACT
UNCLASSIFIED	UNCLASSIFIED	UNCLASSIFIED	SAR

TABLE OF CONTENTS

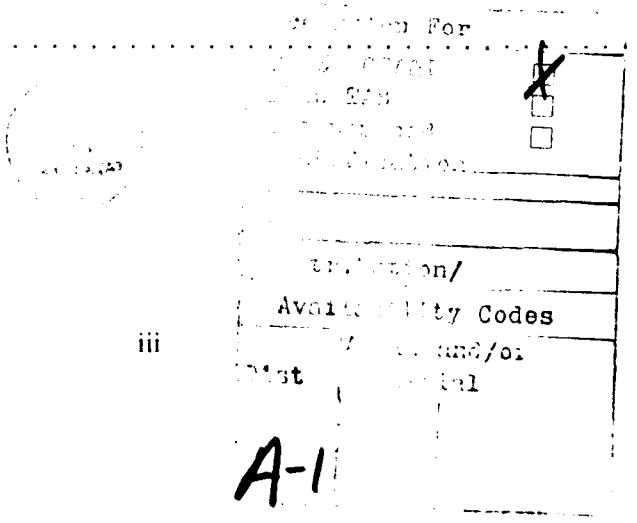

LIST OF FIGURES

LIST OF TABLES

ACKNOWLEDGMENTS

The authors would like to express appreciation to the General Electric Company and Mr. James McCaleb for data used in this report. Data transfer to the BRL was accomplished due to the efforts of Ms. Lou Ann Walter of the General Electric Company and Mr. James Despirito of the Ballistic Research Laboratory. Special thanks are expressed to Ms. Lou Ann Walter and Dr. Inder Magoon of the General Electric Company for their cooperation and help in detailed descriptions of hardware and their assistance with interpretation of experimental results.

1. INTRODUCTION

Regenerative liquid propellant gun (RLPG) technology is sufficiently mature to allow the testing of the first 155 mm liquid propellant gun. In support of the development of this 155 mm technology demonstrator, test fixtures in 30 mm and 105 mm sizes have been built and fired. The data from all three fixtures have been extensively analyzed to better understand the regenerative liquid propellant gun (RLPG) process. In this report, experimental data for the 155 mm Concept VIC configuration are reviewed, and computer simulations of the 155 mm tests are presented. In previous reports[1,2] the 30 mm and 105 mm gun fixtures were discussed.

The structure for the modeling effort discussed in this report was dictated by the criteria for the transition of the liquid propellant (LP) program from the Ballistic Research Laboratory (BRL) to the Army Research, Development and Engineering Center (ARDEC). The transition criteria specify that it should be possible to demonstrate agreement between model and test data for 30 mm, 105 mm, and 155 mm by matching mean, filtered pressure-time data to within 5% for damper, reservoir, chamber, and bore pressures and by matching muzzle velocity to within 2%.[3] The modeling effort was broadened by conducting blind simulations of experimental test firings using a calibration of model parameters based on data from similar test firings.

This report documents the modeling of the 155 mm Concept VIC test firings. First, a description of the Concept VIC fixture is given. The interior ballistic model utilized has been described in previous publications.[4,5] The modifications pertinent to the Concept VIC design were described in detail in the first paper of this series which documented simulations of the 30 mm Concept VIC gun.[1] The choice of input parameters for the 155 mm is described. These parameters are primarily determined from the physical characteristics of the gun. However, some parameters cannot be determined directly and are chosen based on empirical data. To meet the transition criteria, test firings of 2 liter and 5 liter propellant charges are considered. The 7 liter test data were available after the transition of the program. Thus, as a extension of the modeling effort, the baseline parameters from the 5 liter series are used to predict the performance of a 7 liter charge. The igniter used in the 7 liter tests differs from that in the 5 liter test, and differences due to the change in igniter are discussed. In general, simulations of the 7 liter tests are reasonable.

The key feature, and major source of uncertainty, in the regenerative interior ballistic process is the injection, breakup, and combustion of the liquid propellant. A simple droplet breakup and combustion model has been utilized. Droplet size distribution, and, thus, propellant combustion,

show marked sensitivity to other gun parameters. This sensitivity and the related variation of droplet size distributions are discussed.

2. THE CONCEPT VIC LIQUID PROPELLANT GUN

A diagram of a generic VIC liquid propellant gun is shown in Figure 1. The monopropellant in the liquid reservoir is prepressurized and is located between the control rod (inner piston) and the injection piston (outer piston). A primer is ignited and injects hot gas into the combustion chamber. As the chamber is pressurized, the control rod is pushed to the left, opening the injection orifice. The outer piston follows the control rod, injecting the propellant from the reservoir into the combustion chamber.

The motion of the control rod depends on the damper (also referred to as the buffer) assembly. After the initial seal between the injection and control pistons is broken, the liquid pressure has very little effect on the control rod. As the control rod moves to the left, damper fluid is forced between the rod and the extension on the transducer block. The control rod is composed of turned sections which define the damper vent area. Near the end of stroke, the damper vent area becomes small, limiting the flow of fluid from the damper and bringing the control rod to a gradual halt.

The injection piston will track the control rod in response to the differential pressure between the liquid reservoir and the combustion chamber. As the injection piston moves closer to the control rod, the vent area will decrease, the liquid pressure will increase, and the injection piston will slow down. As the piston moves further from the rod, the vent area will increase, the liquid pressure will decrease, and the piston will accelerate.

The fixture utilized in the firings discussed in this report was developed under contract[6] by the General Electric Company, Tactical Systems Department (GE). Figures 1-3 show representative drawings of the piston and damper positions for the GE 155 mm fixture at the initial, midstroke, and end-of-stroke positions of the pistons.

3. BASIC ASSUMPTIONS

The basic physical assumptions of the model and the changes in the governing equations necessary to model a VIC gun fixture were discussed in the first report in this series which focuses on the 30 mm fixture.[1] The second report of the series addresses the 105 mm fixture.[2]

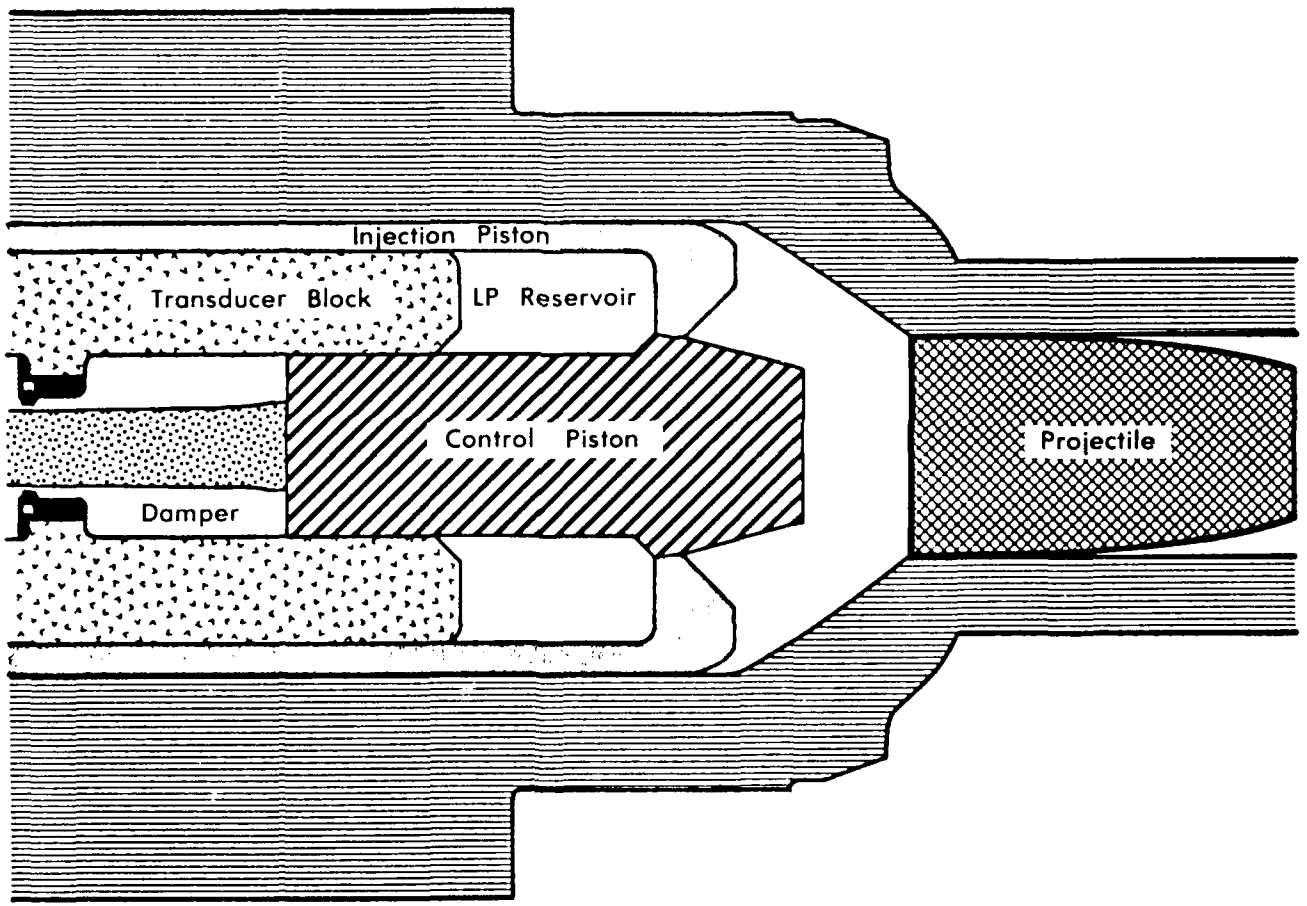

Figure 1. A Concept VIC Regenerative Liquid Propellant Gun, Initial Position.

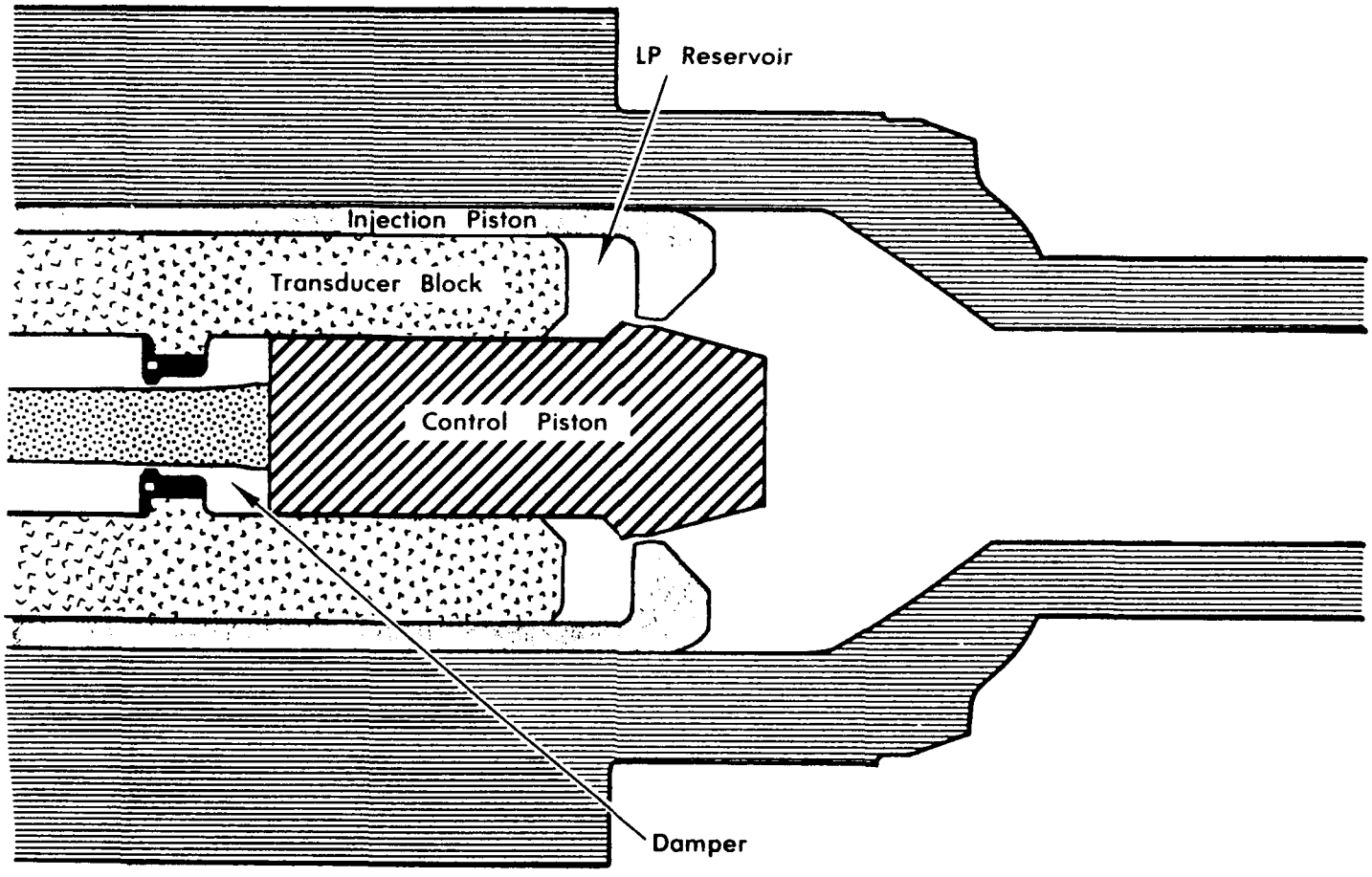

Figure 2. A Concept VIC Regenerative Liquid Propellant Gun, Middle of Stroke.

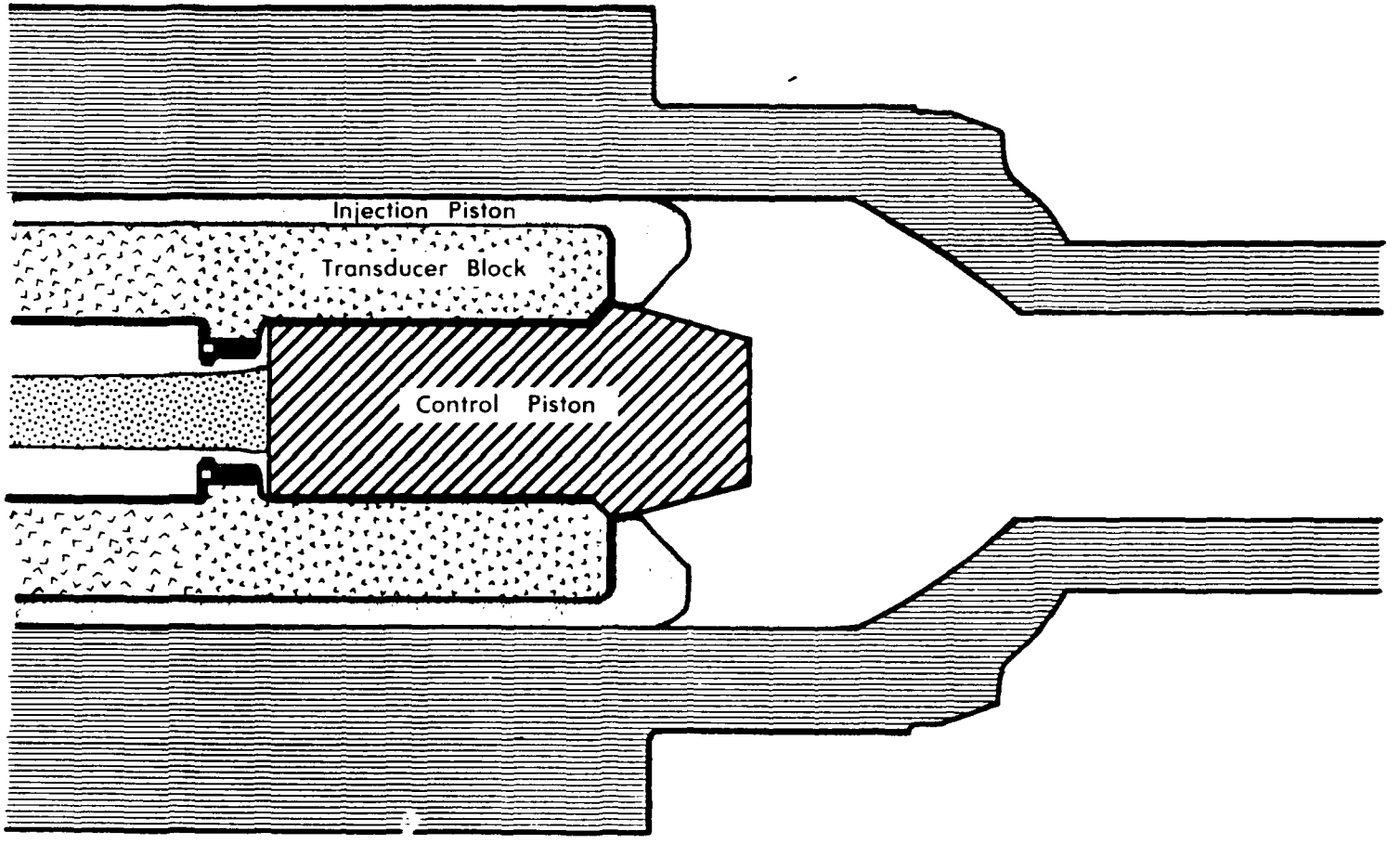

Figure 3. A Concept VIC Regenerative Liquid Propellant Gun, End of Stroke.

4. 155 MM CONCEPT VIC DATA

The 155 mm Concept VIC RLPG was tested using LGP1846 to evaluate Gun 1 ballistic performance with different propellant charge lengths. Table 1 shows the 155 mm shot numbers together with a brief description of the test series. Muzzle velocity and standard deviation in muzzle velocity are given as reported by GE.[7] Shot 24 is excluded from the 2 liter repeatability series since the liquid propellant metering system indicated that the initial charge contained 66 cubic centimeters less liquid propellant than other firings in the series. However, the liquid reservoir was full, the propellant charge being limited by piston stroke. It was hypothesized that the additional volume in the reservoir (66 cc) was occupied by ullage or water from the purge cycle. (The fill system is routinely flushed with water between firings as a safety measure during testing.)

Besides the differences in propellant charge sizes in Table 1, the damper region was modified throughout the firings The damper fluid is Brayco 783 in all cases, and the damper does not contain the 1/32 inch hole associated with the 30 mm gun.[1] Lubricants, 30-weight and 20-weight oils, were pumped during the propellant fill process between the outer piston and chamber wall, outer piston and transducer block, and inner piston and transducer block to lubricate the pistons, provide hydraulic support for the outer piston shaft, and provide a barrier to prevent propellant flow between piston shafts and the transducer block. Two igniters were utilized in the test program: (1) an external solid propellant igniter with an initiator similar to that used in the 30 mm and 105 mm firings, and (2) a hybrid igniter (also called a two-stage igniter) consisting of a small solid propellant igniter which initiates combustion of a liquid propellant "puddle" placed directly in the combustion chamber. The "puddle" combusts and raises the chamber pressure before injection of liquid propellant from the liquid reservoir and is referred to as a pre-positioned charge. Projectile travel is approximately 591.8 cm with a tube length of 609.04 cm.

The experimental firings which are simulated in this investigation are shot 17 (2 liter characterization test), shots 27 and 28 (from the 2 liter repeatability series), shots 48 and 51 (from the 5 liter repeatability series), shot 58 (5 liter with hybrid igniter), and shot 65 (7 liter with hybrid igniter). shot 65 is from a 7 liter characterization series which was fired in preparation for a 7 liter repeatability series to be performed at a later date. All data displayed in this report have been filtered. Units on graphs are centimeters (cm), grams (g), milliseconds (ms) and megapascals (MPa) unless noted otherwise.

Table 1. 155 mm Concept VIC Shot Numbers

Shot numbers	Description
1-19	2-liter characterization, solid propellant igniter
20-30	2-liter repeatability, solid propellant igniter Mean velocity at 200 inches of travel=393.2 m/s with SD=0.44% (shot 24 excluded)
31-46	5-liter characterization, solid propellant igniter
47-56	5-liter repeatability, solid propellant igniter Mean velocity at 200 inches of travel=586.2 m/s with SD=0.25%
57-61	5-liter charge, hybrid igniter characterization
62-65	7-liter characterization, hybrid igniter

Table 2 displays the primary test parameters as reported by GE.[7] The projectile is initially offset approximately 10.16 cm from tube origin with approximately an additional 7.08 cm to the obturating band. The igniter vents perpendicular to the tube axis, just behind the initial position of the projectile. The initial chamber pressure rise due to the igniter alone is determined by water shots, (i.e., test firings in which the reservoir is filled with water). The solid propellant igniter charge is Hercules HC25SS with an M1B1A2 primer; the liquid propellant igniter charge is LGP1846. The initial chamber volume includes the tube volume which results from projectile offset and is determined by GE from a computer aided design (CAD) drawing of the gun. The contours of the inner and outer pistons were altered after the 2 liter characterization series, resulting in a change in initial chamber volume.

Pressure gages used in this analysis include: two gages in the same axial plane near the forward end (tube end) of the combustion chamber, referred to as D-plane gages; two gages in the combustion chamber, located in the same axial plane just behind the initial position of the outer piston, referred to as E-plane gages; two gages in the liquid reservoir, located in the transducer block; two gages in the damper referred to as O-plane gages; and barrel gages B1 at 26.64 cm of

Table 2. 155 mm Concept VIC Test Parameters

Charge	2 liter	2 liter repeat	5 liter repeat	5 liter (hybrid igniter)	7 liter (hybrid igniter)
Shots	17	20-30	47-56	57-61	62-65
Propellant Volume (cm^3)	2134	2233.6	5210	5210	7217
Initial Chamber & Free Tube Volume (cm^3)	10057	10323	10323	10323	10323
Projectile Weight (kg)	43.2	43.2	43.2	43.2	43.2
Total Igniter Charge:					
Solid (g)	455	450	450	280	280
Liquid (g)	0	0	0	133	115.2
Piston Stroke (cm)	4.315	4.453	10.376	10.376	14.387
Shot Start Pressure (MPa)	4.0	4.0	10.0	10.0	20.0
Bore Resistance Pressure (MPa)	0.7	0.7	3.0	3.0	3.0

projectile travel, B3 at 74.497 cm of projectile travel, B5 at 157.013 cm of projectile travel, and B7 at 260.279 cm of projectile travel. The D-plane gages used in this analysis are D33 and D138, where the number corresponds to the angular location of the gages in the D-plane. The E-plane gages used are E222 and E342. Not all barrel gages were activated during each firing. The control and injection piston motions are measured by an external Optrons, and projectile motion is measured by a 15 GHz radar.

The projectile shot-start pressure and resistance profile has been a continual source of concern in the modeling effort. A standard M107 projectile was used in all test firings. A standard 155 mm rifled tube was to have been used. However, during manufacturing, the angle of the forcing cone was incorrectly machined to 1/2 of the specified angle. The effects of this change in the forcing cone on the resistive forces for the M107 were originally felt to be minimal. Thus, as a first approximation, experimental measurement by ARDEC of resistive forces for a M107 projectile in a standard 155 mm tube were utilized.[8,9] These values were found to be poor fits to the experimental projectile motion in LP gun firings as determined from radar data. Therefore, an alternate model of the resistive forces during early projectile motion was introduced. A constant pressure associated with the beginning of projectile motion, loosely referred to in this report as the

projectile shot start pressure, was determined for each set of experimental data analyzed. This resistive force is applied over an initial projectile travel equal to 1.5 times the length of the engraving band (which is 2.54 cm). This is a "rule of thumb" used in solid propellant modeling.[10] The resulting theoretical projectile motion was then compared to the early experimental projectile travel, and in general, the rule of thumb appears to be reasonable.

Beyond the shot start region, the resistance pressure is initially assumed to have a constant value equal to 1% of the maximum chamber pressure, another "rule of thumb" from solid propellant gun modeling for a rifled gun barrel.[10]

The projectile travel, derived from radar measurements for each test series, indicates that the projectile shot start pressure varies in the firings. Radar data are used to establish the shot start pressures presented in Table 2, which give good matches between the model simulations and the radar measurements for early projectile travel. An attempt was made to choose a single value for the down bore resistive pressure for all test series. However, the radar data from the 5 liter firings indicated a substantially different projectile resistance profile than found in the 2 liter firings. In discussions, GE[11] indicated that the gun tube was lubricated after each shot up to shot 46, and after shot 46 the tube was not lubricated. Since shots 48 and 51 were used in the simulation of 5 liter tests, it is assumed that the change in resistance pressure, compared to the 2 liter series, may be related to the change in test procedure as well as (possibly) to differences in the initial pressure rise rate in the combustion chamber. However, interestingly, radar from the 7 liter firing shot 65 indicates that the resistance profile had changed again, although the initial pressure rise, due to the igniter and initial venting of the propellant, is similar to shot 58 in the 5 liter series.

Although more complicated resistive profiles could be devised for a particular shot, a general formulation which would be applicable over all cases of interest is desired. Thus, the shot start pressure is applied over the first 3.81 cm of travel, and a constant resistive pressure is applied to the remainder of the projectile travel. The early projectile motion varies widely as a function of both time and pressure for experimental data obtained in tests with "identical" projectiles. The tolerance in the diameter of the obturating band, 6.214 inches to 6.220 inches, in a tube with fewer than 100 shots is not expected to cause the observed variation in projectile resistive forces. The cause of the observed variation is unknown. The effect of the resistance profile on interior ballistic simulations is examined below.

5. GE 155 MM GUN FIXTURE - 2 LITER SHOT 17

Test shot 17 is a 2 liter, 155 mm, Concept VIC firing from the initial characterization series The experimental muzzle velocity determined from radar measurements is 424 m/s.

The chamber pressure for shot 17 at two gage locations in the D-plane is shown in Figure 4. The chamber pressures measured by the two gages are separated with a difference at peak pressure of about 7%. Data from one liquid pressure gage and one damper gage are available for this shot. Inner and outer piston motion were measured using an Optron. Recoil has been subtracted from the piston travel curves shown using the free recoil model described in the earlier 105 mm report.[2] Unlike the earlier 105 mm case, the recoil has been scaled to give the measured piston travel in the 155 mm case. The shape of the combustion chamber pressure profile in Figure 4 is unusual compared to previous 30 mm and 105 mm (as well as subsequent 155 mm) Concept VIC data, since it is a nearly linear, increasing function up to peak pressure.

Most of the parameters for the gun code are based on physical measurements of the gun fixture or measured propellant or damper fluid properties (see Appendix A). However, some of the parameters cannot be predicted, and the values are selected based on the analysis of experimental data. One such parameter is the propellant discharge coefficient, which is derived from the experimental chamber and liquid pressures and the experimental piston travels using the assumption of steady-state Bernoulli flow. An inverse code[12, 13] is utilized to derive values for the liquid reservoir and damper discharge coefficients, shown in Figures 5 and 6, respectively. The value of the reservoir discharge coefficient, Figure 5, is greater than 1.0 for a large portion of the firing cycle. This result is not physically meaningful and is probably due to small errors in the measured piston travels, which lead to large errors in the computed vent area and/or the pressures. The damper discharge coefficient, shown in Figure 6, is close to 1.0, a reasonable value considering the relatively large exit area. Thus, model values of the two discharge coefficients are fixed at a constant value of 0.95.

The interior ballistic model is first applied in an optional mode using experimental chamber pressure gage D138 as a boundary condition. The results are shown in Figures 7-10. The comparison with the experimental liquid pressure, Figure 7, is good until late in the firing cycle. The comparisons with piston travels, in Figure 8, and damper pressure, in Figure 9, are quite good with some minor differences. The projectile shot start pressure was initially chosen as 4.0 MPa,

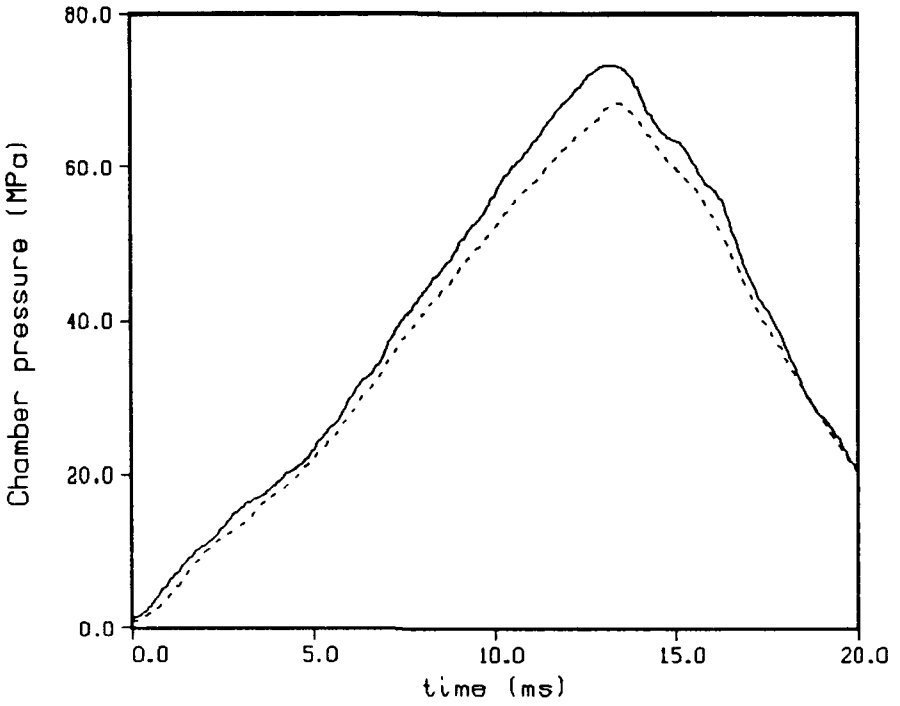

Figure 4. Experimental Chamber Pressure. Round 17 - Gage D138 (line) and Gage D33 (dot).

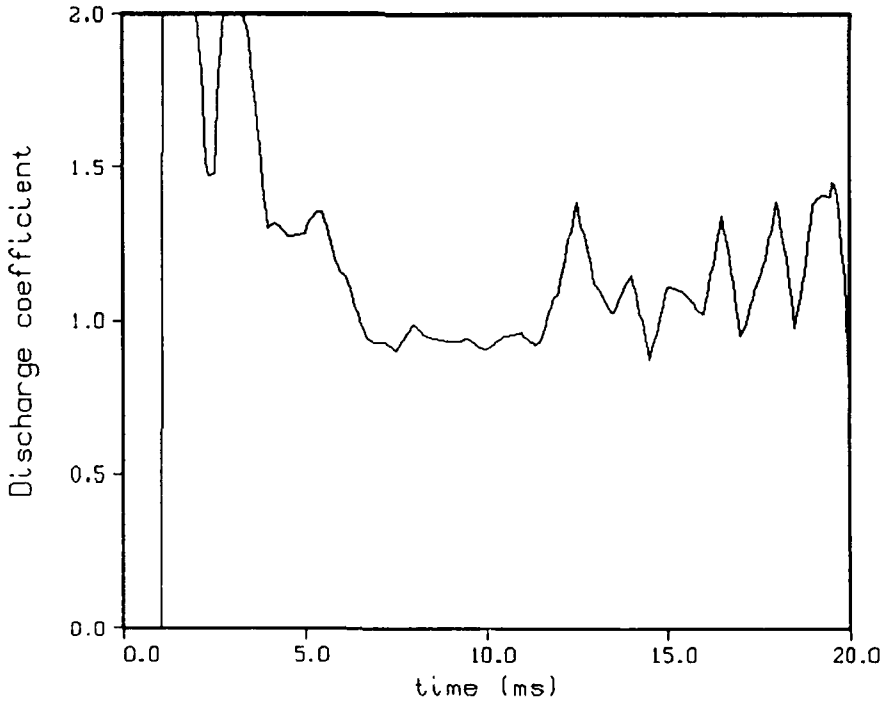

Figure 5. Results From Inverse Code - Reservoir. Discharge Coefficient (line) - Round 17. Based on the Gage D138.

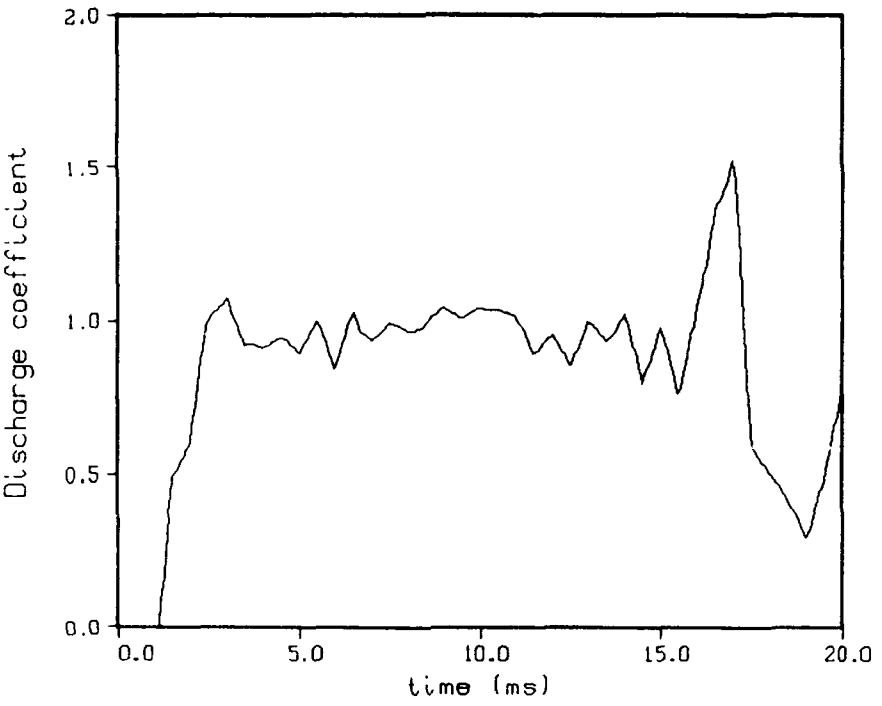

Figure 6. Results From Inverse Code - Damper. Discharge Coefficient (line) - Round 17. Based on the Damper Gage.

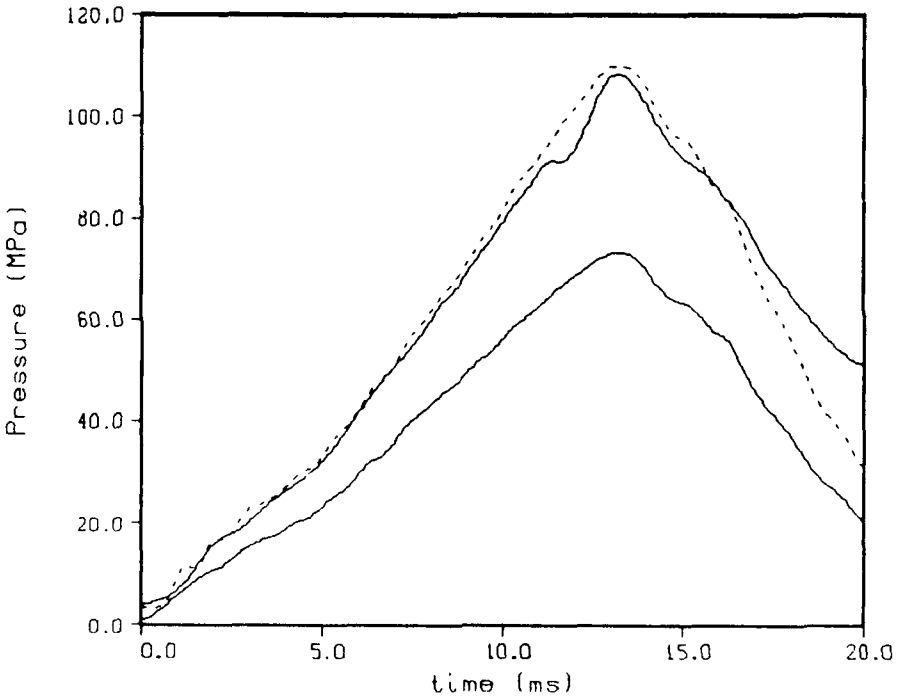

Figure 7. Liquid Pressure and Chamber Pressure - Round 17 (line). Liquid Pressure From Model With Chamber Pressure D138 (dot).

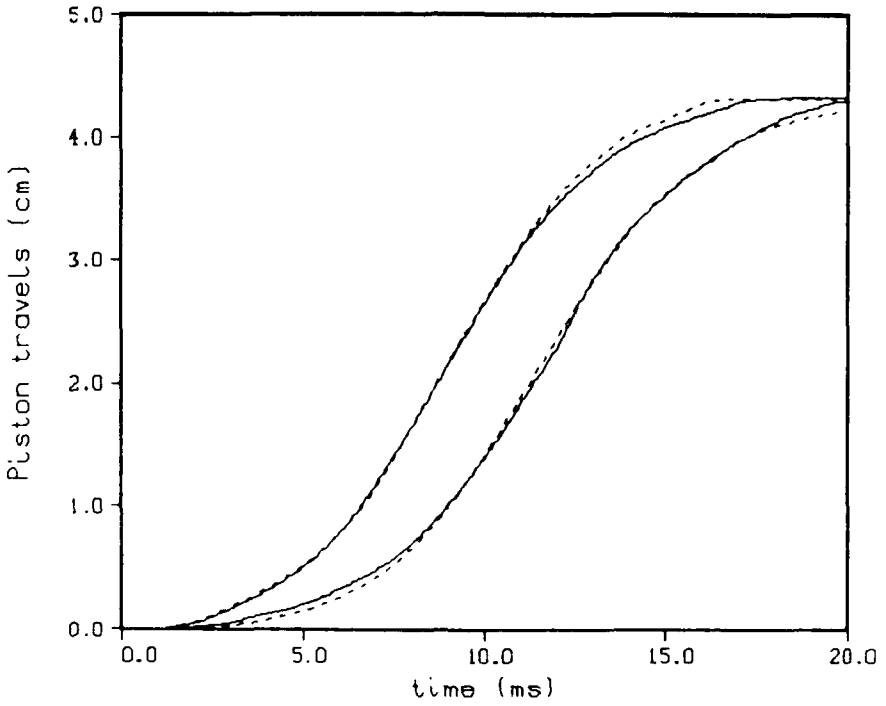

Figure 8. Piston Travel - Round 17 (line). Piston Travel From Model With Chamber Pressure D138 (dot).

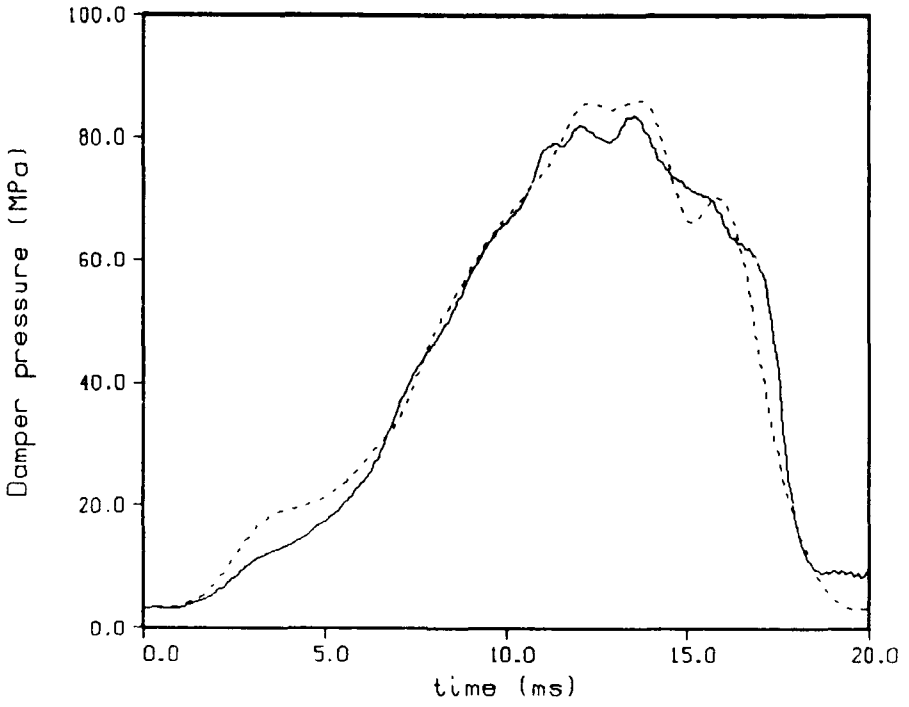

Figure 9. Damper Pressure - Round 17 (line). Damper Pressure From Model With Chamber Pressure D138 (dot).

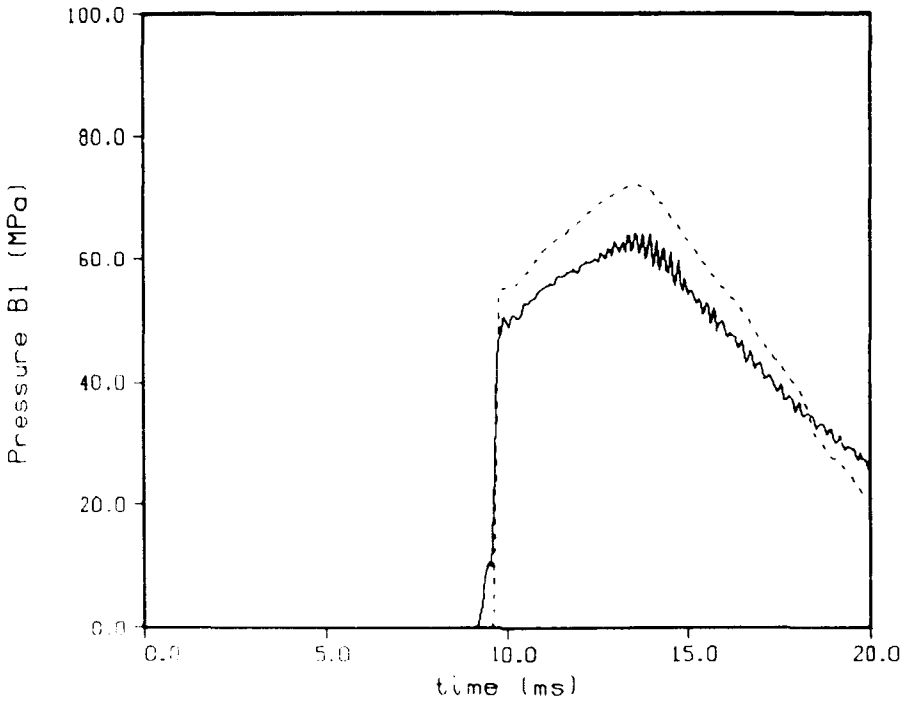

Figure 10. Barrel Pressure, Gage B1 - Round 17 (line). Barrel Pressure From Model With Chamber Pressure D138 (dot).

with a barrel resistive pressure of 0.7 MPa based on an analysis of shot 27 radar data. The resulting comparison with the tube gage B1, located at 26.642 centimeters of projectile travel, is shown in Figure 10. The projectile passes the gage position at the correct time in the simulation. However, there is some difference in the magnitudes of the experimental and predicted pressures. The pressure in the tube at gage B1 rises after the gage is uncovered, since the chamber pressure is still rising at this point in time, and the projectile is moving relatively slowly.

To determine the effect of accumulation on the ballistic process, the code is run assuming instantaneous combustion of the propellant as it enters the combustion chamber. The comparison of experimental and simulated chamber pressures is shown in Figure 11. Piston travels are presented in Figure 12. As can be seen in Figure 11, combustion is fairly efficient in this shot, and the chamber pressure is not strongly affected by accumulation. These pressure traces lack the slowly increasing pressure in the startup regime, indicative of accumulation, which is a characteristic of other Concept VIC data analyzed. The igniter vents approximately 10.16 cm from tube origin and is not expected to influence the enhanced early combustion. However, the chamber

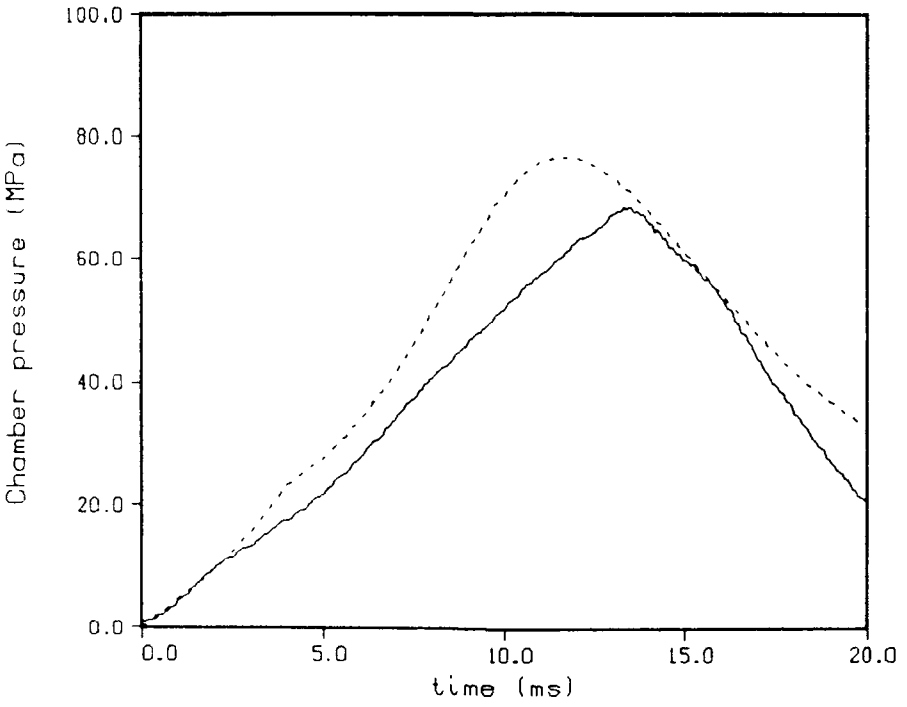

Figure 11. Chamber Pressure - Round 17 - Gage D138 (line), Model With Instantaneous Burning (dot).

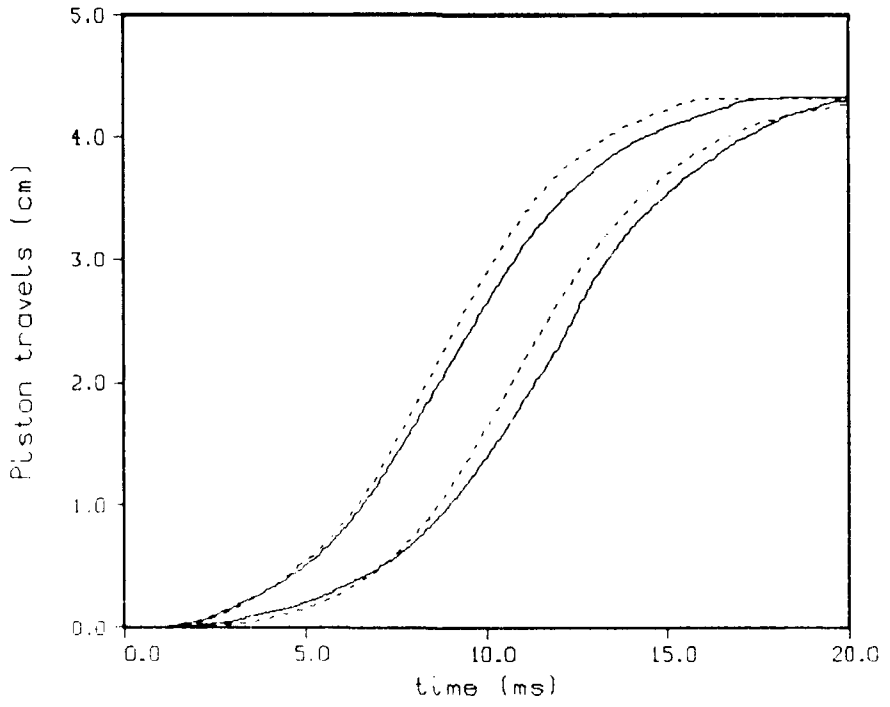

Figure 12. Piston Travel - Round 17 (line), Model With Instantaneous Burning (dot).

pressures are substantially lower than in the 30 mm and 105 mm data. The lack of significant accumulation may simply be due to the low pressures and correspondingly slower pistons and injection rate, which allows the injected propellant increased time to heat and combust. The shape of the pressure curve may also be related to the burn rate of the propellant. Some experimental evidence[14] indicates that the burn rate of the propellant is substantially lower below 100 MPa than it is above 100 MPa. Since accumulation is not significant, the assumption of instantaneous combustion produces approximately the correct muzzle velocity, a predicted value of 429 m/s compared to the experimental velocity of 424 m/s.

However, Figure 11 suggests that there is a small amount accumulation as evidenced by the slower rise to maximum pressure in the experiment. The simulation can be improved with a finite rate combustion model. In the combustion model it is assumed that the propellant jet instantaneously breaks into droplets as it enters the combustion chamber. The number and size of the droplets define a surface area for propellant combustion, and all droplets burn according to a pressure-dependent, linear surface regression law, which is derived from experimental strand burner data.[14,15] For simplicity, it is assumed that the droplets all have the same diameter at any given time and that the total liquid surface area is conserved (i.e., the Sauter mean diameter is utilized). The droplet diameter is input as a function of chamber pressure. The droplet profile in Table 3 is derived by adjusting the droplet profile until the model results match the experimental chamber pressure. Table 3 indicates that the average droplet diameter is a constant 100 μm from 0.0 to 20.0 MPa, decreases linearly from 100 μm to 75 μm from 20.0 to 40.0 MPa, and remains at a constant 75 μm during the remainder of the process.

Table 3. Round 17 Mean Droplet Diameter Profile

Chamber pressure, MPa	Droplet diameter, μm
0.0	100
20.0	100
40.0	75

The liquid accumulation and the droplet mean diameter can also be derived from the inverse code based upon measured piston positions to determine the vent area and amount of propellant injected into the chamber. However, approximations must be made, and the results are less

accurate than the computed discharge coefficients. Computed liquid accumulations and the mean droplet profiles upon which the simulations are based are presented in Figures 13 and 14, respectively. There is some discrepancy at early times when a small amount of liquid propellant has been injected. The droplet profile in Table 3 is chosen to be as simple as possible to approximate the effect of accumulation and, arbitrarily, to be a decreasing function of pressure. The mean diameter computed from experiment suggests a droplet profile which begins as a fine spray, increases to a maximum droplet size and then decreases. Although physically more appealing as the vent area increases during the startup, little liquid is involved in the startup, and the simple droplet profile is adequate to simulate accumulation.

A comparison of the model using the droplet profile in Table 3 with experimental data is shown in Figures 15-22. The model chamber pressure in Figure 15 is not as linear as the experiment, but remains within the experimental gage measurements. The model liquid pressure in Figure 16 compares well with the experiment, but again is not as linear. The two piston travels in Figure 17 show overall good agreement, with a discrepancy between the model and experiment in the early injection (outer) piston motion. It is noted that, since 1.0 millimeter of injection piston travel results in injection of approximately 75 grams of liquid propellant, a small error can significantly alter the computed liquid accumulation. The damper pressures in Figure 18 are in reasonable agreement. In order to match the experimental muzzle velocity of 424 m/s, the resistive pressure is lowered to 0.7 MPa, with the resulting comparisons with the barrel gages shown in Figures 19-22. The predicted timing of the gage responses to the passage of the projectile appears accurate. There is an apparent loss of gage signal in Figures 20-22. There is a discrepancy in the magnitude of the pressure (recorded by the gage) and the model prediction in Figure 19. A similar discrepancy is noted and discussed in the next section on the 2 liter repeatability series. Interestingly, the projectile shows almost zero shot start pressure. Discussions with GE[11] revealed that the gun tube was lubricated between each firing in the characterization series, which may contribute to the low shot start pressure.

6. GE 155 MM GUN FIXTURE - 2 LITER SHOTS 27, 28

The ten shots in the repeatability series for the 2 liter charge consist of shots 20-23 and 25-30. Two shots, 27 and 28, are compared to assess repeatability. In addition, the model is used to analyze the data. The mean velocity for the 2 liter repeatability series at 200 inches of travel is 393.2 m/s, with a standard deviation of 0.44%, excluding shot 24, as discussed in Section 4.[7] The initial liquid reservoir volume contains approximately 50 cubic centimeters of oil injected during the

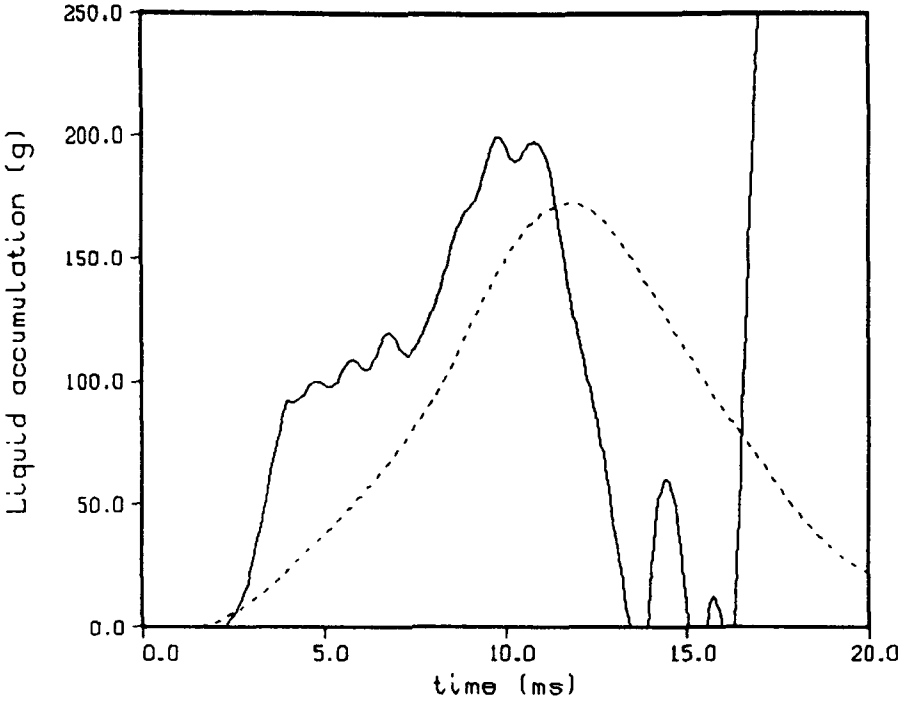

Figure 13. Liquid Accumulation - Round 17. Inverse Code (line). Model With Droplet Burning (dot).

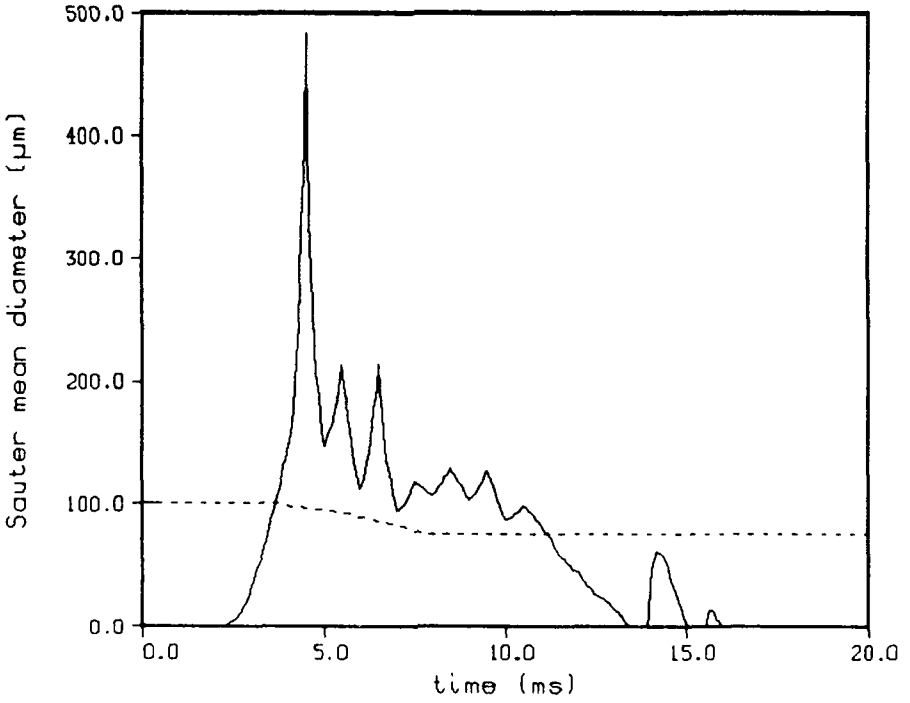

Figure 14. Sauter Mean Diameter - Round 17. Inverse Code (line). Model With Droplet Burning (dot).

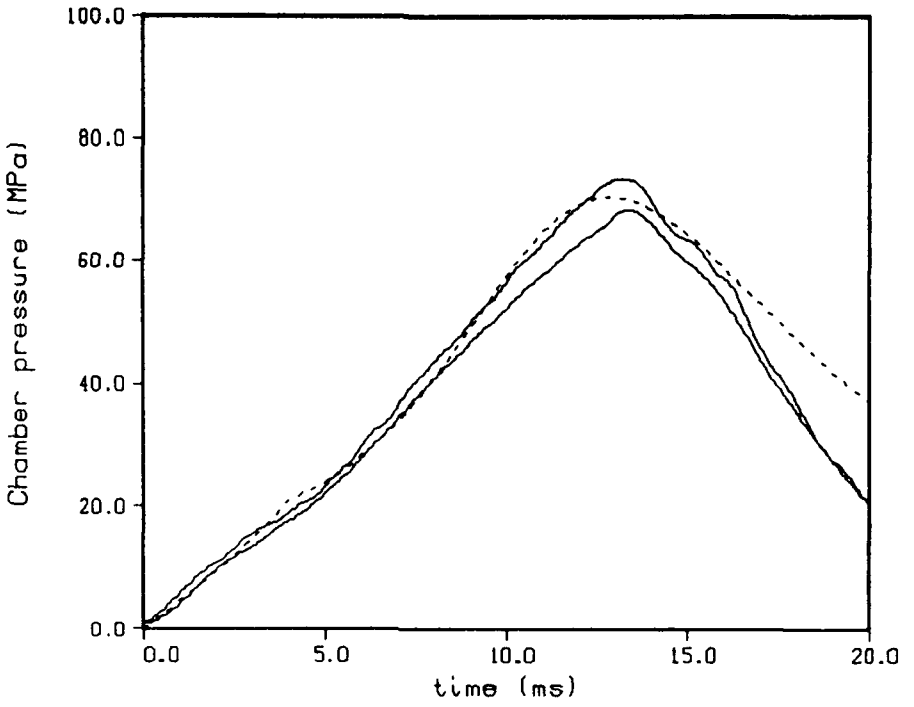

Figure 15. Chamber Pressure - Round 17 (line). Model With Droplet Burning (dot).

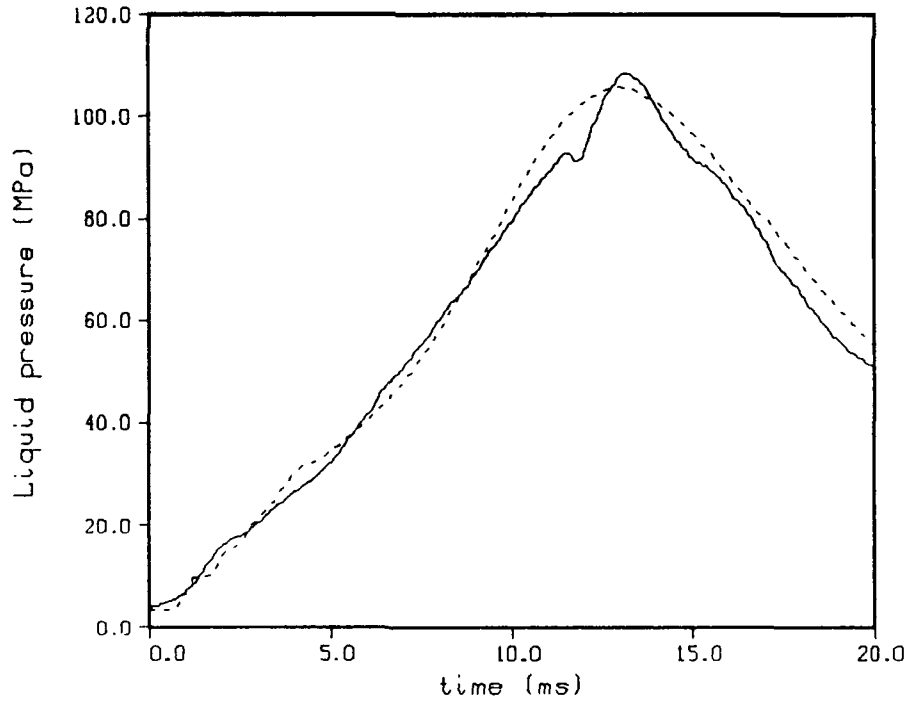

Figure 16. Liquid Pressure - Round 17 (line). Model With Droplet Burning (dot).

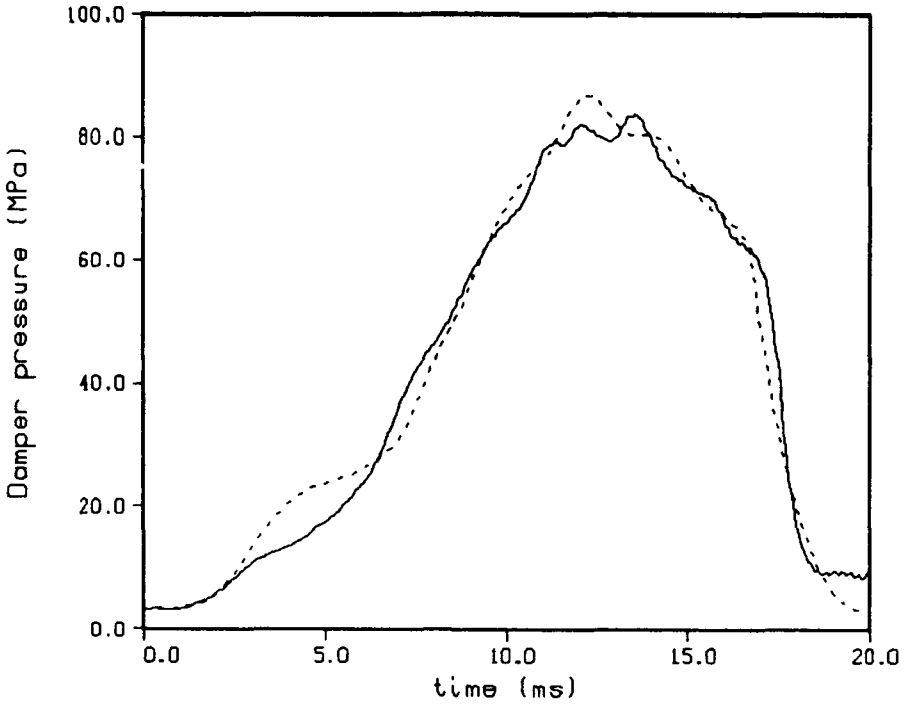

Figure 17. Damper Pressure - Round 17 (line). Model With Droplet Burning (dot).

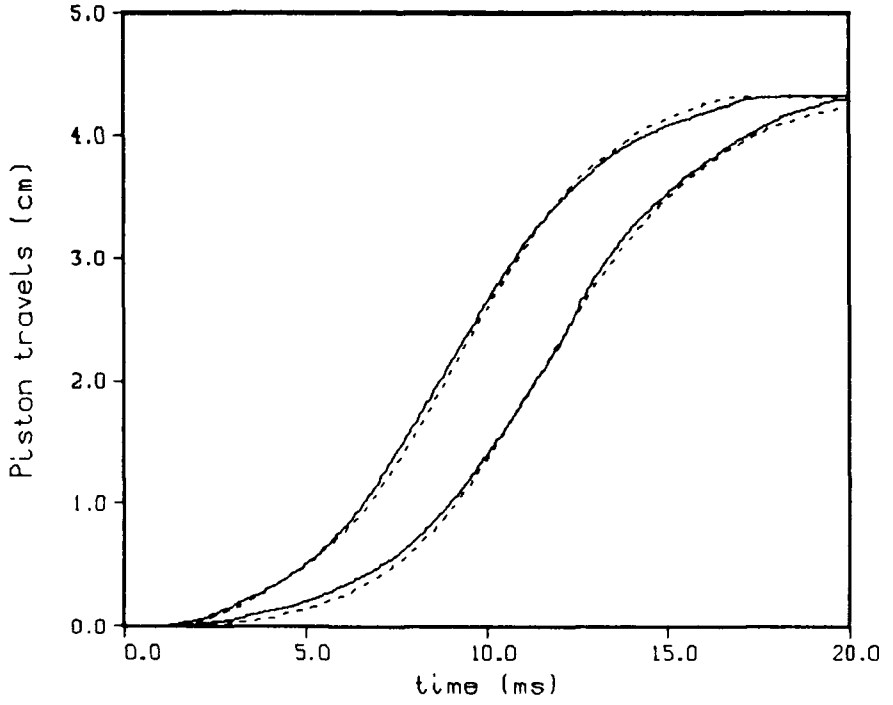

Figure 18. Piston Travel - Round 17 (line). Model With Droplet Burning (dot).

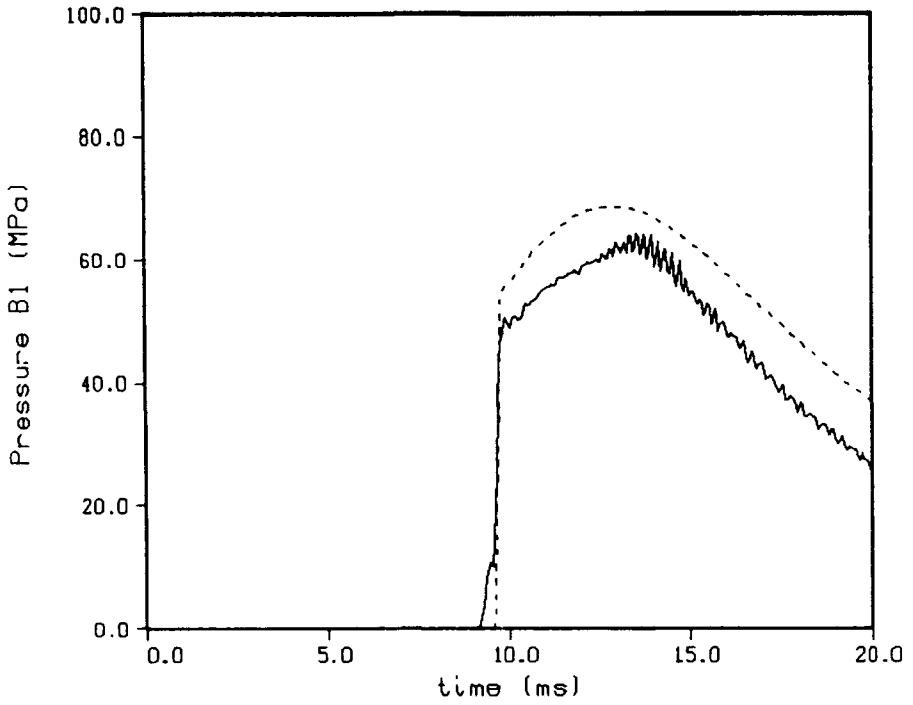

Figure 19. Barrel Pressure, Gage B1 - Round 17 (line). Model With Droplet Burning (dot).

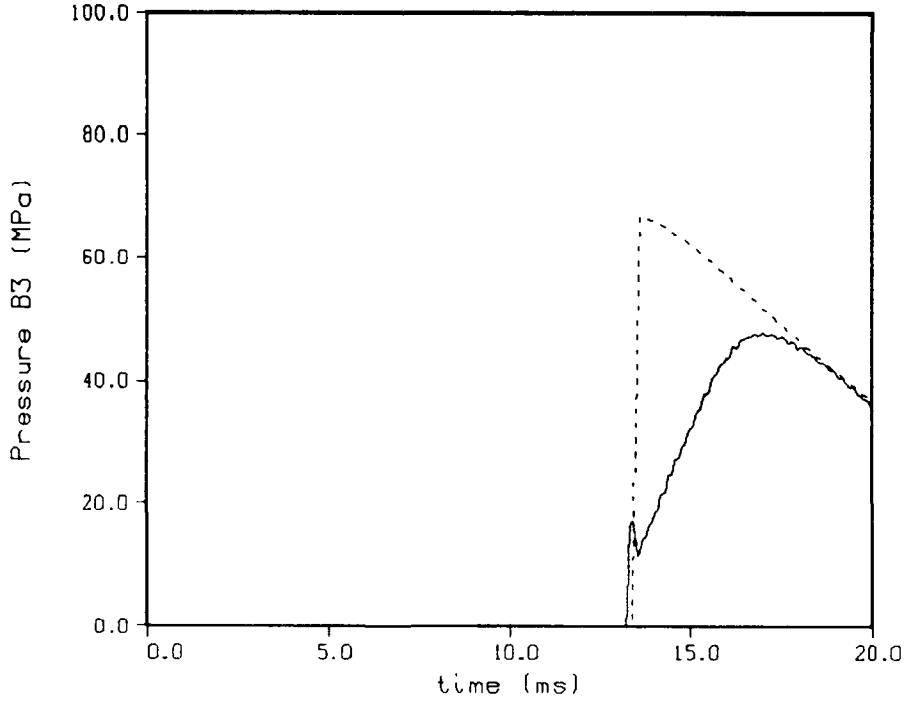

Figure 20. Barrel Pressure, Gage B3 - Round 17 (line). Model With Droplet Burning (dot).

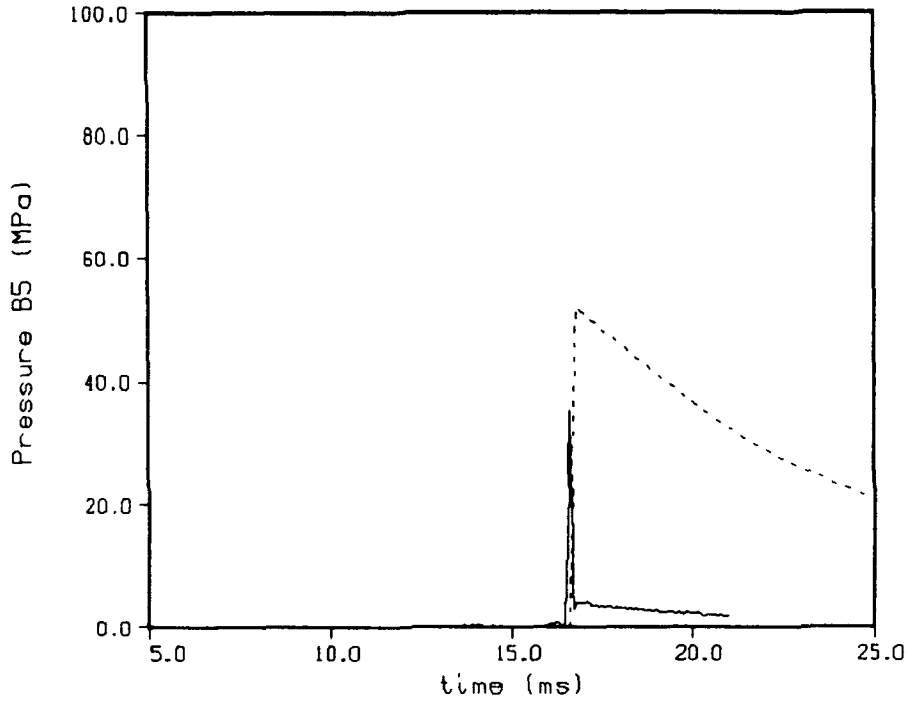

Figure 21. Barrel Pressure, Gage B5 - Round 17 (line). Model With Droplet Burning (dot).

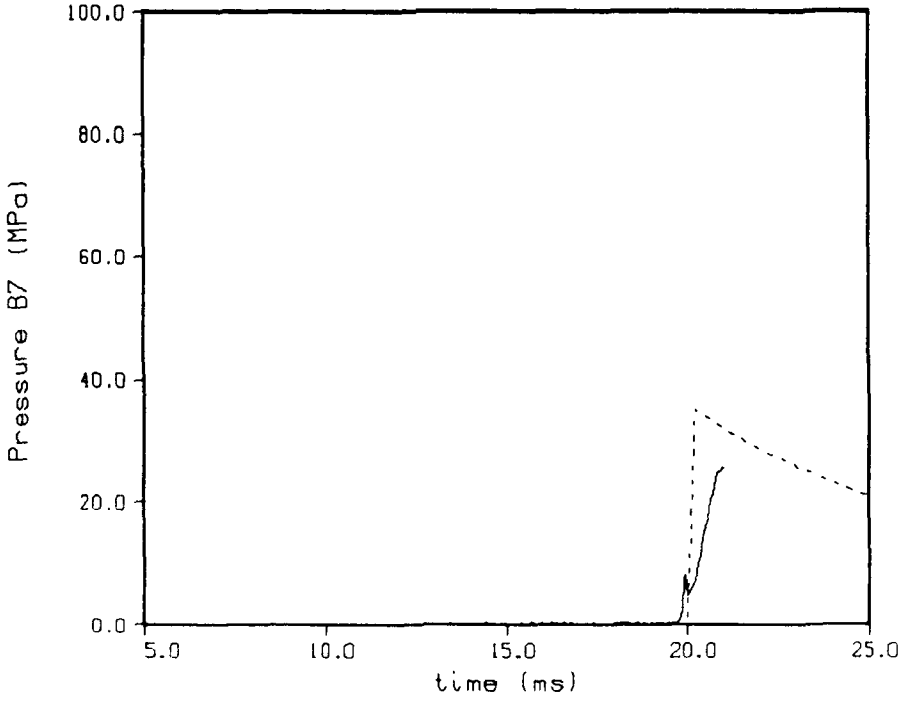

Figure 22. Barrel Pressure, Gage B7 - Round 17 (line). Model With Droplet Burning (dot).

propellant fill cycle to seal the space between the transducer block and the outer piston. The effect of the oil on the propellant combustion and thermochemistry is ignored, since GE[11] reports that the oil is most likely deposited in the rear of the liquid reservoir and does not mix easily with the propellant. However, in the model, we assume the liquid reservoir contains only propellant with the volume chosen to be consistent with recorded piston travel.

The piston and control rod in the damper were modified from the shot 17 configuration. This modification results in slightly different initial liquid volume, initial chamber volume (as derived from a CAD analysis), and piston travels. The primer mass is slightly less than that in shot 17, but otherwise the primer is the same. The values of the key gun parameters are listed in Table 2. A standard M107 projectile was used in this test series. The projectile-tube interface was the same as in shot 17.

A comparison of the experimental chamber and liquid pressures from shots 27 and 28 are shown in Figures 23 and 24. The gages display the discrepancies associated with much of the Concept VIC data. The four chamber pressure gages in Figure 23 record pressures consistent in the startup region, but the pressures then diverge by about 7% at maximum pressure. In shot 28, both a higher pressure and a lower pressure were recorded, bounding the shot 27 data which are more consistent. The four recorded liquid pressure histories in Figure 24 diverge in the startup region and show a difference of approximately 9% at maximum pressure. There appears to be little correlation between the shots (i.e., the highest chamber pressure is recorded for shot 28, but the highest liquid pressure is recorded for shot 27). This may indicate calibration errors in the chamber gages. Comparisons of piston travel, damper pressures, and barrel pressures at gage B1 for shots 27 and 28 are not presented; however, agreement is good. It is noted that recoil has already been subtracted from the piston travel curves. The results of the free recoil model are not as accurate as the 105 mm results;[2] therefore, the recoil model was adjusted to give the correct maximum piston travel.[7]

In an effort to obtain a more accurate history of the combustion chamber pressure, GE[7] suggested that the pressure recorded at the D-plane gage location be supplemented by the pressure recorded by the E-plane combustion chamber gages. The D-plane gages are located at the front of the combustion chamber, just before the taper into the gun tube. Differences between these gages and other chamber gages have been observed in much of the other 155 mm data. The differences have been attributed to gage drift caused by heating due to increased gas flow and turbulence since the gage is located in the chambrage of the chamber; also, the gage holes were milled too

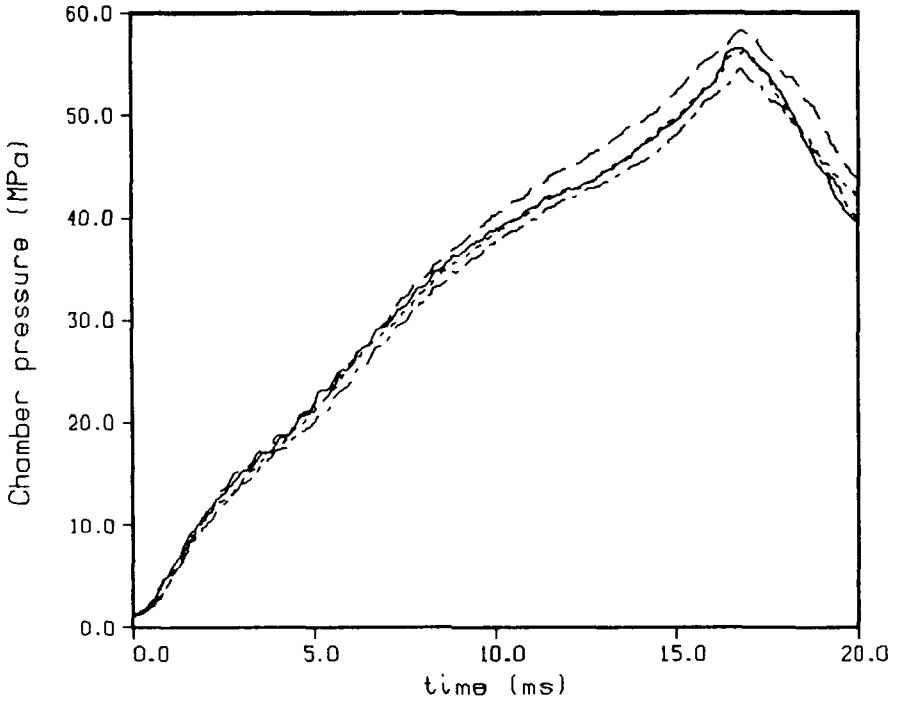

Figure 23. Experimental Chamber Pressure. Round 27 - Gage D138 (line) and Gage D33 (dot) Round 28 - Gage D138 (dash) and Gage D33 (dot-dash).

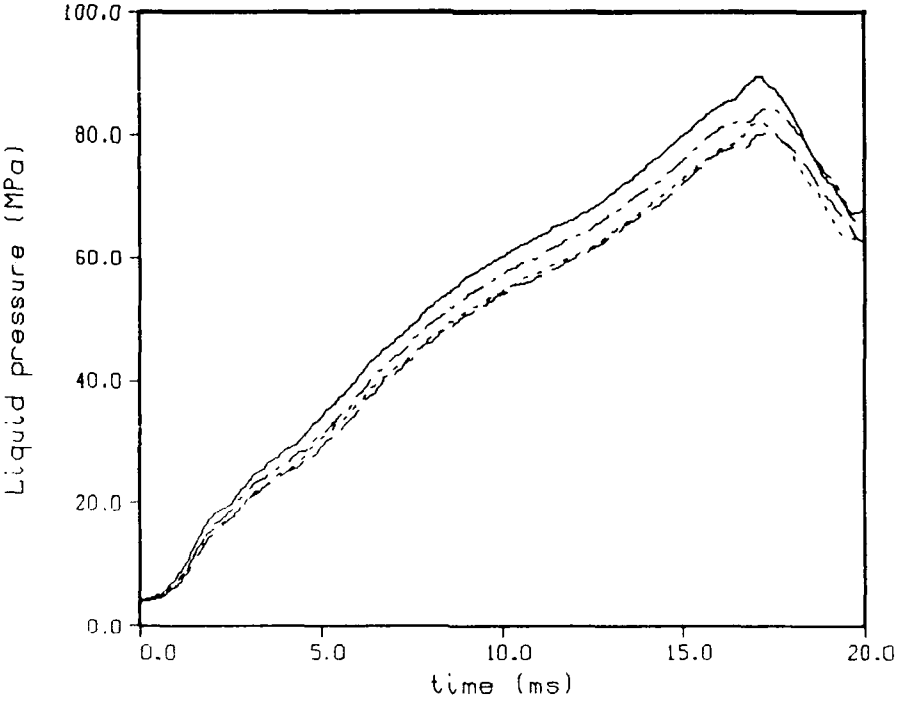

Figure 24. Experimental Liquid Pressure. Round 27 - Gage LP270 (line) and Gage LP90 (dot). Round 28 - Gage LP270 (dash) and Gage LP90 (dot-dash).

large. The two E-plane gages are initially covered by the outer piston and do not provide a record of the early chamber history. However, they are exposed to the combustion chamber environment soon after the start of piston travel. In Figure 25, the recorded pressures at the D and E-plane gages for Shot 28 are compared. A close inspection shows that the recorded pressures at D138 and E342 are high and in relative agreement, and at D33 and E222 are low and in relative agreement. The spread between the recorded pressures is on the order of 14%. Since there is no apparent evidence of systematic differences between the D and E-plane gages, no attempt was made to combine recorded pressures. The D-plane gages are used in subsequent analyses to be consistent with earlier simulations.

The inverse code is applied to the data to determine values of the discharge coefficients for the liquid reservoir and the damper. The derived discharge coefficients from the two shots using gages D138 and LP270 are shown in Figures 26 and 27 for the reservoir and damper, respectively. Values above 1.0 are not physically meaningful and indicate error in pressure measurement or piston travel. It has been noted that the pressure gages are not in good agreement and that the measured piston travel was adjusted by the recoil model. Thus, the data in Figure 26 are taken to suggest little flow loss, and the discharge coefficient for the liquid reservoir is chosen to be a constant 0.95. Similarly, Figure 27 suggests a discharge coefficient of 0.95 for the damper. Identical values were used in Shot 17 simulations.

The projectile resistive pressure is determined from radar data using the chamber pressure, D138 gage, as a boundary condition in Shot 28. A shot start pressure of 4.0 MPa applied over 1.5 times the length of the engraving band with the resistive pressure of 0.7 MPa along the remainder of the bore provides good agreement between experimental and predicted projectile travel (see Figure 28). The radar signal is temporarily lost and regained during firing, producing the break in the experimental data in Figure 28. A comparison of experimental and predicted pressures at the B1 gun tube gage, the only barrel gage recorded for this shot, is shown in Figure 29.

Initially, the model is applied with the Shot 27 chamber pressure, D138 gage, as a boundary condition. The results are shown in Figures 30 and 31. The liquid pressure is reproduced accurately in Figure 30, but the piston travels in Figure 31 are in poor agreement. Although not shown, the damper pressure agreement is adequate, and the early projectile travel, as shown in Figure 28, is good. To investigate the inconsistency between the predicted and experimental piston travels in shot 27, the model is applied to Shot 28 with chamber pressure, D138 gage, as a boundary condition. These results are shown in Figures 32 and 33. The liquid pressure agreement

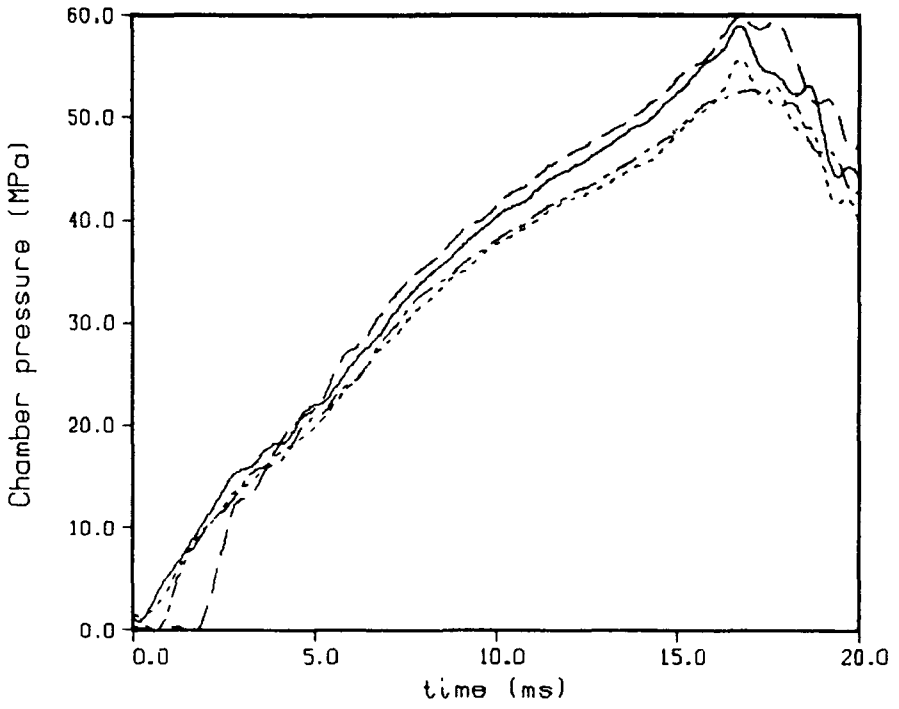

Figure 25. Experimental Chamber Pressure. Round 28 - Gage D138 (line) and Gage D33 (dot). Round 28 - Gage E342 (dash) and Gage F222 (dot-dash).

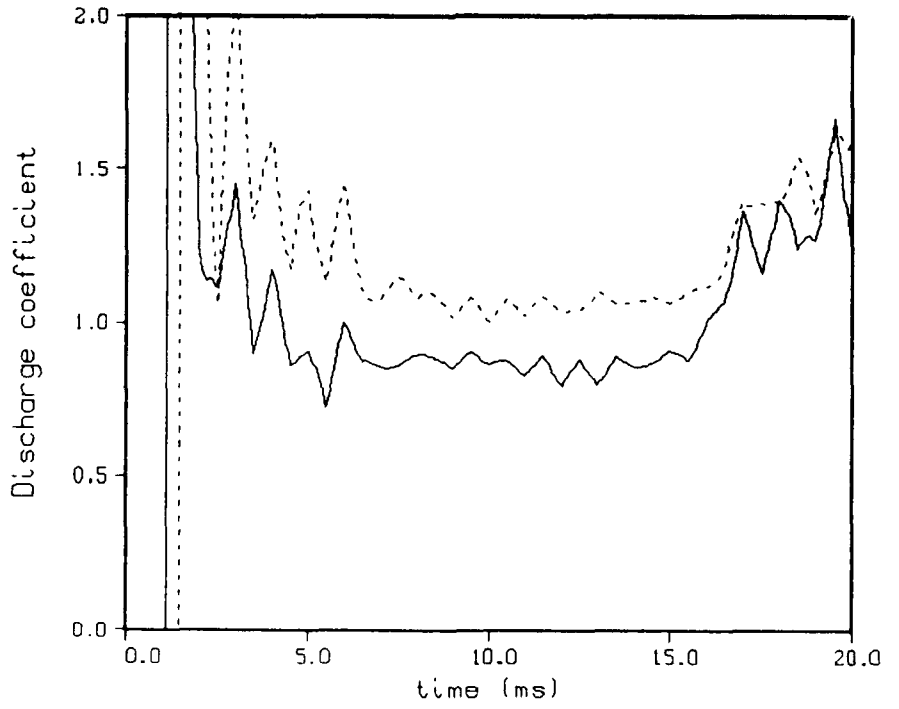

Figure 26. Results From Inverse Code - Reservoir. Discharge Coefficient (line) - Round 27. Discharge Coefficient (dot) - Round 28. Based on the Gages D138 and LP270.

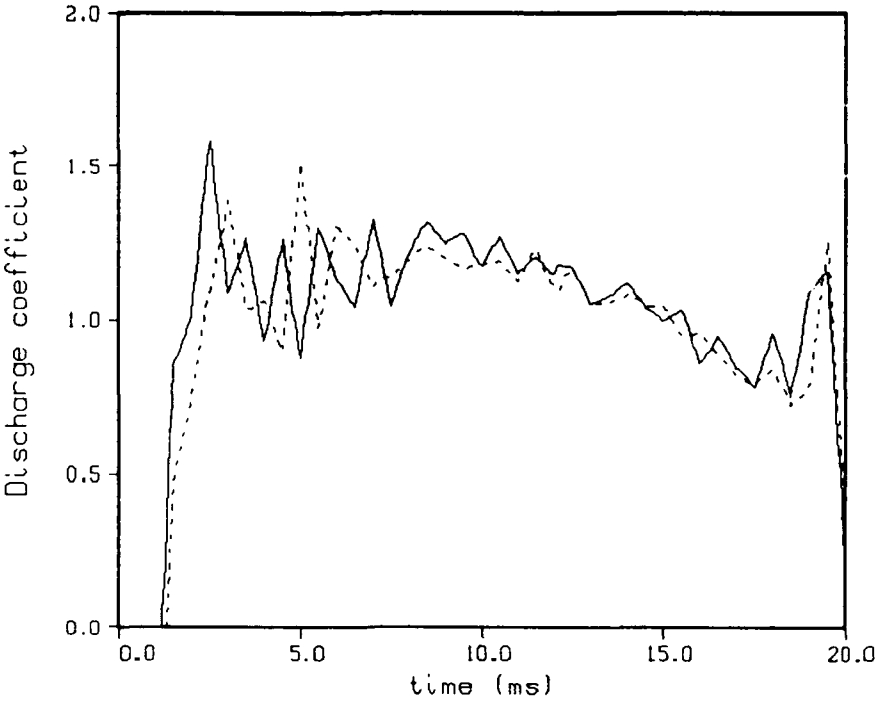

Figure 27. Results From Inverse Code - Damper. Discharge Coefficient (line) - Round 27. Discharge Coefficient (dot) - Round 28. Based on the Damper Gage.

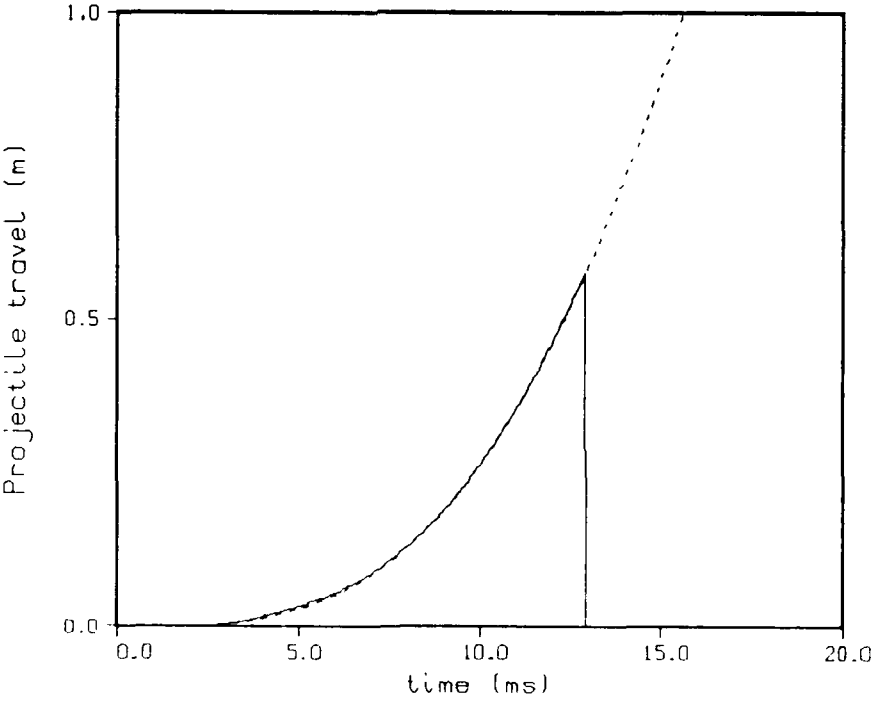

Figure 28. Initial Projectile Travel - Round 27 (line). Model With Chamber Pressure D138 (dot).

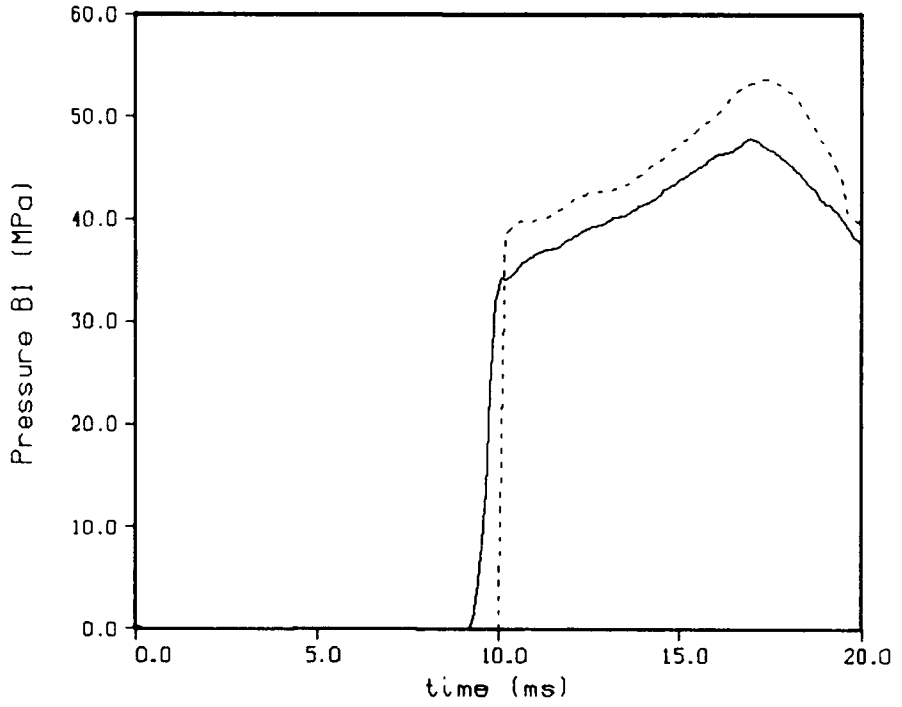

Figure 29. Barrel Pressure, Cage B1 - Round 27 (line). Model With Chamber Pressure D138 (dot).

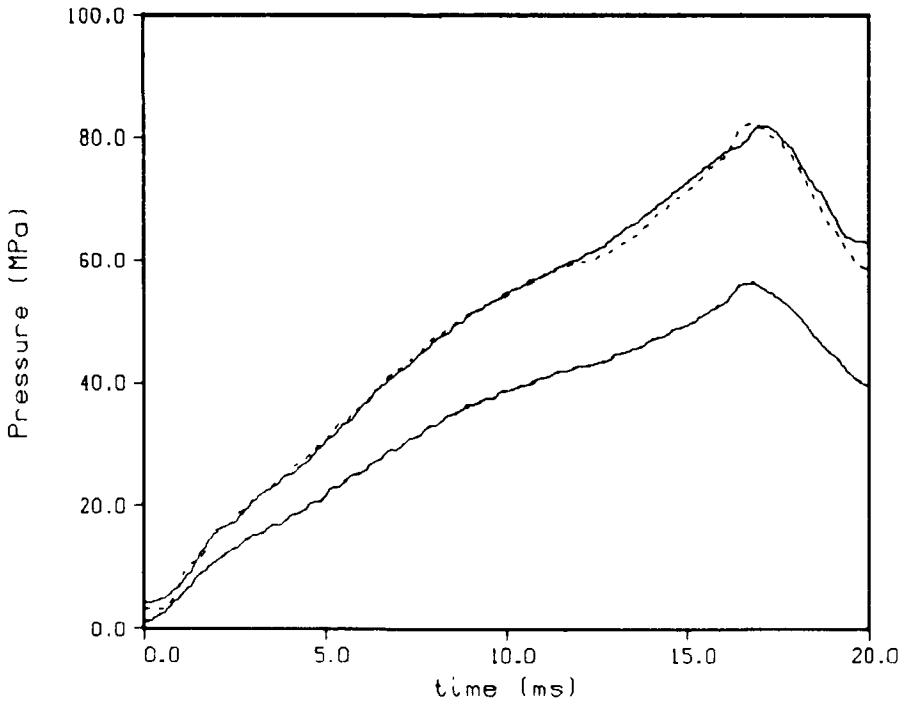

Figure 30. Liquid Pressure and Chamber Pressure - Round 27 (line). Liquid Pressure From Model With Chamber Pressure D138 (dot).

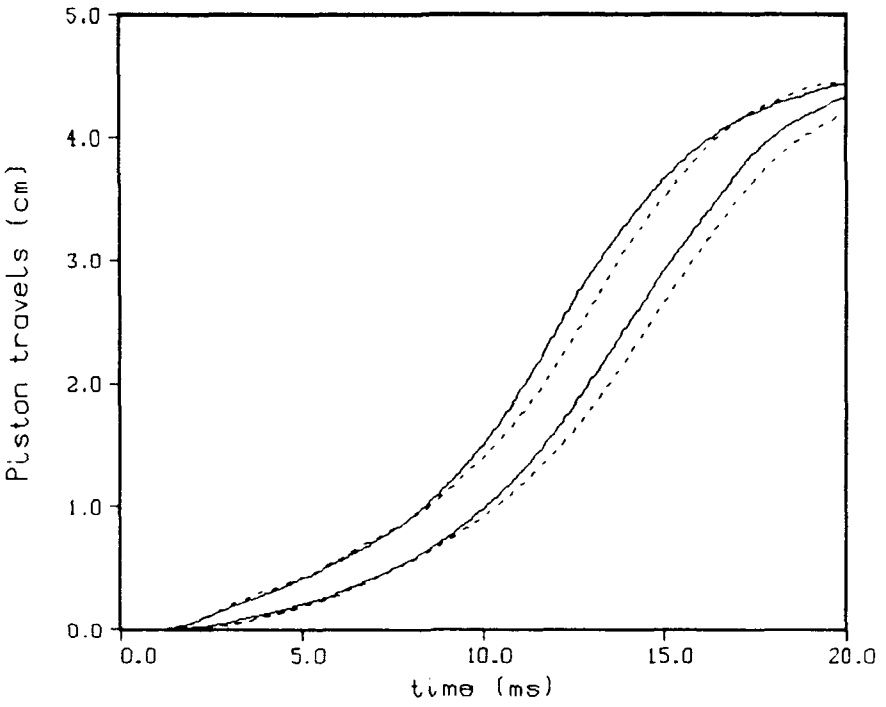

Figure 31. Piston Travel - Round 27 (line). Model With Chamber Pressure D138 (dot).

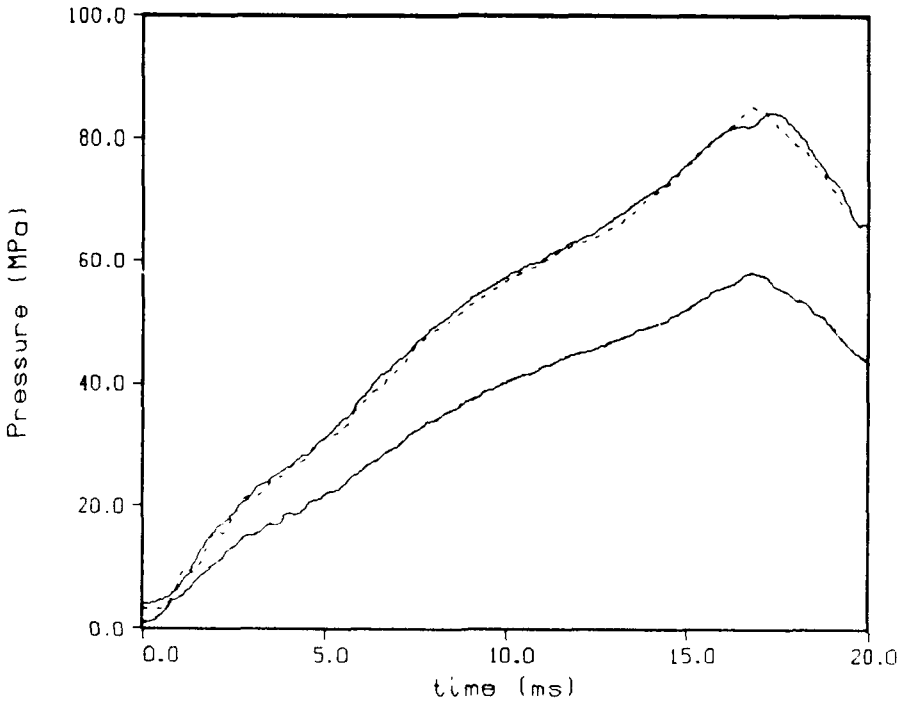

Figure 32. Liquid Pressure and Chamber Pressure - Round 28 (line). Liquid Pressure From Model With Chamber Pressure D138 (dot).

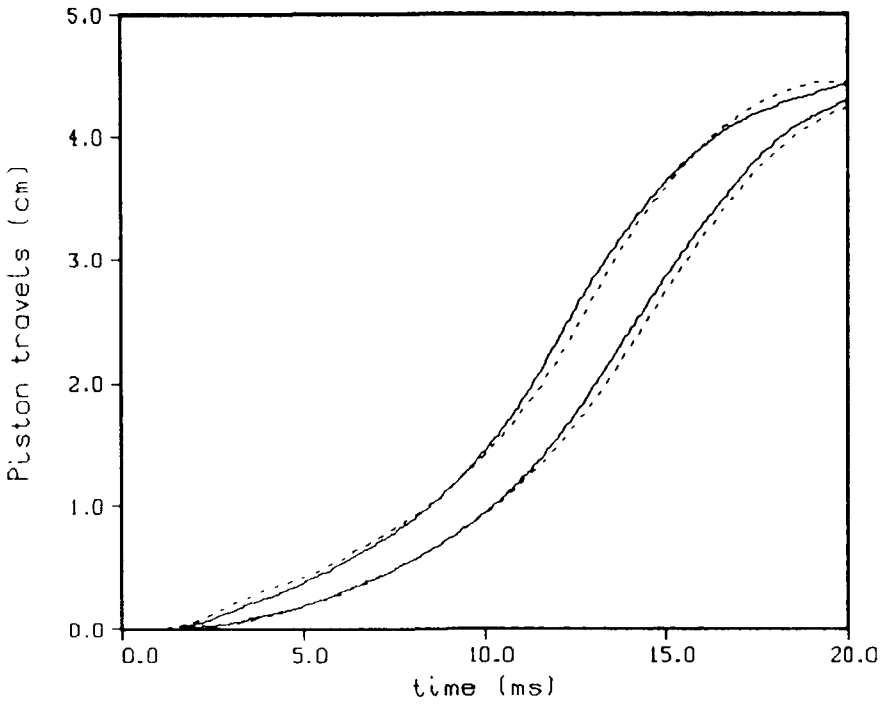

Figure 33. Piston Travel - Round 28 (line). Model With Chamber Pressure D138 (dot).

in Figure 32 is good, and the piston travel agreement in Figure 33 is much improved. The results again indicate the uncertainty in the chamber pressure gage measurements.

Instantaneous burning is assumed in the comparisons of liquid and chamber pressures and piston travels, shown in Figures 34 and 35, respectively, for Shot 28. It can be seen that accumulation is an important factor in the ballistic cycle. The instantaneous combustion assumption results in a predicted maximum chamber pressure significantly higher than that recorded. Interestingly, the opposite situation is seen in 30 mm and 105 mm data[1,2] where the rapid burn-off of the accumulated propellant together with the combustion of entering propellant produces a higher experimental maximum chamber pressure than the model assuming instantaneous combustion. Although there is less accumulation in Shot 17 than in Shot 28, the energy release is spread over a longer period of time in Shot 28. The maximum chamber pressure is reached in Shot 17 (Figure 11) at approximately 13 ms compared to approximately 18 ms in Shot 28 (Figure 34). Over this longer time period, the gas volume is increasing as a result of projectile motion. Thus, the slower

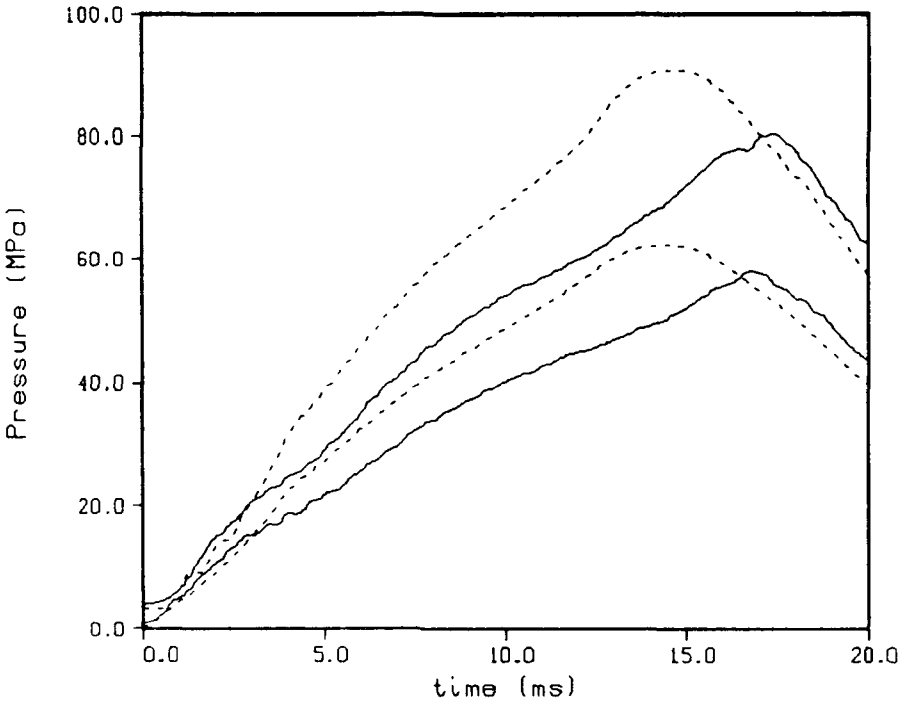

Figure 34. Liquid Pressure and Chamber Pressure - Round 28 (line). Model With Instantaneous Burning (dot).

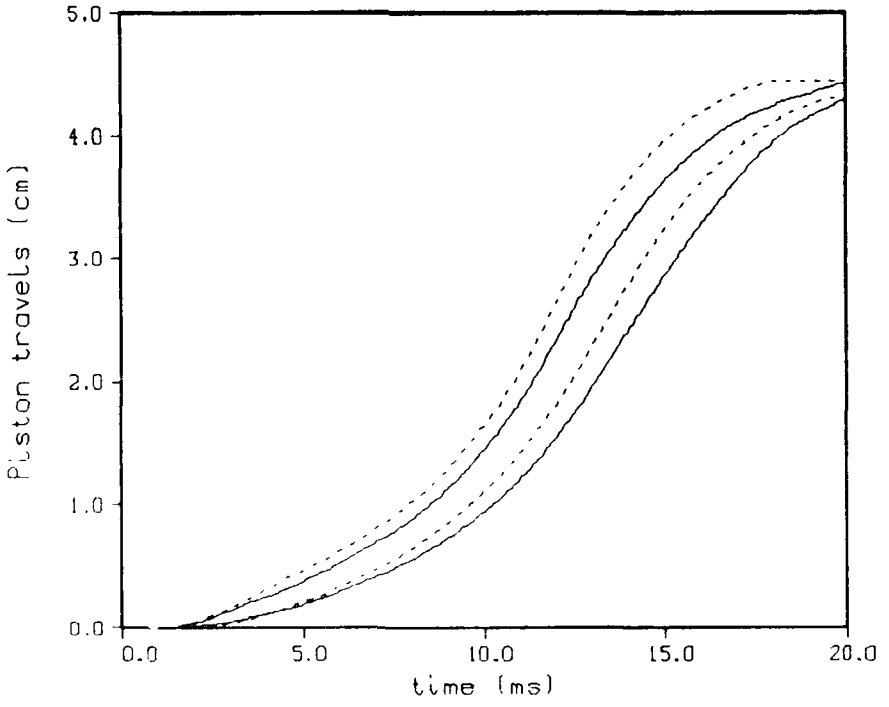

Figure 35. Piston Travel - Round 28 (line). Model With Instantaneous Burning (dot).

event and larger gas volume result in a chamber pressure which is lower than that obtained assuming instantaneous combustion. The higher predicted liquid pressure (Figure 34) and faster predicted piston motion (Figure 35) simply reflect the higher predicted combustion chamber pressure. The experimental data are similar to those of shot 17 in the lack of the relatively long, flat pressure during the startup. However, a comparison of chamber pressures for shot 17 (Figure 11) and for shot 28 (Figure 34) indicates significantly more accumulation in shot 28. The predicted projectile velocity at 200 inches of travel is 405 m/s, 3.1% higher, due to the higher predicted pressures, than the experimental value of 393 m/s.

Accumulation is modeled by developing a droplet profile for the liquid propellant in the combustion chamber to match the experimental chamber pressure recorded at the gage D138 location. The resulting droplet profile is shown in Table 4.

Table 4. Round 28 Mean Droplet Diameter Profile Derived From Chamber Pressure Recorded at Gage D138

Chamber pressure, MPa	Droplet diameter, μm
0.0	100
20.0	100
40.0	100

A comparison of the model predictions, using the droplet profile in Table 4, with experimental data is shown in Figures 36-41. A comparison of the chamber and liquid pressures is shown in Figure 36. The agreement is good, although the model does not produce the experimental dip in pressure between 12 and 14 ms. The piston travels in Figure 37 show good overall agreement with some slight discrepancies between the prediction and experiment. The computed damper pressure in Figure 38 is high and only qualitatively correct. The inaccuracy may reflect an incorrect damper exit-area profile due to the initial seating of the bushing. The projectile travels in Figure 39 show good agreement in the early motion. The model accurately predicts the time of the uncovering of gages B1 and B3; however, the magnitudes of the pressures at these locations are incorrect (see Figures 40 and 41). The predicted projectile velocity at 200 inches of travel is 397 m/s, which is 1.0% high.

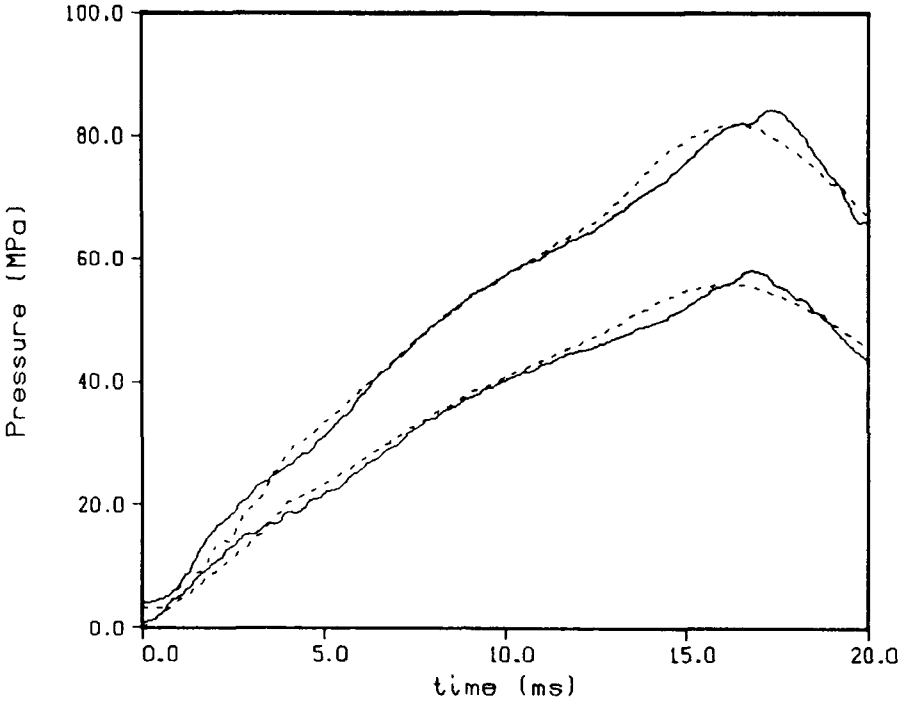

Figure 36. Liquid Pressure and Chamber Pressure - Round 28 (line). Model With Droplet Burning (dot).

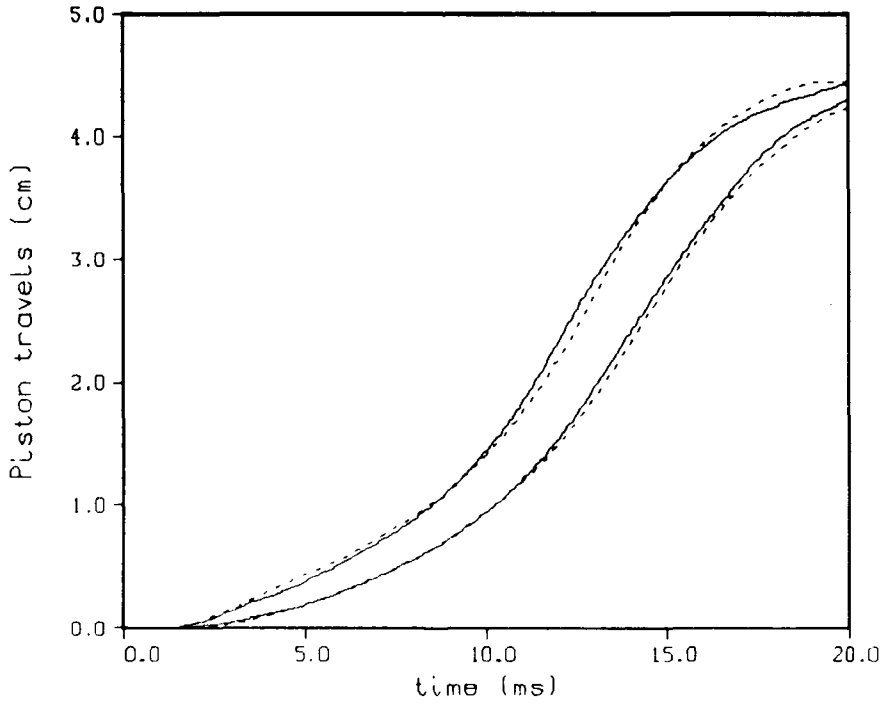

Figure 37. Piston Travel - Round 28 (line). Model With Droplet Burning (dot).

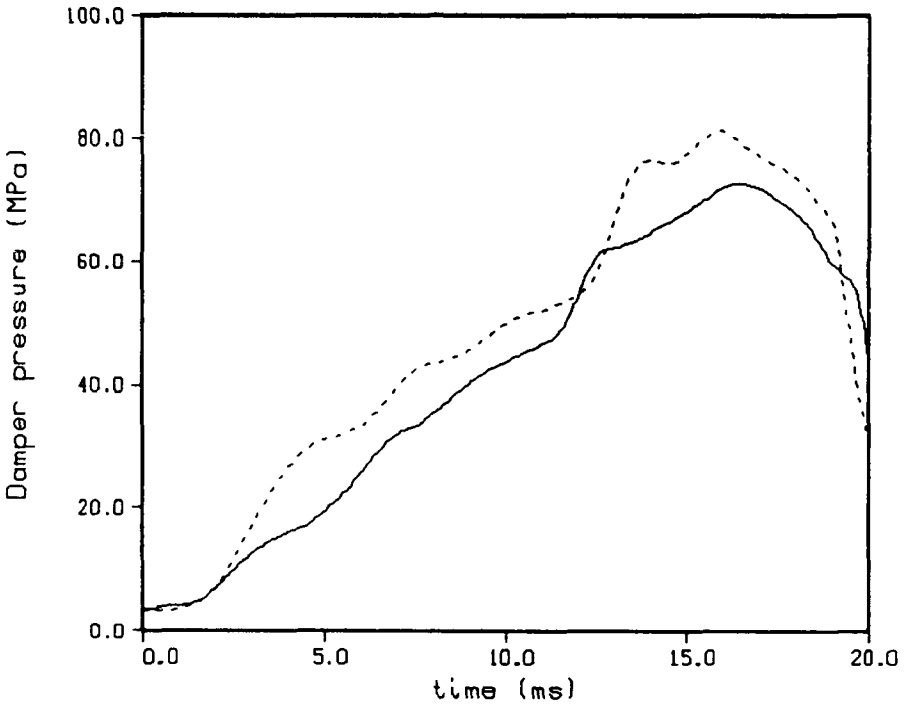

Figure 38. Damper Pressure - Round 28 (line). Model With Droplet Burning (dot).

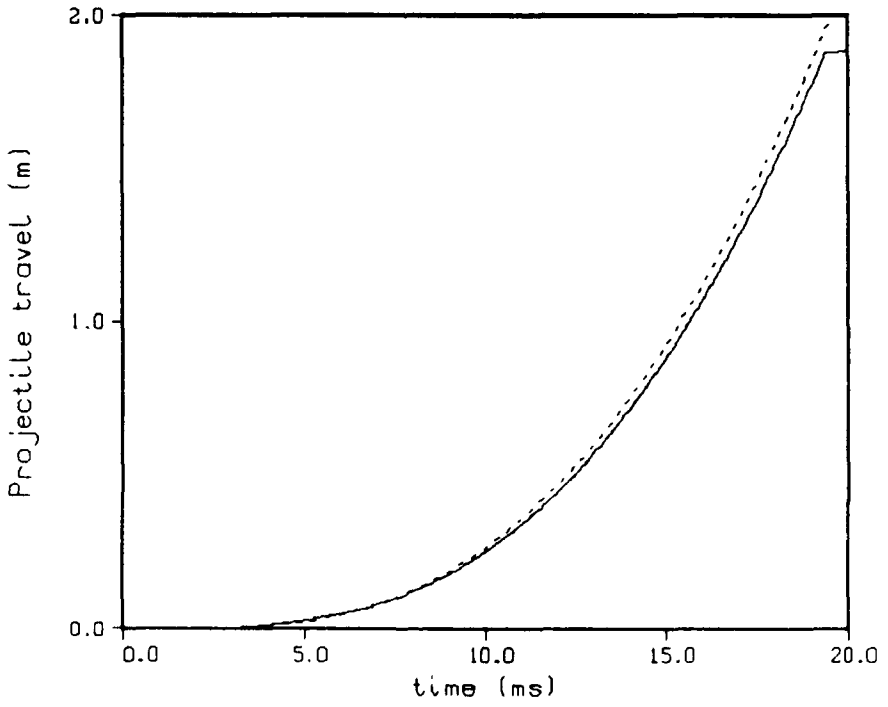

Figure 39. Initial Projectile Travel - Round 28 (line). Model With Droplet Burning (dot).

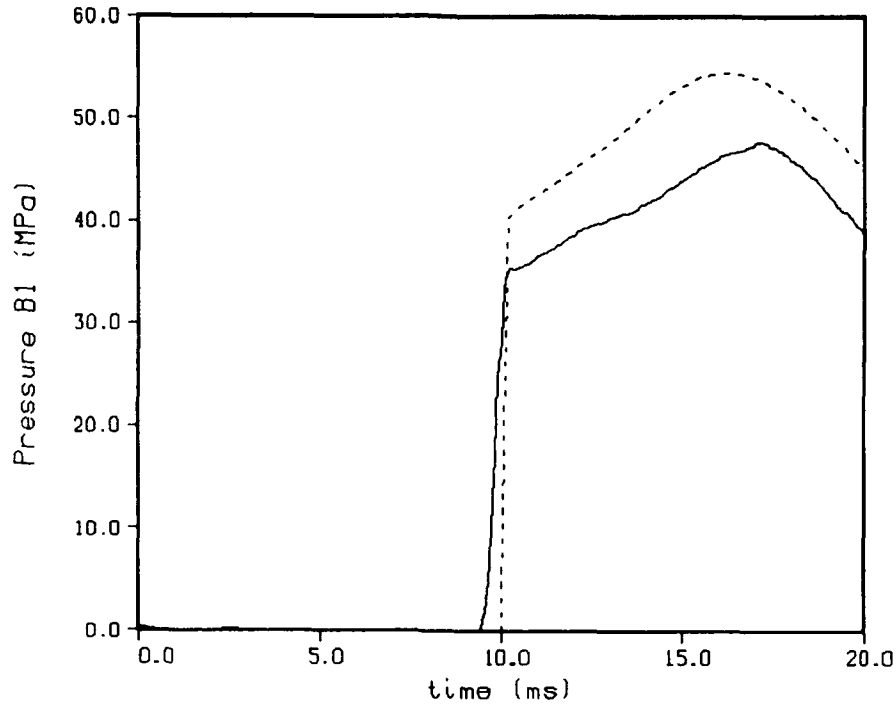

Figure 40. Barrel Pressure, Gage B1 - Round 28 (line). Model With Droplet Burning (dot).

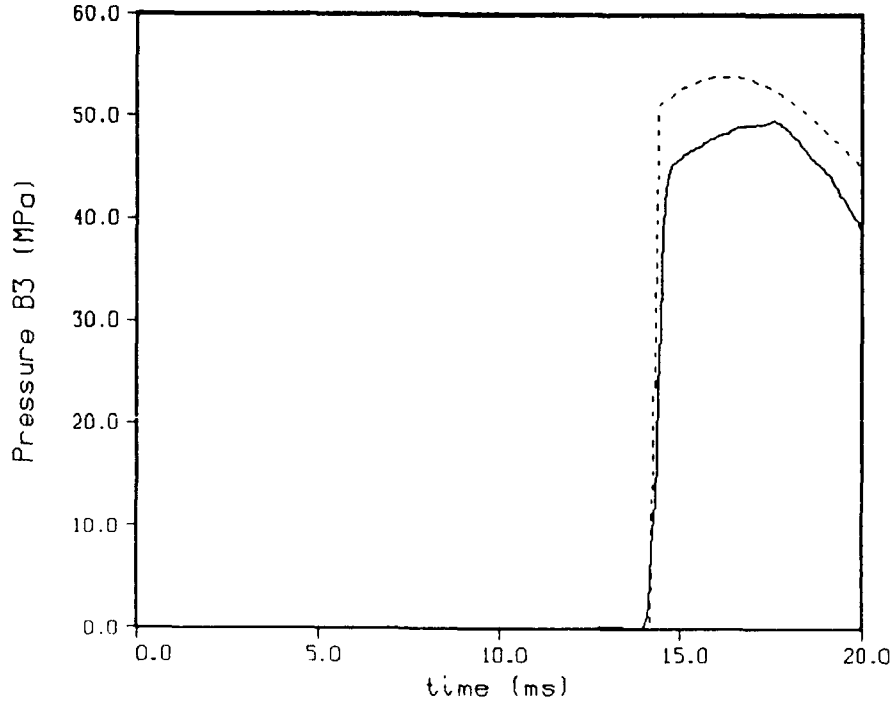

Figure 41. Barrel Pressure, Gage B3 - Round 28 (line). Model With Droplet Burning (dot).

Unfiltered data were reviewed for Shot 28 in order to investigate the discrepancies in the magnitudes of the predicted and experimental barrel pressures seen in Figures 40 and 41. A comparison of unfiltered data with the filtered data showed good agreement. Thus, data reduction is not considered to be a cause of the discrepancy. Comparisons between the two chamber pressure gages, D138 and D33, and the two barrel gages, B1 and B3, are shown in Figure 42. B1 is located at 26.642 centimeters of projectile travel, and B3 is located at 79.497 centimeters of projectile travel. It is noted that the recorded maximum pressure at the gage B3 location is higher than that at gage B1. Although it is physically possible, due to a rarefaction wave, for a gage further down tube to temporarily record a higher pressure than a gage closer to the chamber, no physical mechanism can be identified which would maintain such a pressure difference. In addition, since the chamber pressure is low, and the projectile is moving slowly, the model predicts no noticeable rarefaction wave. The predicted chamber and barrel pressures, shown in Figure 43, show a small pressure drop from the chamber to the first barrel gage and an imperceptible drop from the first barrel gage to the second, physically reasonable events. Thus, it appears that there is a calibration problem with one or both barrel gages.

To probe this discrepancy between the barrel gages further, a simulation of Shot 28 using the lower chamber pressure recorded at D33 is developed. The recoil model is first applied to the raw Optron data in Figure 44 using chamber pressure measurements from D138 and D33. Both calculations give a maximum piston travel which is too small. However, the lower pressure results in less recoil and, hence, longer apparent piston travel. Since the pressure would have to be significantly lower than recorded in the experiment to produce the actual piston travel with the recoil model used, it is more likely that the recoil model is inadequate. However, as can be seen in Figure 44, the piston motion is not highly dependent on the exact recoil until end of stroke. This does not appear to be a major factor in the analysis, and the GE supplied piston travel is used.

In order to produce a simulation of the lower chamber pressure measurement at D33, the constant droplet size is increased from a constant 100 μm to a constant 250 μm, as shown in Table 5. To match the experimental piston travel curves using the droplet profile in Table 5, the damper discharge coefficient is changed from 0.95 to 1.05. Although the discharge coefficient physically cannot be greater than 1.0, the larger value in the Bernoulli equation is a simple way to uniformly increase the damper area. (It was noted to be in question in the discussion above.) The resulting comparisons with the experiment are shown in Figures 45-50. The predicted projectile

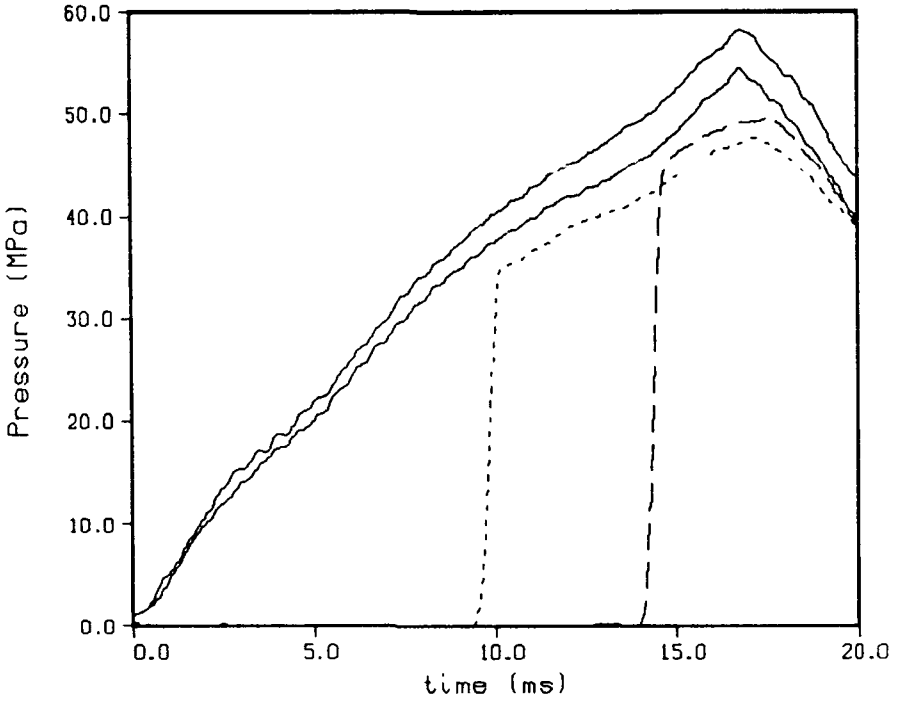

Figure 42. Chamber Pressures and Barrel Pressures - Round 28. Gage D138, Gage D33 - Round 28 (line). Barrel Gage B1 (dot). Barrel Gage B3 (dash).

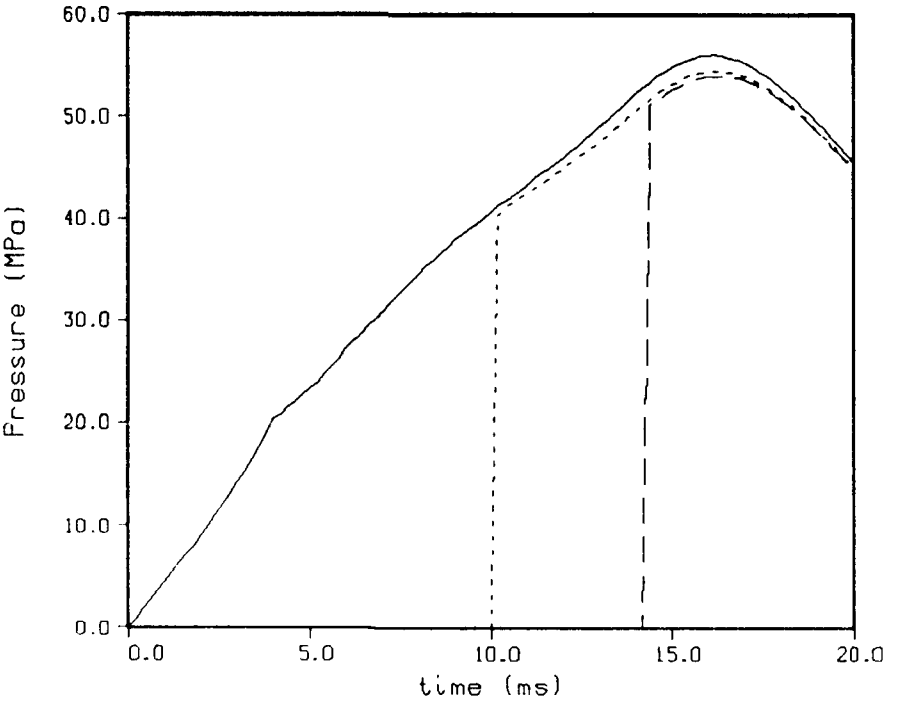

Figure 43. Chamber Pressures and Barrel Pressures - Model. Chamber Pressure - Model (line). Barrel Gage B1 (dot). Barrel Gage B3 (dash).

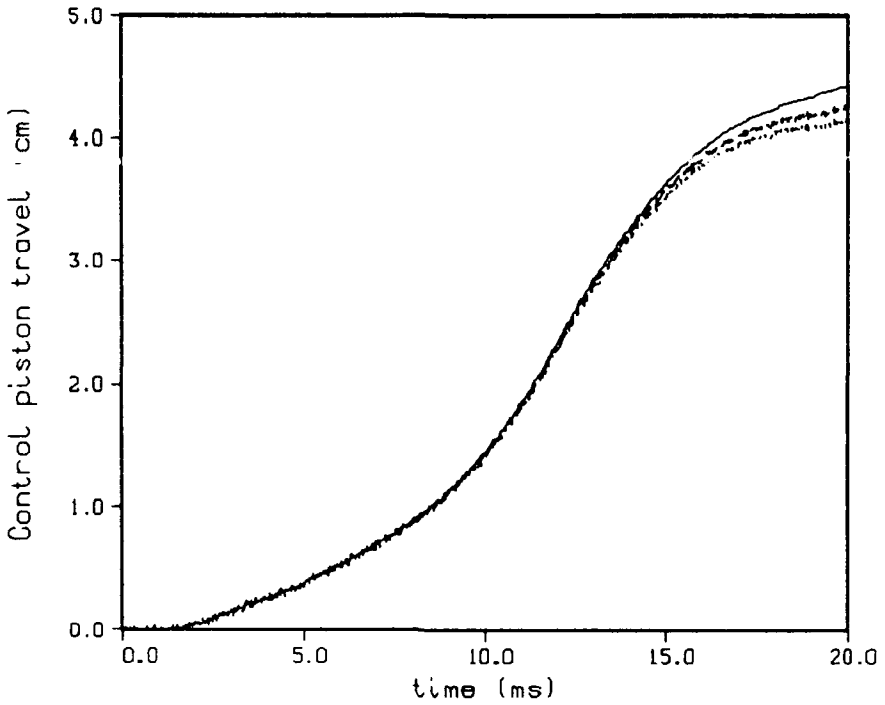

Figure 44. Piston Travel - Round 28. Reported by GE (line). Computed From Optron Measurement Using Gage D138 (lower curve). Computed From Optron Measurement Using Gage D33 (middle curve).

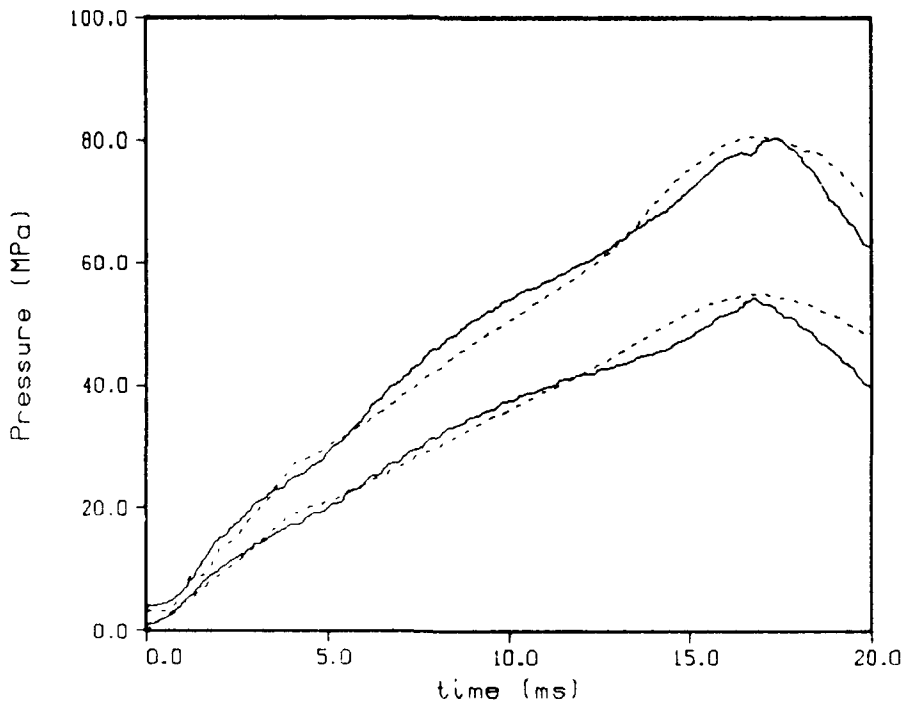

Figure 45. Liquid Pressure and Chamber Pressure - Round 28 (line). Model With Droplet Burning (dot).

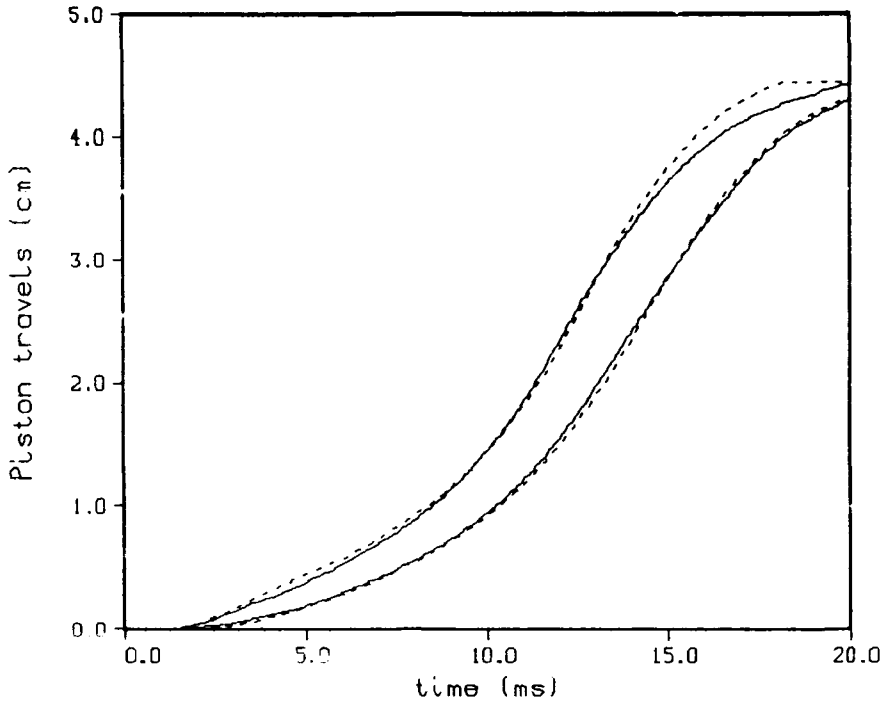

Figure 46. Piston Travel - Round 28 (line). Model With Droplet Burning (dot).

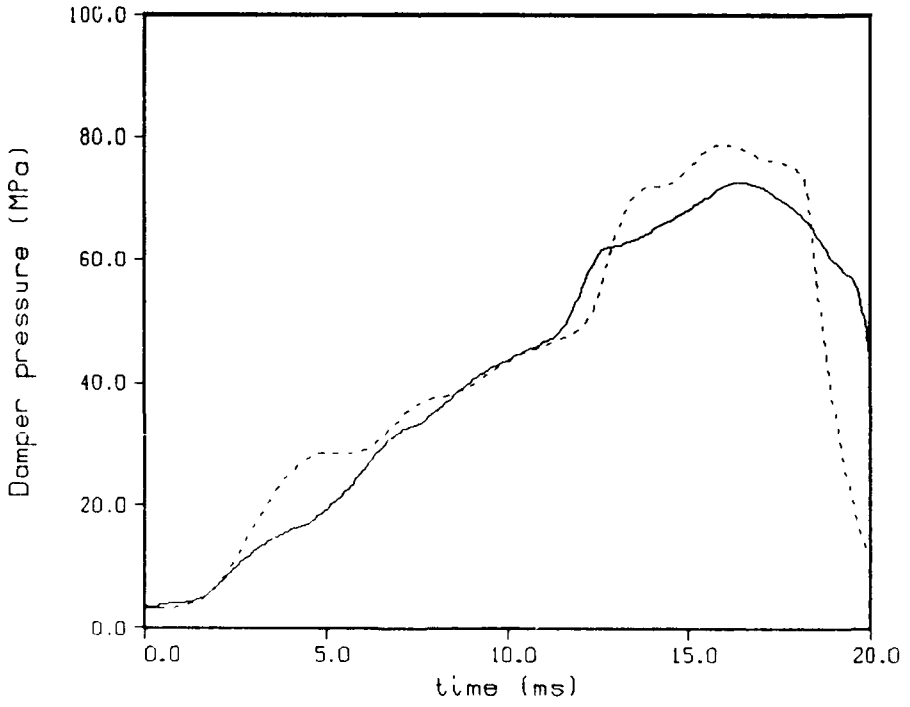

Figure 47. Damper Pressure - Round 28 (line). Model With Droplet Burning (dot).

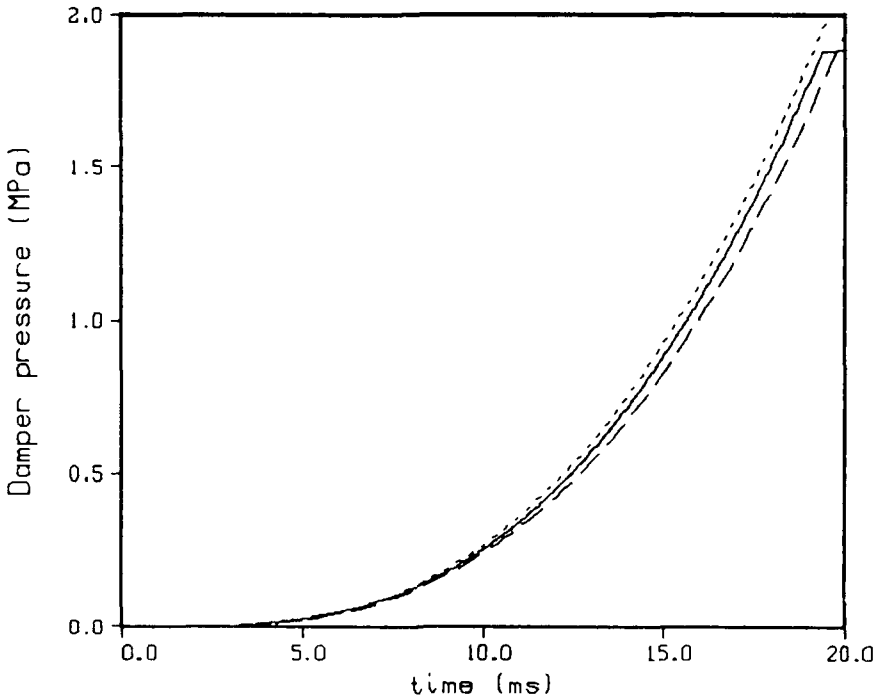

Figure 48. Initial Projectile Travel - Round 28 (line). Model With Droplet Burning - Based on D138 (dot), Based on D33 (dash).

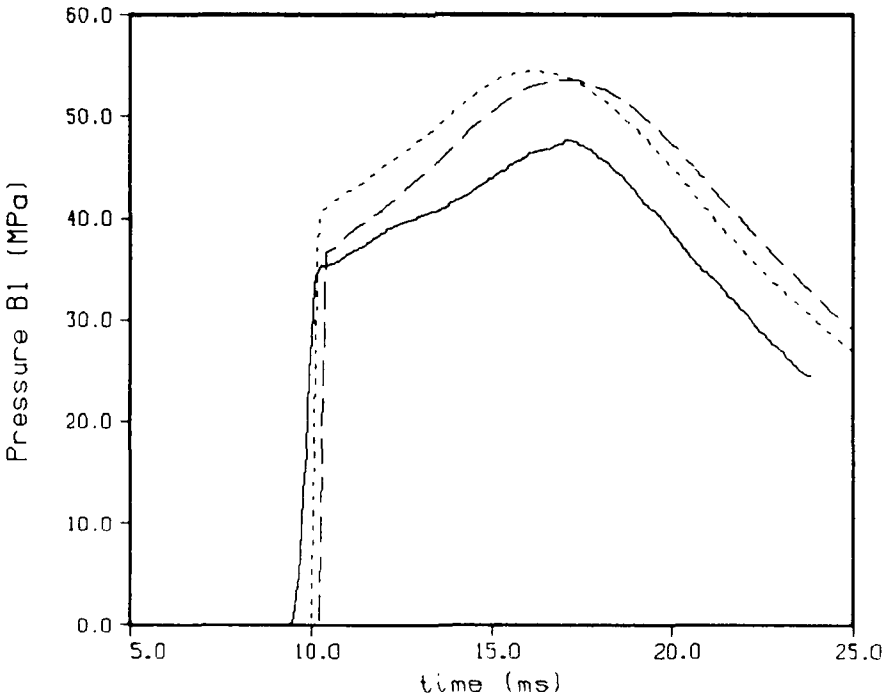

Figure 49. Barrel Pressure, Gage B1 - Round 28 (line). Model With Droplet Burning - Based on D138 (dot), Based on D33 (dash).

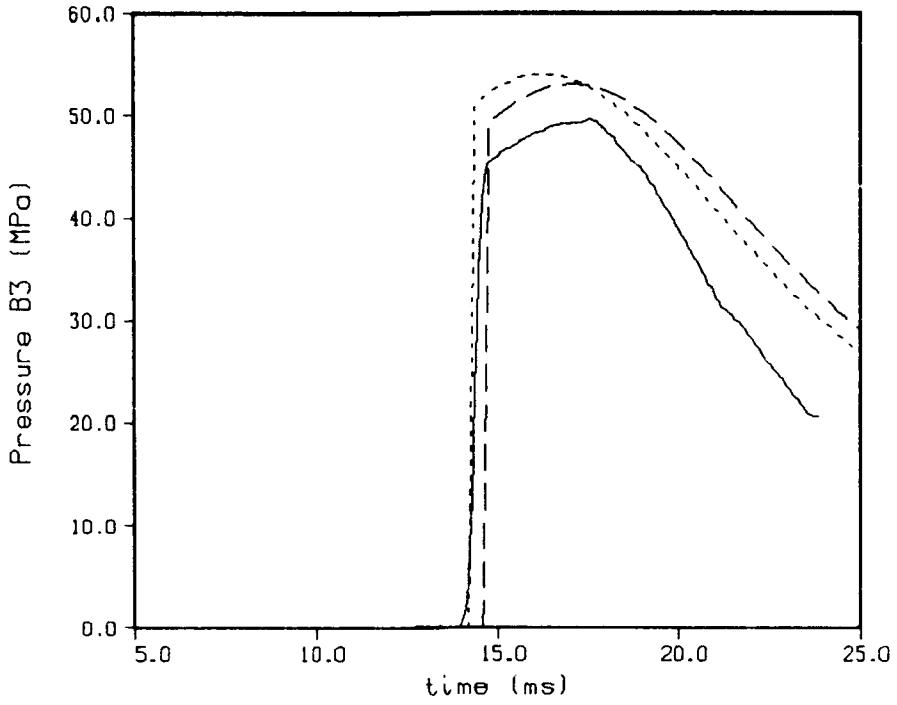

Figure 50. Barrel Pressure, Gage B3 - Round 28 (line). Model With Droplet Burning - Based on D138 (dot), Based on D33 (dash).

velocity at 200 inches of travel is now 392 m/s compared to an experimental velocity of 393 m/s. The previous predicted velocity was 397 m/s using the previous droplet size profiles cited in Table 4. The chamber and liquid pressures in Figure 45 are in reasonable agreement. Similarly, the piston travels in Figure 46 compare well. The agreement between damper pressures in Figure 47 is somewhat improved compared to Figure 38. However, the agreement of early projectile motions in Figure 48 (using Table 5) is somewhat poorer than obtained in the previous simulation (using Table 4). Comparisons of experimental and predicted pressures at the B1 and B3 locations using both droplet size profiles are presented in Figures 49 and 50, respectively. Figure 49 shows that in the simulation, using Table 5, the projectile arrives late at the B1 location, and the resulting pressure-time curve is qualitatively different than the experimental curve in shape. The quantitative discrepancy is also not improved. Similarly, in the simulation, the projectile arrives late at the B3 location. It appears that, if the amplitude of the experimental barrel pressure were matched exactly, the predicted projectile velocity would be lower than experimentally observed. Thus, it appears that the pressures recorded at the barrel gage locations are in error, and the droplet size profile in Table 4 provides the best overall simulation of the experimental data.

Table 5. Round 28 Mean Droplet Diameter Profile Derived From Chamber Pressure Recorded at Gage D33

Chamber pressure, MPa	Droplet diameter, μm
0.0	250
20.0	250
40.0	250

7. GE 155 MM GUN FIXTURE - 5 LITER SHOTS 48, 51

The 5 liter repeatability series consists of shots 47-56. Two of these firings, shots 48 and 51, are analyzed. The mean velocity reported by GE[7] at 200 inches of travel for this series is 586.2 m/s, with a standard deviation of 0.25%. The liquid volume of 5205 cubic centimeters used in the simulation to match the reported piston stroke (varies slightly from GE reported liquid volume) includes approximately 84 cubic centimeters of oil, which is pumped during the propellant fill cycle to seal the passage between the transducer block and the outer piston. The oil is expected to remain segregated from the propellant, and thus, the properties of the liquid propellant are not expected to change. The oil volume is included as propellant. The tube was not lubricated after shot 46, and it is hypothesized that increases in the projectile shot start and resistive pressures shown in Table 2 are a result of the change in the tube lubrication procedure.

Comparisons of the experimental data from shots 48 and 51 are shown in Figures 51-56. Overall, the data are quite reproducible. The piston travels in Figure 51 show excellent agreement. However, recoil has already been subtracted from this data. The recoil model was calibrated to give the correct maximum piston travel, and the actual comparison between piston travels in these experiments is obtainable only by direct observation of the raw data. The agreement among liquid pressures in the two experiments (two gages in the same plane in the liquid reservoir) shown in Figure 52 is excellent. The recorded chamber pressures in the D-plane in Figure 53 show discrepancies, particularly at peak pressure and afterwards. A close observation of Figure 53 shows that, prior to peak pressure, the recorded pressure is higher at one gage location in each shot. However, at peak pressure, both D-plane gages in shot 51 record pressures which are higher than shot 48 by approximately 5%. It is not clear which pressure data are more accurate.

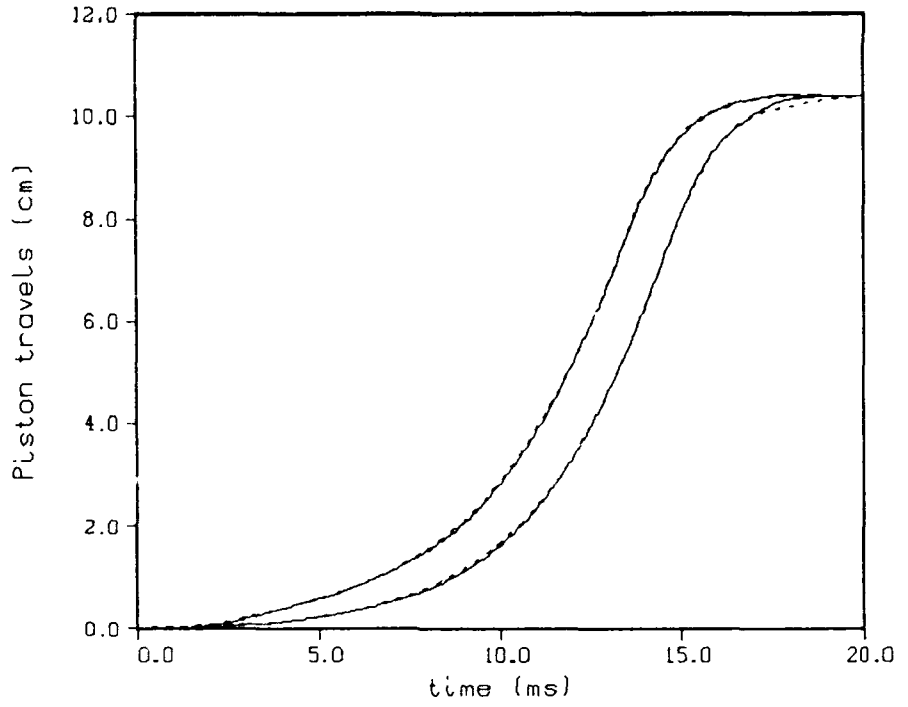

Figure 51. Piston Travel - Round 48 (line). Round 51 (dot).

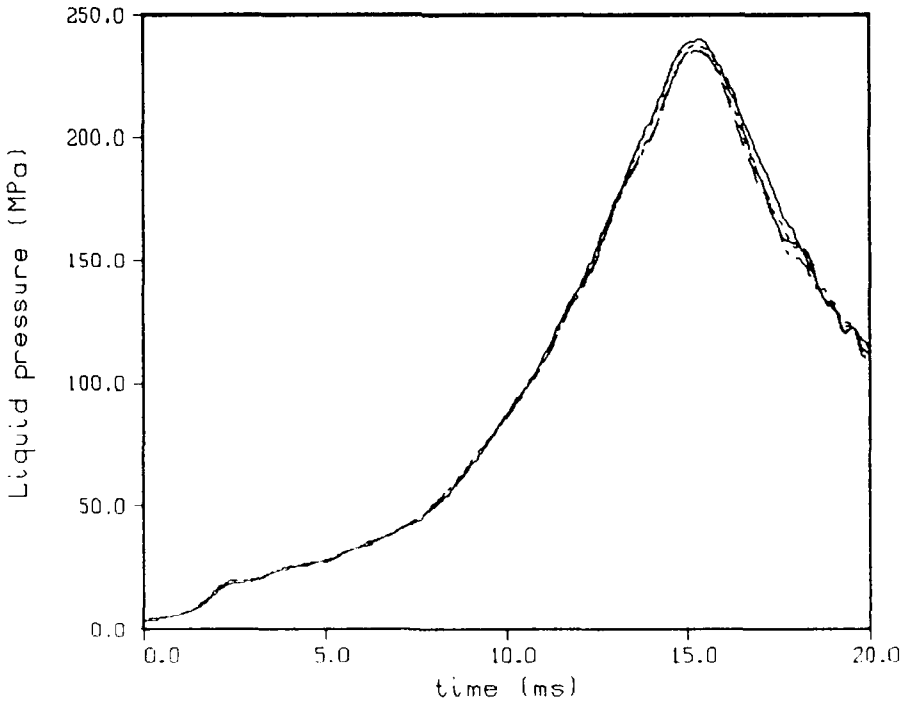

Figure 52. Experimental Liquid Pressure. Round 48 - Gage LP270 (line) and Gage LP90 (dot). Round 51 - Gages LP270 (dash) and Gage LP90 (dot-dash).

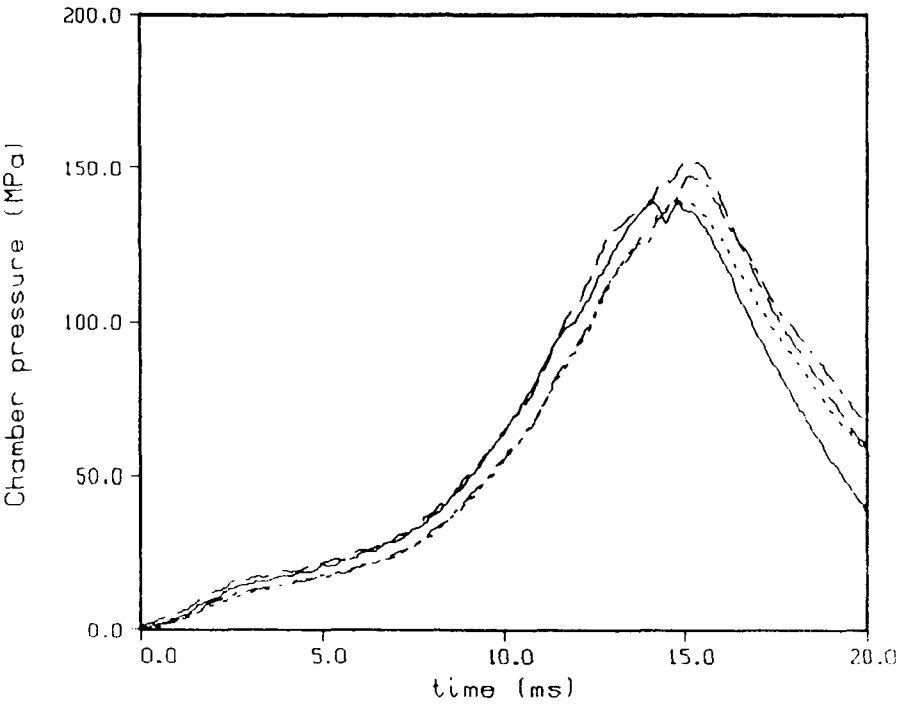

Figure 53. Experimental Chamber Pressure. Round 48 - Gage D138 (line) and Gage D33 (dot). Round 51 - Gage D138 (dash) and Gage D33 (dot-dash).

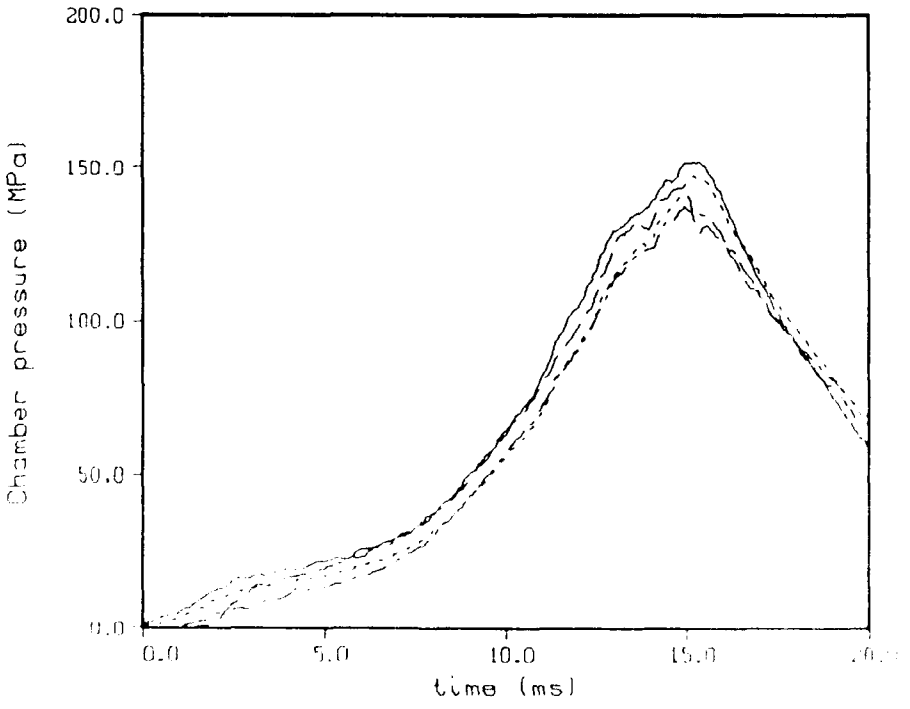

Figure 54. Experimental Chamber Pressure. Round 51 - Gage D138 (line) and Gage D33 (dot). Round 51 - Gage E342 (dash) and Gage E222 (dot-dash).

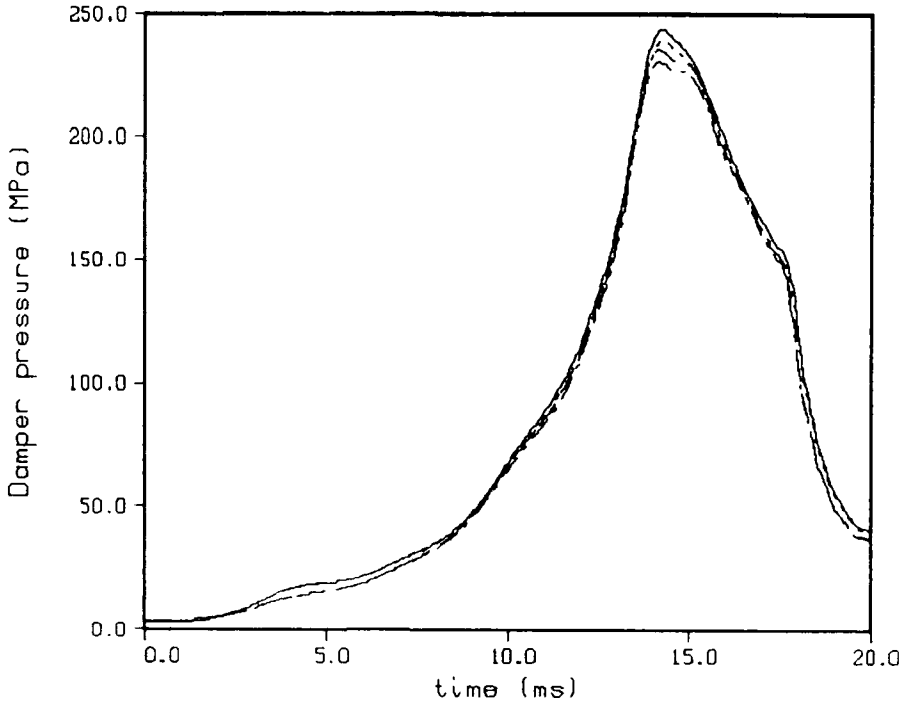

Figure 55. Experimental Damper Pressure. Round 48 - Gage O90 (line) and Gage O270 (dot). Round 51 - Gages O90 (dash) and Gage O270 (dot-dash).

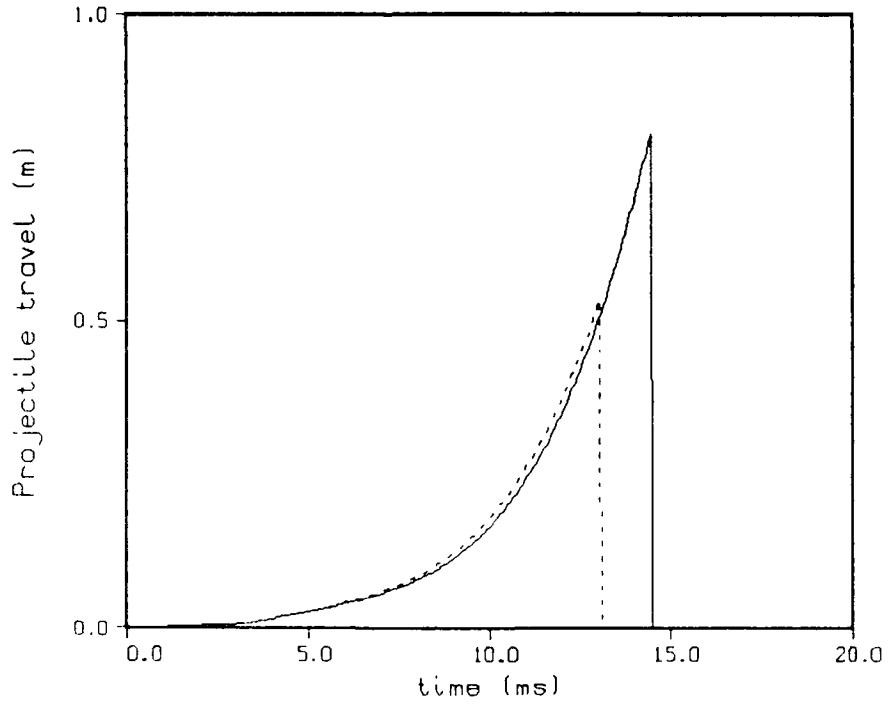

Figure 56. Initial Projectile Travel - Round 48 (line). Round 51 (dot).

Figure 54 compares the pressures recorded by the D and E-gages for Shot 51. A close inspection shows that the D138 and E342 pressures are high and in relative agreement, and that the D33 and E222 pressures are low and in relative agreement. The spread between the two sets of recorded pressures is on the order of 5-10%. Again, since there is no evidence of systematic differences between the D and E-plane pressures, the D-plane data are used in subsequent analyses, if only to be consistent with earlier analyses.

The comparison of the recorded damper pressures in Shots 48 and 51 shown in Figure 55 shows excellent agreement. The projectile travels (derived from radar data), as shown in Figure 56, are in good agreement. Overall, the ballistic cycle appears reproducible, with differences in the measured combustion chamber pressures possibly due to gage inaccuracy.

As a first approximation, the experimental chamber pressure recorded at the D138 location is used as a boundary condition with a value of 0.95 for the discharge coefficients for the reservoir and the damper, as in the 2 liter experiments. The resulting comparison of predicted and experimental liquid pressures is shown in Figure 57 for Shot 48 and in Figure 58 for Shot 51. The agreement in Figure 57 is poor, while in Figure 58 it is good. Due to the inconsistency of 5-10% in the experimental chamber pressure data, these results are interpreted as indication that the pressure measurement in Shot 51 at the D138 location is more accurate. Therefore, the comparison of the model prediction and experiment for the 5 liter repeatability series is based on Shot 51.

In order to model the effects of propellant accumulation, the droplet profile shown in Table 6 is developed, using the pressure recorded for Shot 51 at the D138 location. The droplet sizes are not significantly different than those in the 2 liter repeatability droplet profile in Table 5 up to 40 MPa, but are substantially larger than those in Table 4, which gave the best overall agreement with the experimental data. The higher chamber pressure in the 5 liter shots requires an extended profile. Comparisons of the model predictions using Table 6 with experimental data from Shot 51 are presented in Figures 59-63. The agreement of chamber and liquid pressures in Figure 59 is good, while the piston travels in Figure 60 show some deviation. The agreement of damper pressures in Figure 61 is reasonable, except at peak pressure where a difference of approximately 15% is seen. The experimental and predicted projectile travel curves in Figure 62 deviate at the beginning of motion; but the comparison in Figure 63 of pressure curves at the B1 gage location, the only recorded barrel gage in this test, shows good agreement both in time of projectile arrival and magnitude of the pressures. It is again assumed that the shot start pressure acts over 1.5 times the length of the obturating band. Overall, the comparisons between the model predictions and

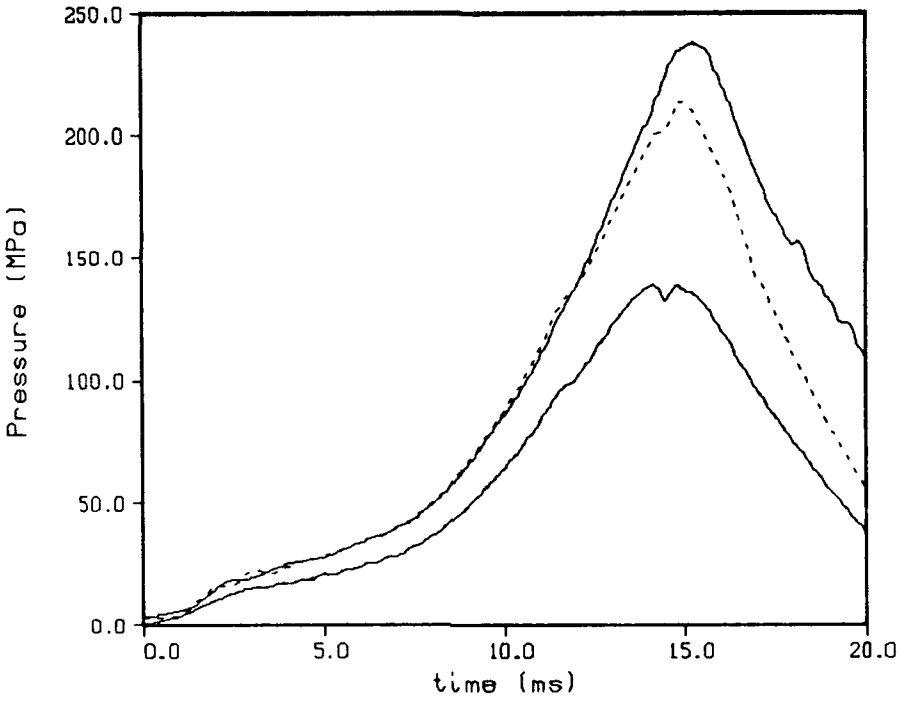

Figure 57. Liquid Pressure and Chamber Pressure - Round 48 (line). Liquid Pressure From Model With Chamber Pressure D138 (dot).

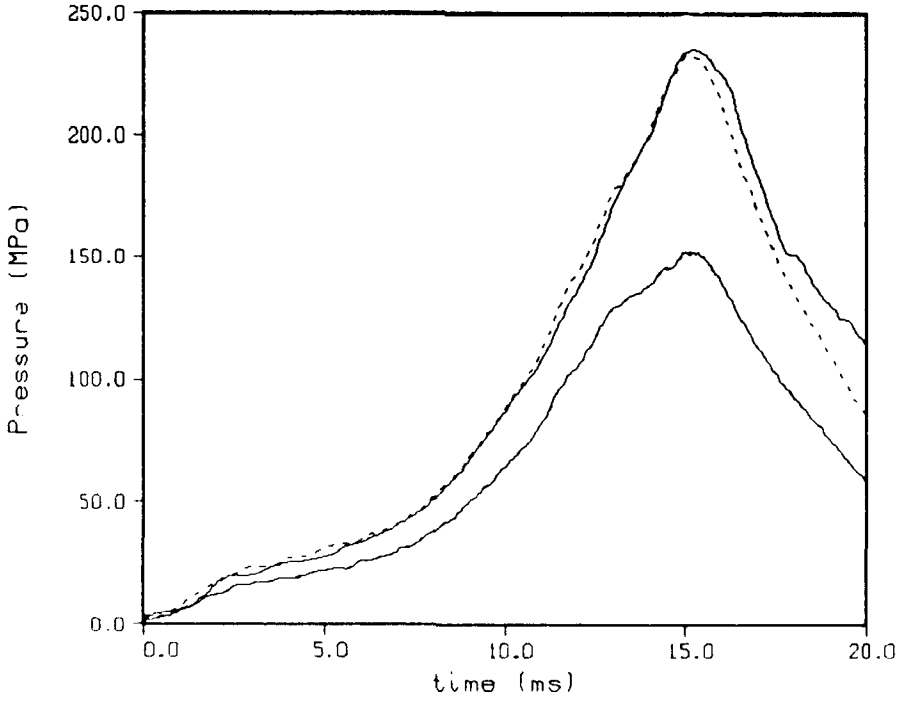

Figure 58. Liquid Pressure and Chamber Pressure - Round 51 (line). Liquid Pressure From Model With Chamber Pressure D138 (dot).

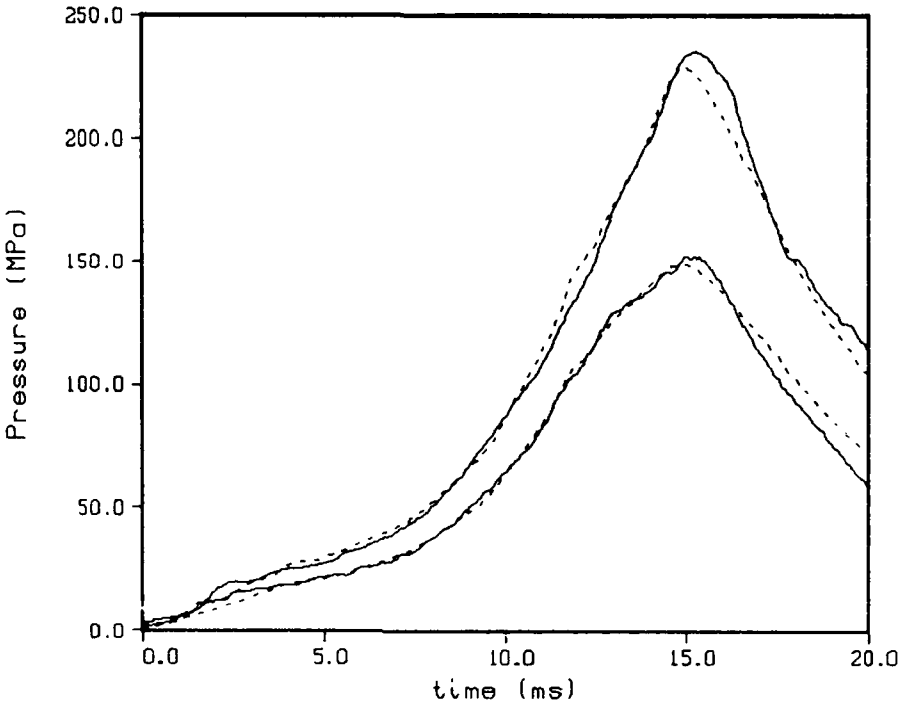

Figure 59. Liquid Pressure and Chamber Pressure - Round 51 (line). Model With Droplet Burning (dot).

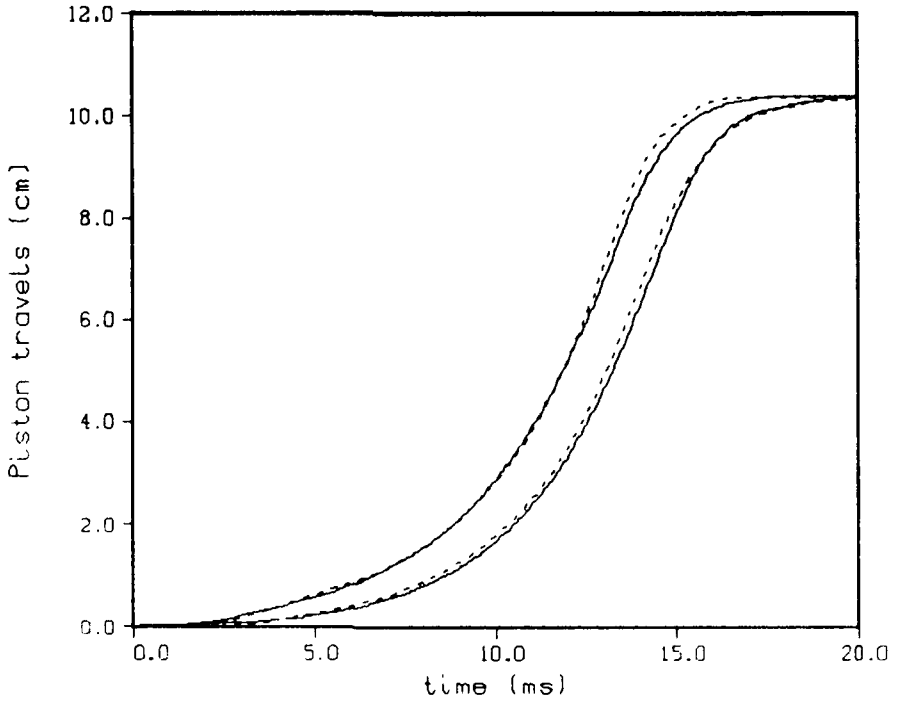

Figure 60. Piston Travel - Round 51 (line). Model With Droplet Burning (dot).

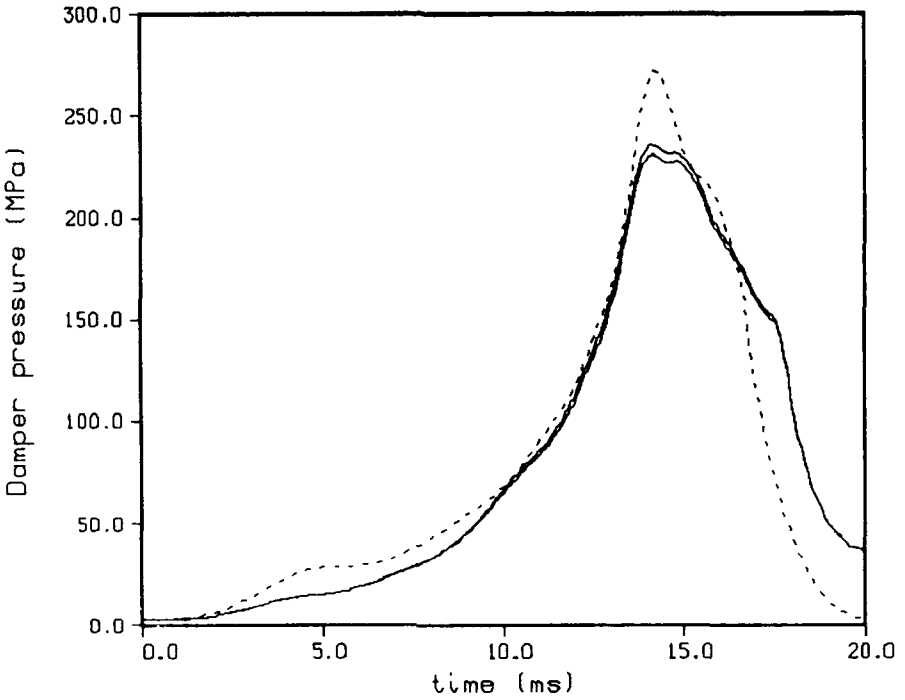

Figure 61. Damper Pressure - Round 51 (line). Model With Droplet Burning (dot).

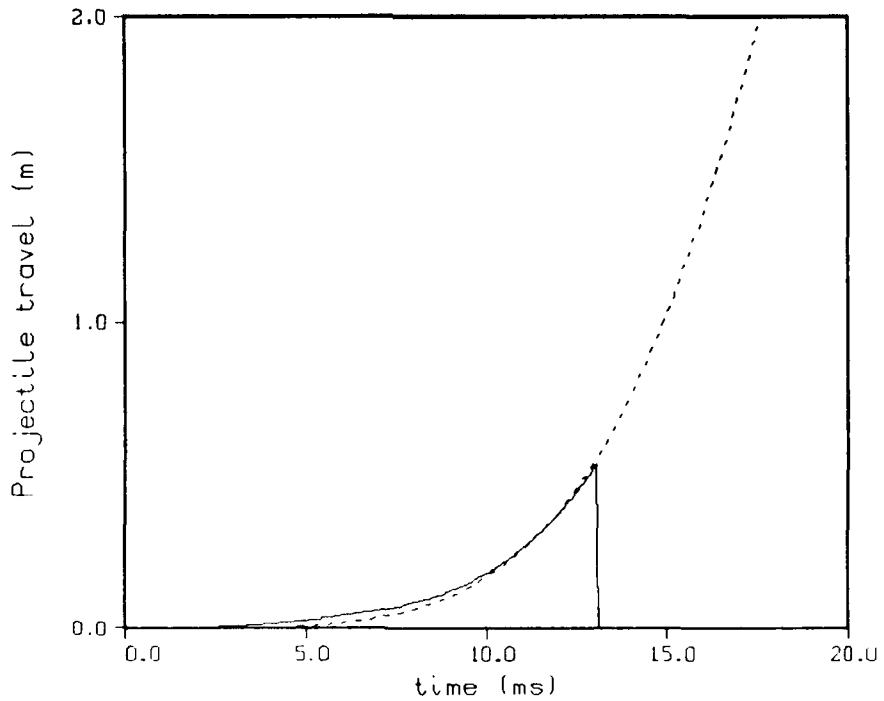

Figure 62. Initial Projectile Travel - Round 51 (line). Model With Droplet Burning (dot).

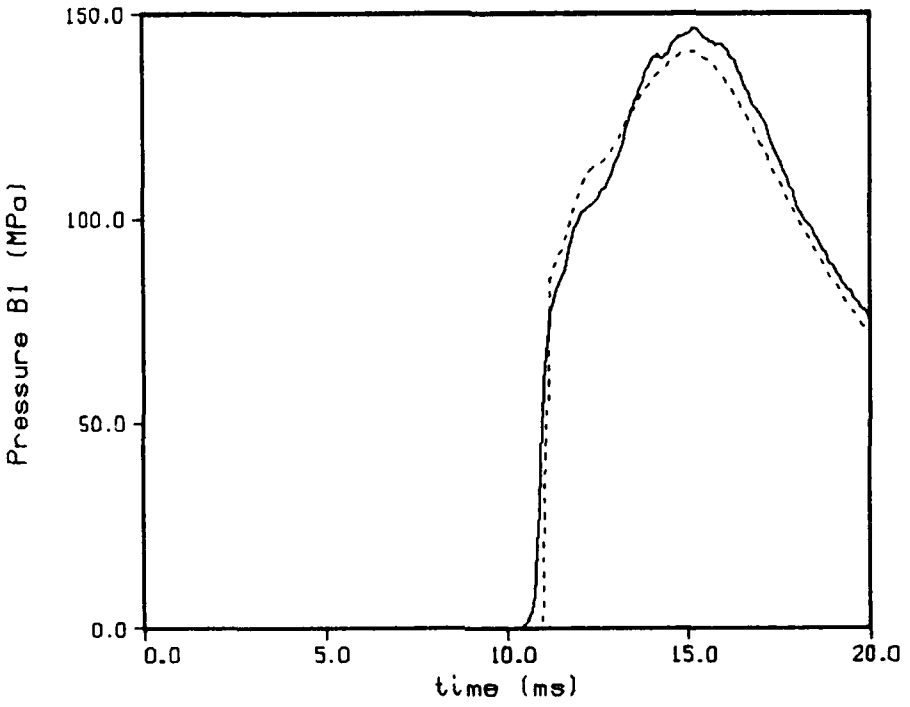

Figure 63. Barrel Pressure, Gage B1 - Round 51 (line). Model With Droplet Burning (dot).

Table 6. Round 51 Mean Droplet Diameter Profile Derived From Chamber Pressure Recorded at Gage D138

Chamber pressure, MPa	Droplet diameter, μm
0.0	300
30.0	300
40.0	200
50.0	200
60.0	100
70.0	100
100.0	25

experiment show more discrepancies than earlier efforts. The major difference is in the predicted and experimental damper maximum pressures.

In order to evaluate possible causes of the differences between the model and experimental damper pressures in Shot 51, a number of hypotheses are examined. The first involves the calculation of the damper vent area. In the model, the vent area is calculated as the minimum flow area between the bushing on the transducer block and the contoured damper rod, as shown in Figure 64. Thus, the location of the defining point on the bushing is initially taken as point A. As the rod moves to the left (the bushing is stationary), the defining point on the rod is relocated to point B due to the curvature of the rod. The changeover location occurs near the maximum vent area (minimum bolt radius) when the areas at points A and B are the same. At that time, the location of the maximum vent area is assumed to instantaneously move the 0.16 cm from point A to point B. This assumption is of interest since this transition occurs near peak damper pressure, and the true maximum vent area which occurs between points A and B is not reached in the model with the redefinition of the vent. Removing the assumption and defining the flow area only in terms of point A, however, produced only minor changes in the damper pressure. Thus, the method of calculation of the vent area does not explain the difference between the model prediction and experiment.

As a second approach, it was hypothesized that the damper control rod geometry is inaccurate. The computer model is applied with the recorded chamber pressure at the D138 location in Shot 51 as a boundary condition. The damper exit area near peak damper pressure is then adjusted to attempt to match the experimental data. Figure 65 is a comparison of the vent area computed from the engineering drawings and that required to match the experimental damper pressure. Figure 66 shows the effect on the calculated damper pressure. The results in Figures 65 and 66 show that the vent area must be increased substantially, and as a result, the predicted end of stroke occurs too soon. If the experimental damper pressure is matched from the beginning of the firing cycle by adjusting the entire vent area profile, the result is a predicted end of stroke which occurs much too soon. If the experimental damper pressure is matched from the beginning of the firing cycle by adjusting the entire vent area profile, the result is a predicted end of stroke which occurs much too soon, as shown in Figure 67. Thus, the maximum predicted damper pressure can be lowered to agree with the experiment by increasing the damper vent area, but this change adversely impacts the piston motion. It appears that, if the recorded chamber pressure is accurate, the recorded damper pressure may be too high. It is also possible that the model is not correctly capturing the

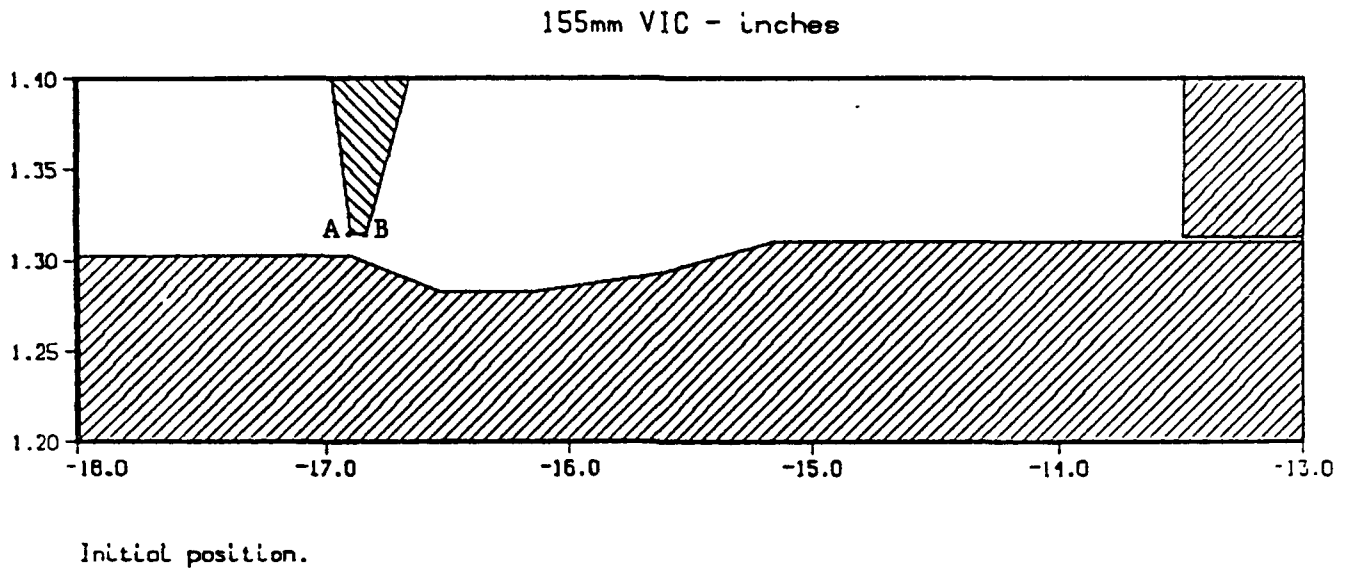

Figure 64. Damper Control Rod and Bushing in Initial Position.

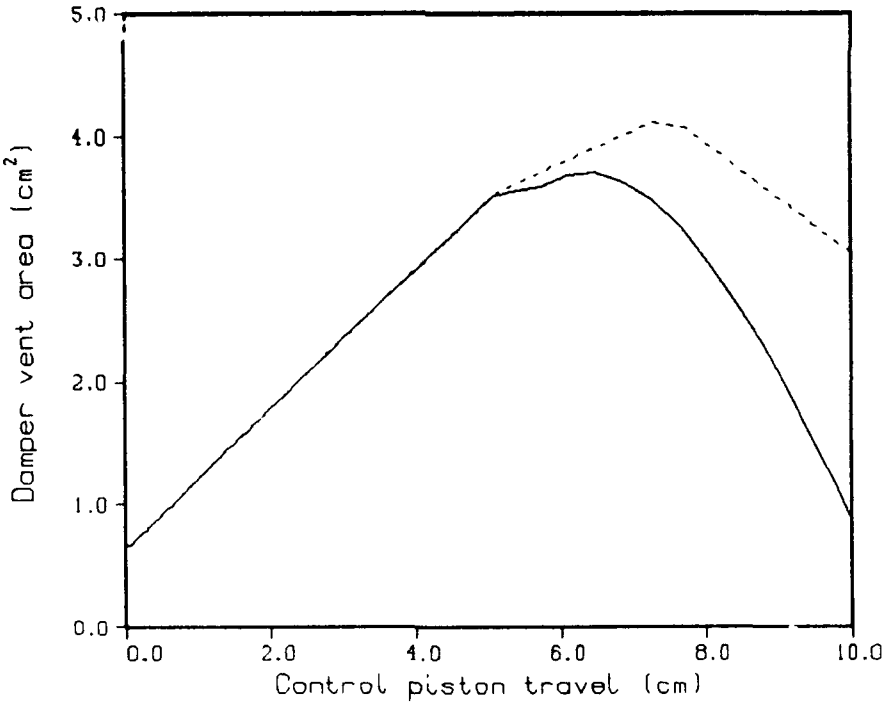

Figure 65. Vent Area - Engineering Drawings (line). Computed From Gage D138 (dot).

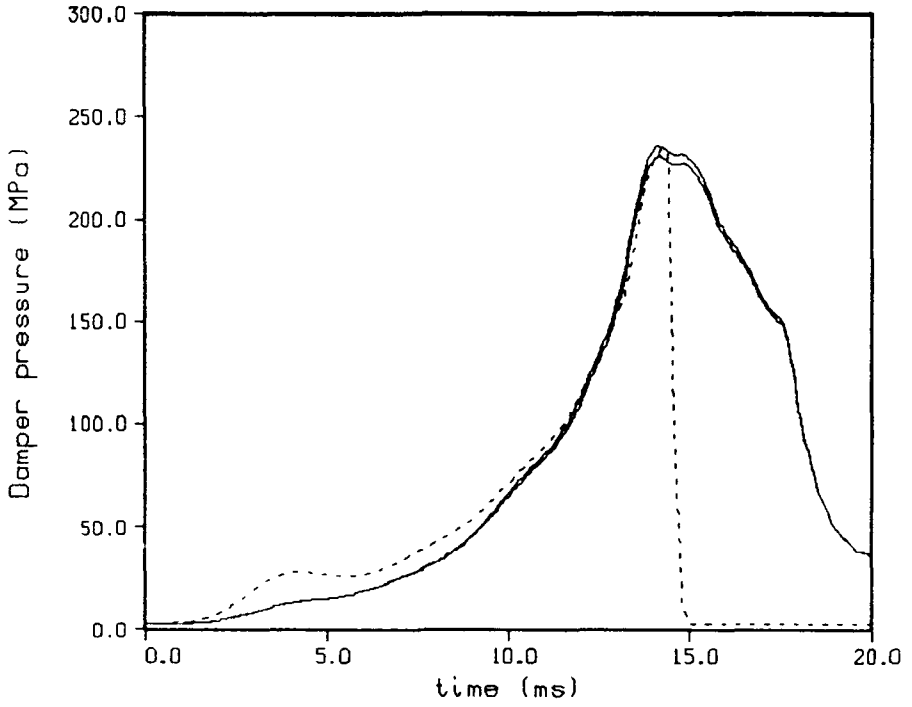

Figure 66. Damper Pressure - Round 51 (line). Computed From Gage D138 (dot).

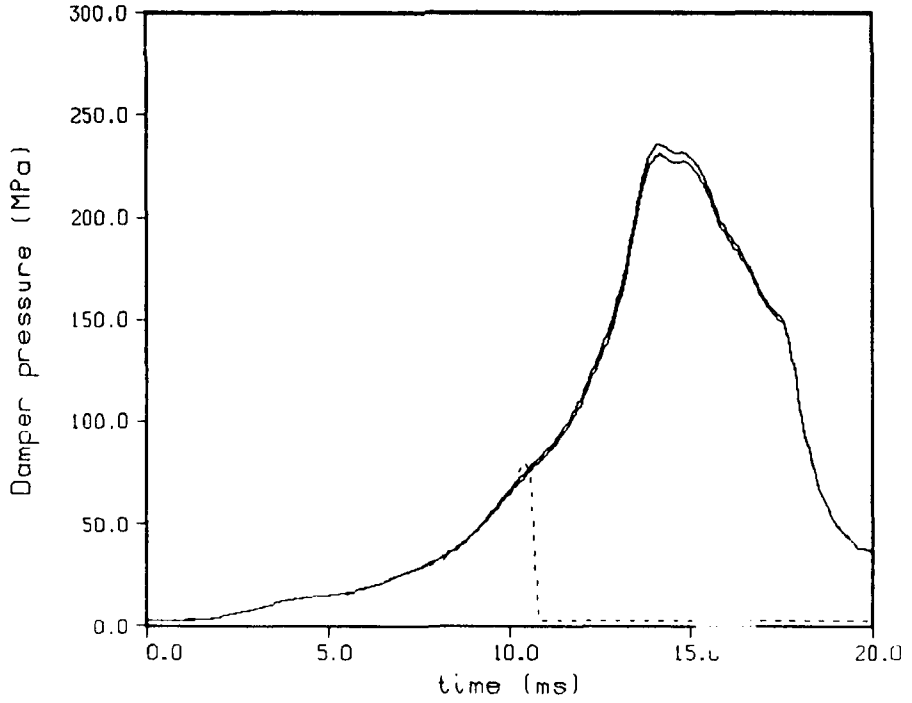

Figure 67. Damper Pressure - Round 51 (line). Using Vent Area Computed From Gage O90 (dot).

complicated feedback between the damper and chamber pressures. The chamber pressure is found to be consistent with liquid pressure in Figure 58. Although the predicted damper pressure typically deviates from the experiment more than other measurements, damper pressure predictions do not exhibit as large a pressure deviation in any other shot from the 30 mm, 105 mm, and 155 mm firings.

As another hypothesis, it is assumed that the damper pressure gage is miscalibrated. The result of multiplying the experimental damper pressure by 1.15 and then comparing it to the model prediction is shown in Figure 68. The agreement is now much improved. However, no firm conclusion can be drawn from this result.

As a final hypothesis, GE[16] speculates that the higher calculated peak damper pressure is attributable to excluding damper compliance in the damper pressure calculation. As the damper wall expands at high pressures, the measured damper pressure lowers. In the GE code, an effective bulk modulus is calculated to account for the damper compliance. Our analysis has indicated that this correction is small and is not sufficient to explain the difference between experimental and model damper pressures.

In summary, no satisfactory explanation was found for the difference in predicted and experimental damper pressures shown in Figure 61. It has been assumed that simple Bernoulli flow, with a constant value of 0.95 for the discharge coefficient, is sufficient to describe the flow in the damper vent. This hypothesis has proven reasonable for similar configurations. It is possible that a complex discharge coefficient model is required due to the sharp corner on the bushing and to the contour of the rod. (Note that a variable discharge coefficient only at maximum pressure would require a value greater than 1.0 to match experimental data, since the model pressure is too high.) Although the plateau in the experimental data near peak damper pressure appears physically meaningful, no mechanism is identified to match the recorded experimental pressure curve with the given geometric description.

8. GE 155 MM GUN FIXTURE - 5 LITER shot 58

In order to evaluate the effectiveness of a hybrid igniter, the 155 mm Concept VIC fixture was employed in the configuration used in the 5 liter repeatability series. An external solid propellant igniter was used in all Concept VIC firings before shot 57. In preparation for a totally liquid

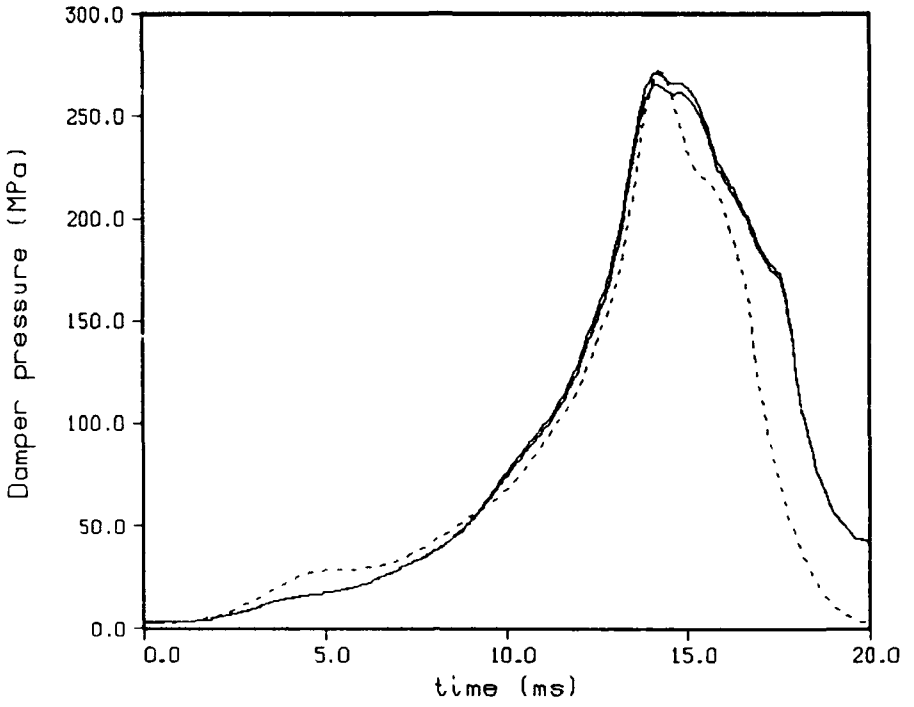

Figure 68. Damper Pressure - Round 51 times 1.15 (line). Model With Droplet Burning (dot).

propellant igniter, an intermediate hybrid (also called a two-stage) igniter was tested. The hybrid igniter consists of a small external solid propellant charge, which vents into the gun tube just behind the initial position of the projectile, and an unrestrained liquid propellant puddle (also called a pre-positioned charge) in the bottom of the combustion chamber. The pre-positioned charge is introduced into the chamber through the fill lines in the transducer block just before the pistons are sealed and the liquid reservoir is filled. The liquid igniter fill has the added benefit of flushing the liquid reservoir. Other than the change in the igniter, the gun configuration is identical to that used in 5 liter repeatability series.

The igniter model implemented in the code is simple. An option is added to the gun code to allow liquid droplets to be initially introduced into the chamber. The size of the liquid droplets and the burning rate of the propellant determine the initial pressure rise rate. The burning rate and the thermochemistry of the "igniter" droplets are taken to be the same as those of the propellant injected from the reservoir.

A comparison of chamber pressures for shot 51 using the solid propellant igniter and shot 58 using the hybrid igniter is shown in Figure 69. The gage D138 record was lost at about 10 ms in shot 58. However, the initial pressure rise in shot 58 is much more rapid than in shot 51, apparently due to the energy release directly in the chamber. The totally solid propellant igniter vents through a long, narrow passage; and igniter gases experience high heat loss. The rate of pressure rise with the hybrid igniter indicates fast, efficient combustion of the liquid puddle. The input parameters for the model for shot 58 are identical to those of shot 51, except for the solid propellant primer and the droplet profile. The droplet profile is modified as a result of propellant being injected from the reservoir into a hotter and higher pressure chamber environment. A comparison between the droplet profiles is shown in Table 7 and Figure 70. Since the droplet profiles are strongly affected by small changes in the igniter, damper, and projectile shot start pressure, the droplet sizes should not be interpreted literally. However, the comparison indicates more efficient combustion in shot 58, reflecting the differences in chamber pressures.

Table 7. Round 58 and Round 51 Mean Droplet Diameter Profiles

Round 51		Round 58	
Chamber pressure, MPa	Droplet diameter, μm	Chamber pressure, MPa	Droplet diameter, μm
0.0	300	0.0	300
30.0	300	25.0	300
40.0	200	50.0	100
50.0	200	75.0	75
60.0	100	100.0	20
70.0	100	125.0	10
100.0	25	150.0	1

Comparisons of model simulation and experimental data for shot 58 are shown in Figures 71-74. The chamber and liquid pressures in Figure 71 are in good agreement. The predicted control piston travel in Figure 72 shows a comparatively large deviation from the experimental travel, although the injection piston travels agree well. Errors in either the chamber pressure or the predicted damper pressure are possible. The comparison of experimental and

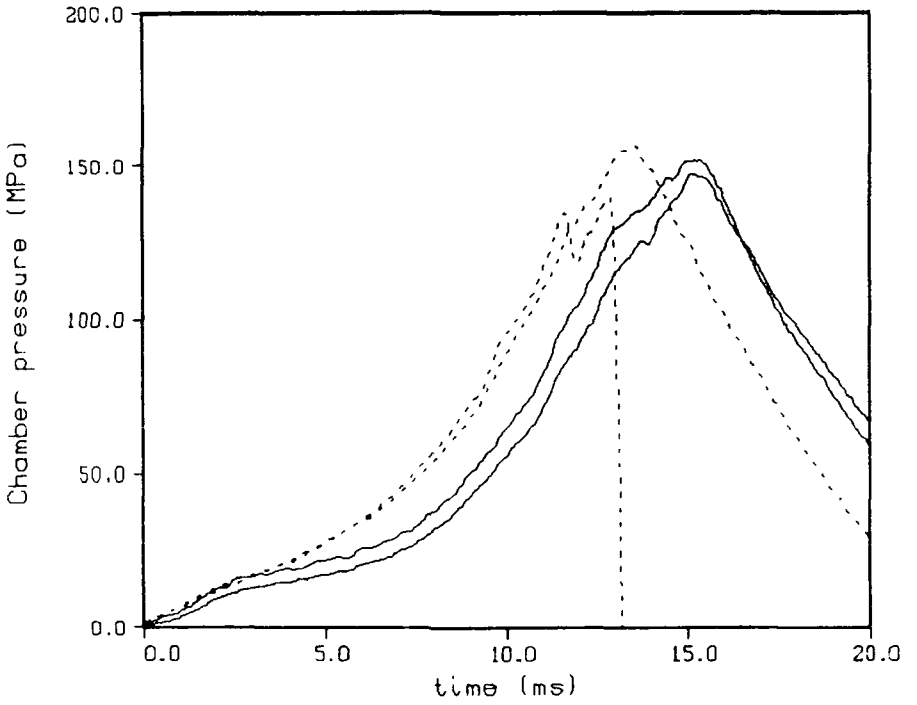

Figure 69. Experimental Chamber Pressure - Round 51 (line). Round 58 (dot).

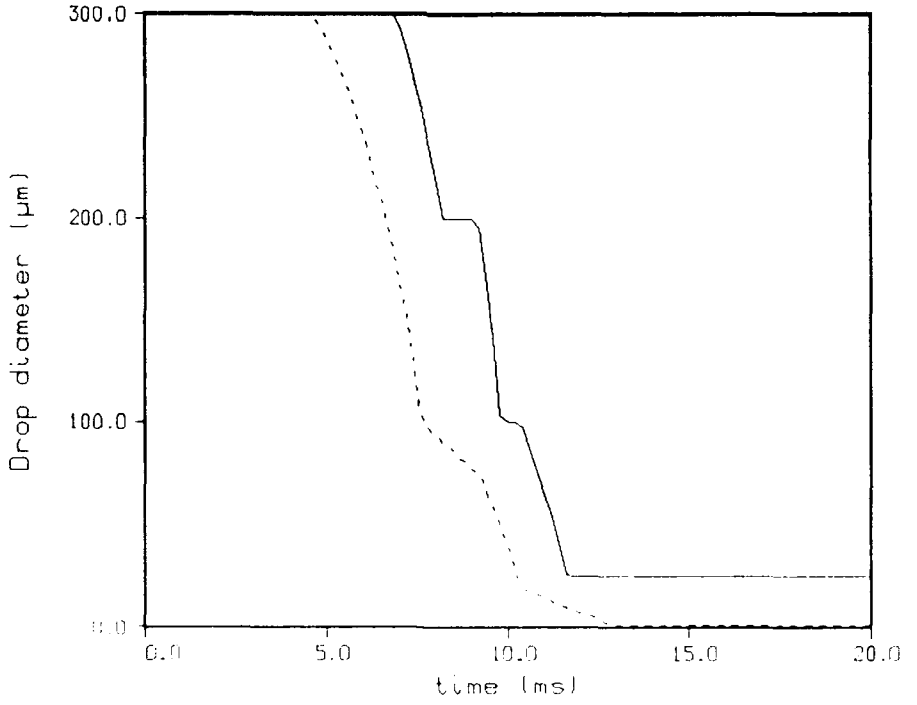

Figure 70. Droplet Profile - Round 51 (line). Round 58 (dot).

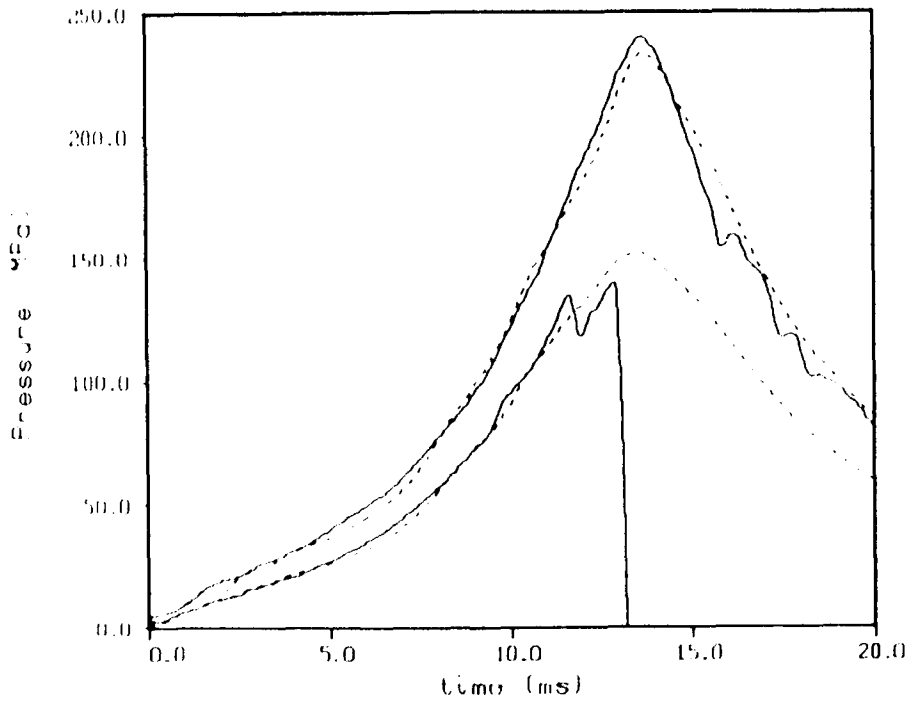

Figure 71. Liquid Pressure and Chamber Pressure - Round 58 (line), Model With Droplet Burning (dot).

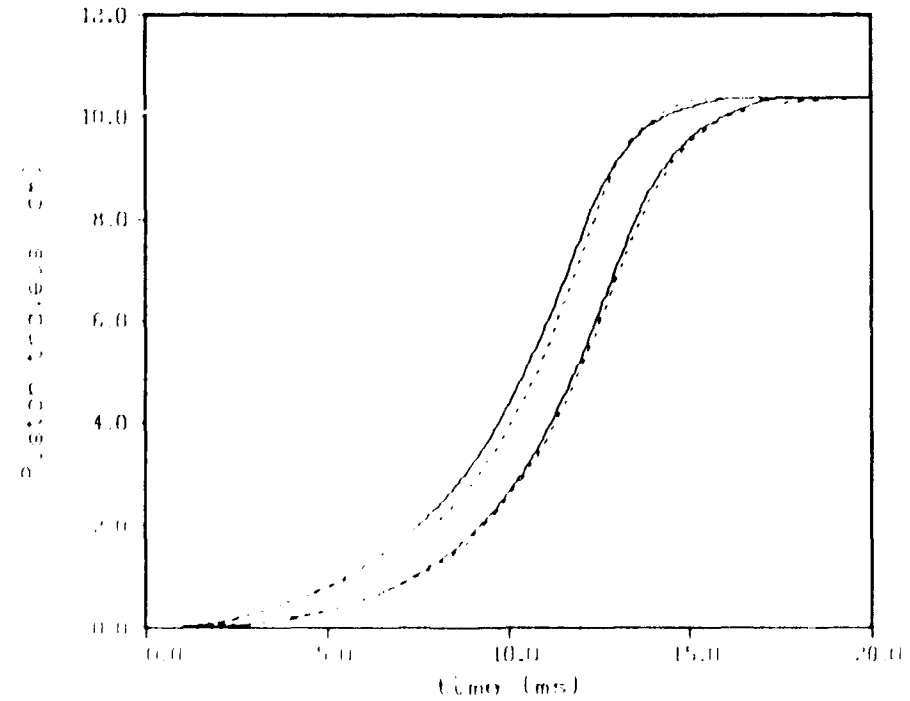

Figure 72. Piston Travel - Round 58 (line), Model With Droplet Burning (dot).

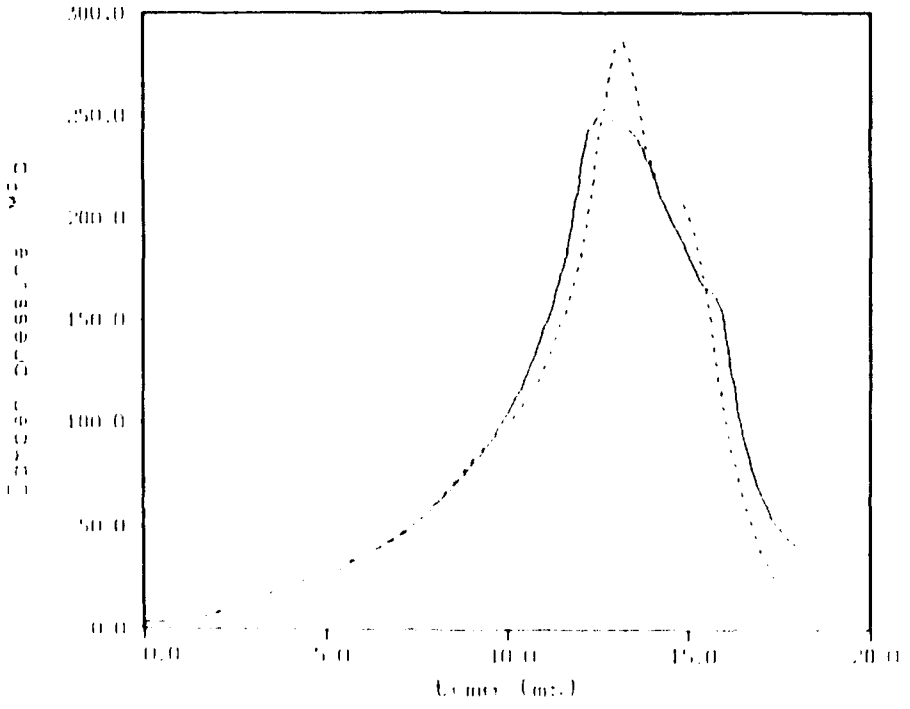

Figure 73. Damper Pressure - Round 58 (line), Model With Droplet Burning (dot).

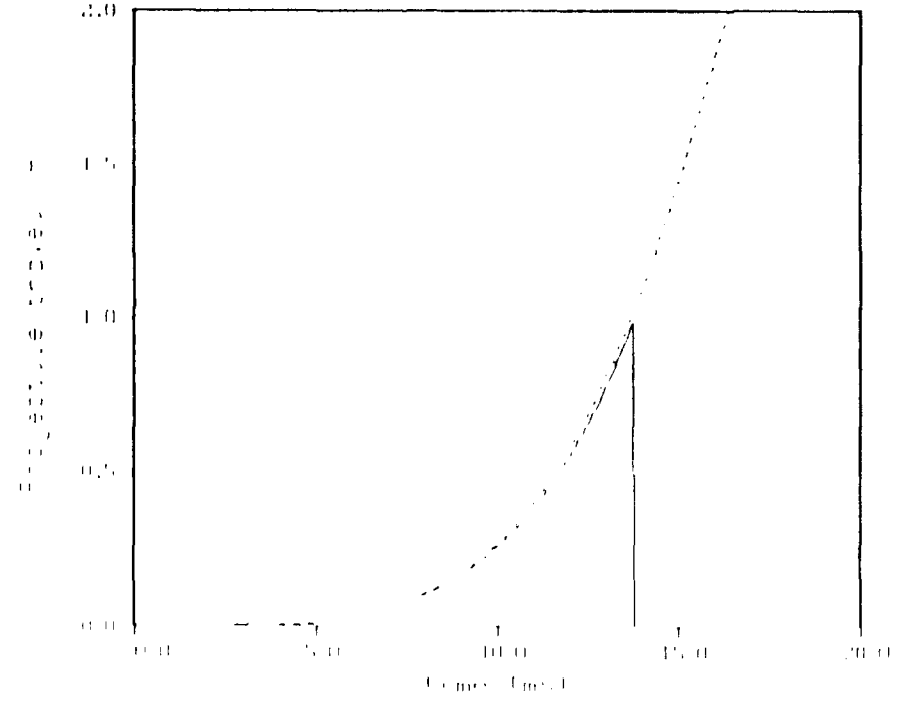

Figure 74. Initial Projectile Travel - Round 58 (line), Model With Droplet Burning (dot).

predicted damper pressures is shown in Figure 73. Not unexpectedly, the predicted damper pressure is high compared to the experiment at peak pressure as in Shot 51. The early predicted and experimental projectile travels shown in Figure 74 are in reasonable agreement. The experimental velocity at 200 inches is 596 m/s, vs. a predicted velocity of 597 m/s.

The hybrid igniter appears to provide enhanced gun ignition and more efficient combustion of the injected liquid propellant. A simple igniter model is sufficient to model the hybrid igniter. The resulting comparisons between the model prediction and experiment are similar to previous results.

9. GE 155 MM GUN FIXTURE - 7 LITER SHOT 65

Shot 65 is part of a 7 liter characterization series consisting of rounds 62-65. The gun configuration is similar to that used in the 5 liter firings. The transducer block is moved rearward to accommodate the additional liquid in the reservoir, resulting in a longer piston travel. The hybrid igniter is used with slightly less liquid propellant in the pre-positioned charge (liquid puddle) than for Shot 58. The initial chamber volume and pistons are unchanged from the 5 liter repeatability series. The damper rod is extended by inserting a 1.75 inch straight section near the middle of the piston stroke to accommodate the longer piston travel.

The droplet profile shown in Table 8 is developed based on the experimental chamber pressure recorded at the D33 location, since the signal from pressure gage D138 was apparently lost later in the ballistic cycle. Initial analyses, based on the experimental chamber pressure and projectile displacement, indicated that the shot start pressure must be doubled from 10.0 MPa in the 5 liter test series to 20.0 MPa in the 7 liter series, even though the projectiles are all M107 projectiles, and the initial chamber pressure rise rates in the two experiments are similar. As before, the shot start pressure is applied over 1.5 times the length of the obturating band, a total of 3.81 cm to obtain reasonable comparison with the experimental data. This will be discussed in more detail below. The comparisons between the model predictions and experiment are presented in Figures 75-80.

The comparison of predicted and experimental chamber pressures in Figure 75 shows good agreement up to peak pressure, with the usual deviation during the expansion phase. The model does not predict the flattened chamber pressure curve near peak pressure. The gage with the higher

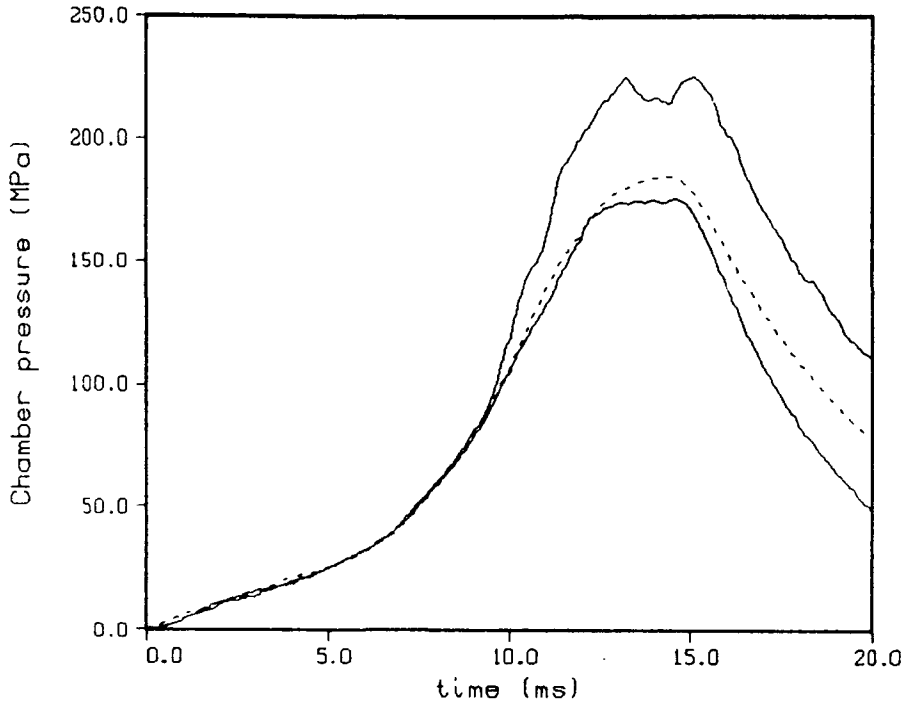

Figure 75. Chamber Pressure - Round 65 (line). Model With Droplet Burning (dot).

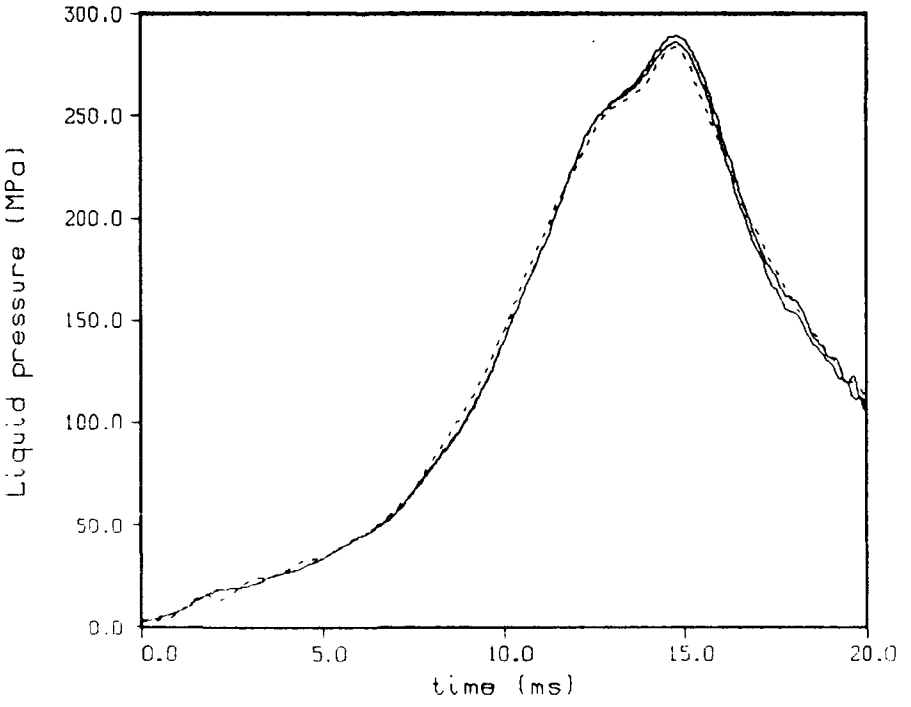

Figure 76. Liquid Pressure - Round 65 (line). Model With Droplet Burning (dot).

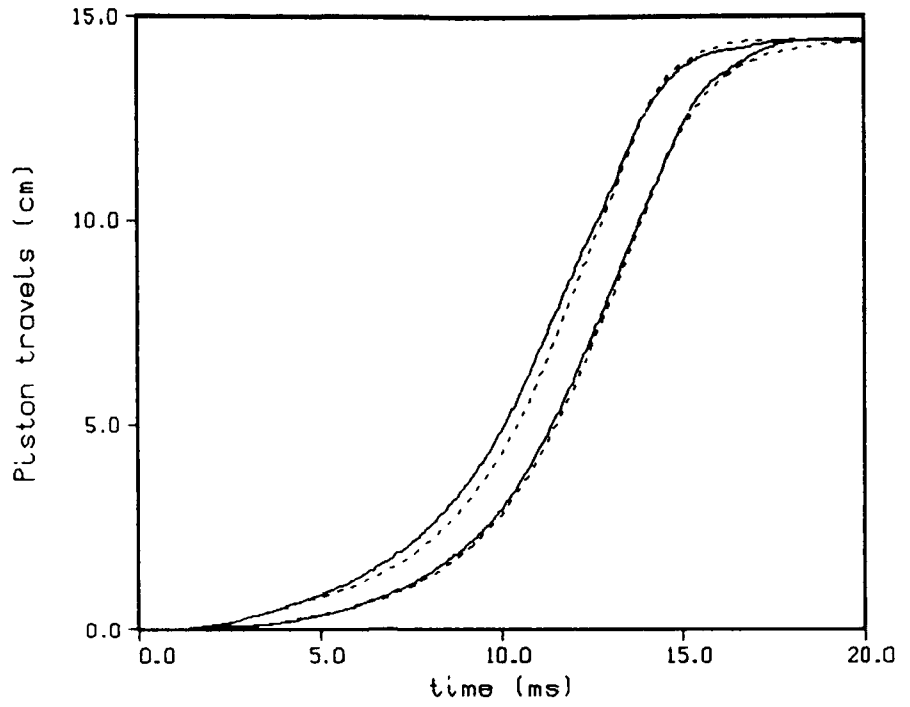

Figure 77. Piston Travel - Round 65 (line). Model With Droplet Burning (dot).

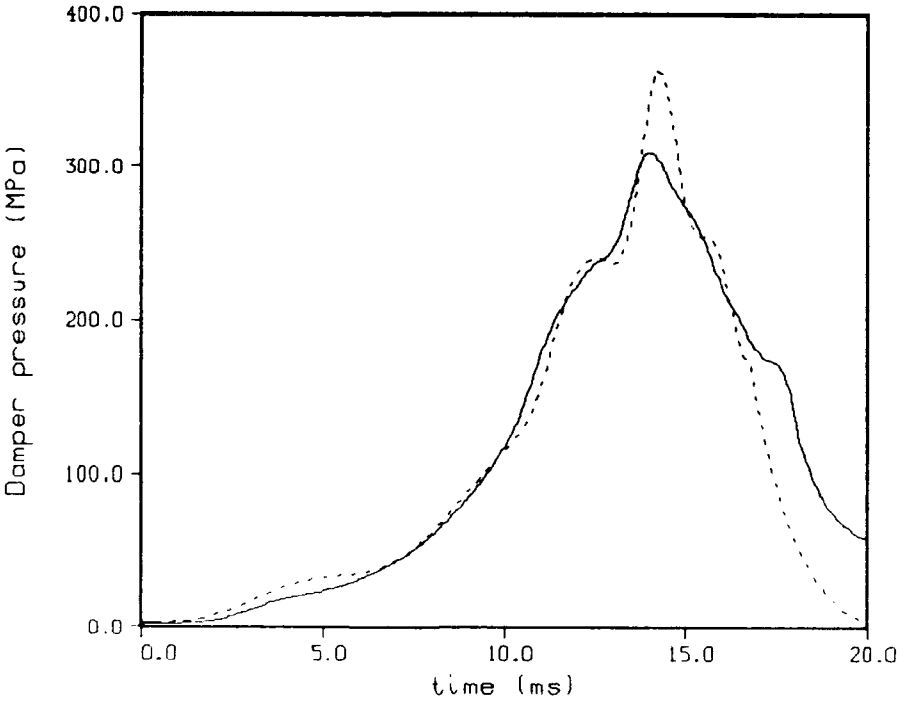

Figure 78. Damper Pressure - Round 65 (line). Model With Droplet Burning (dot).

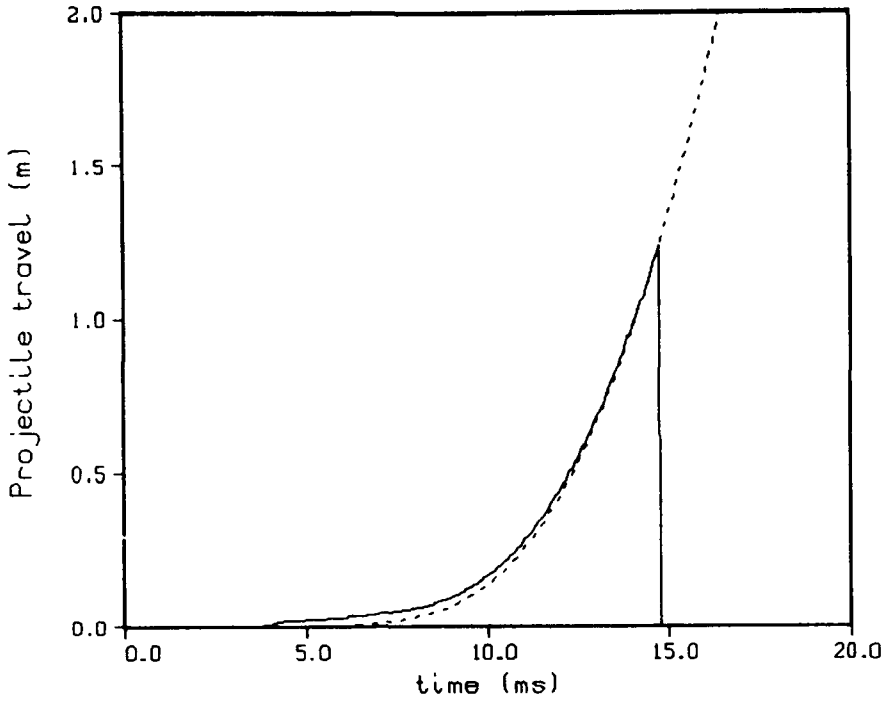

Figure 79. Initial Projectile Travel - Round 65 (line). Model With Droplet Burning (dot).

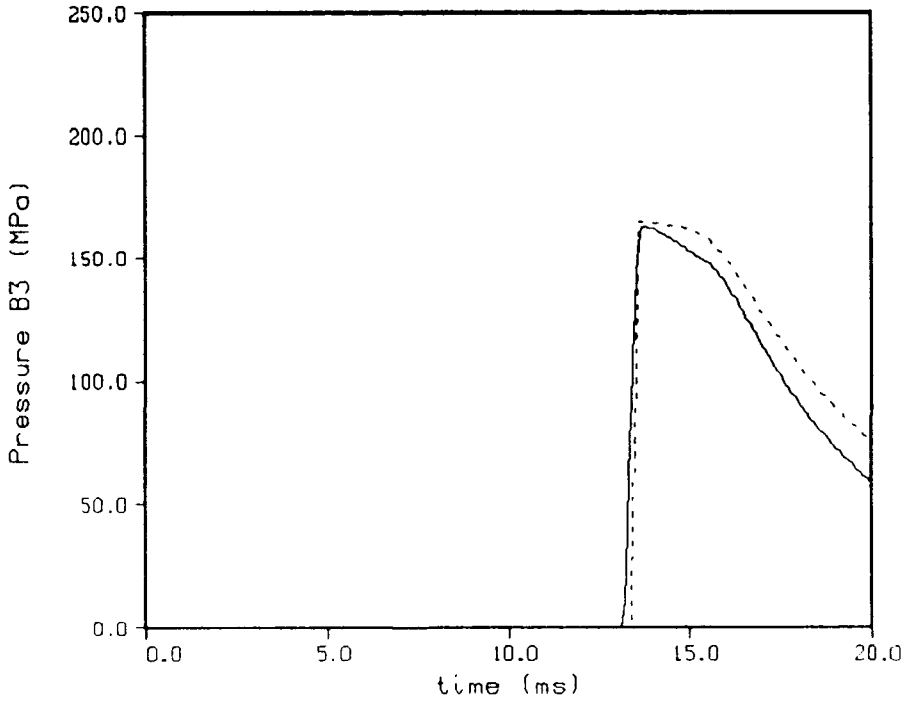

Figure 80. Barrel Pressure, Gage B3 - Round 65 (line). Model With Droplet Burning (dot).

Table 8. Round 65 Mean Droplet Diameter Profile Derived From Chamber Pressure Recorded at Gage D33

Chamber pressure, MPa	Droplet diameter, μm
0.0	300
25.0	300
50.0	125
75.0	100
100.0	60
125.0	30
150.0	15

recorded pressure, D138, lost the pressure signal during the ballistic cycle. The agreement between predicted and experimental liquid pressures in Figure 76 is excellent. The injection piston travels, Figure 77, are in good agreement; however, there the control piston travels show some deviation. The same characteristic was noted in the 5 liter test series, shot 58. The predicted damper pressure in Figure 78 is in good overall agreement with experiment with an overpressure at peak. Predicted and experimental projectile travels, Figure 79, are in good agreement, although the early projectile motion in the experiment occurs somewhat sooner. The one recorded barrel gage B3 comparison in Figure 80 is good. The experimental muzzle velocity is 683 m/s at 200 inches of travel, while the predicted velocity is 682 m/s.

The flattened chamber pressure curve in Figure 75 has not been observed in experimental data since medium caliber testing early in the liquid propellant program. It is due to the straight section on the damper rod which allows the system to reach a near steady state condition. The regenerative pistons pass the straight section on the control rod just before the plateau in the chamber pressure and achieve a near steady state condition during the travel over this straight section. As the damper vent area begins to close, the piston momentum maintains the equilibrium condition for a short time. The control piston then decelerates in response to the decreasing vent area, and the injection piston momentum causes the sharp rise in the liquid pressure at approximately 15 ms (see Figure 76). As the injection piston decelerates, the injection area is reduced, and chamber pressure decreases.

The hybrid igniter appeared to function well in the 7 liter test as it did in the 5 liter Shot 58. The only anomalies in the data are the increased projectile shot start pressure and higher amplitude pressure oscillations than previously observed, particularly in the damper. The pressure oscillations will not be discussed in this report and are the subject of a separate, ongoing investigation.

10. FURTHER MODELING - PREDICTION OF 7 LITER, SHOT 65

Although the model results presented above demonstrate excellent agreement with the experimental data, values of the empirical parameters, discharge coefficients for the reservoir, and the damper and the mean droplet diameter size distribution are derived from the experimental data. A longer-term goal of the liquid propellant interior ballistic modeling program is prediction of performance for untested gun designs. Therefore, it is desirable to obtain values of these parameters which are independent of a particular fixture. Thus, parameters derived for the 5 liter, Shot 58 are used in a simulation of the 7 liter, Shot 65.

A constant value of 0.95 for the discharge coefficient for both the liquid reservoir and the damper was used in all the 155 mm modeling. The droplet profile for the 5 liter igniter, Shot 58, is used since the igniter is similar and vents into the same volume in both fixtures. The prediction is then not dependent on the igniter model. The results are shown in Figure 81 using the droplet size distribution in Table 7. The initial chamber pressures, which are due primarily to the igniter, agree well as expected, but the predicted and experimental pressures deviate at 5.0 ms. The subsequent predicted pressure rise is too slow, and although the maximum pressures are within 5%, the shape of the curve is incorrect. The predicted velocity at 200 inches of projectile travel is 660 m/s, while the experimental velocity is 683 m/s, a difference of -3.4%.

The inconsistency can be traced to the early projectile motion. Although the initial chamber pressure rise rate due to the igniters is similar, as shown in Figure 82, the early projectile motion varies considerably. Shown in Figures 83 and 84 are the experimental projectile travels derived from radar for Shots 58 and 65 vs. chamber pressure and time, respectively. The two projectiles are "identical" and yet behave quite differently. The model uses a resistive pressure determined by applying a constant shot start value over the first 3.81 cm of travel, the first small segment of the curves in Figures 83 and 84. A constant shot start value of 10 MPa simulates Shot 58 well, but a shot start pressure of 20 MPa is needed to simulate Shot 65. It is not apparent why the resistive profiles are so different between these two shots. The physical mechanism for the difference is not apparent and is the subject of current study.

However, if the change in projectile shot start pressure is recognized by the model, the result of the prediction of shot 65 from shot 58 is much improved, as shown in Figure 85. The predicted and experimental chamber pressures are now in better qualitative agreement. The comparison at peak pressure is about the same as in Figure 81, (0.7%). The predicted projectile velocity at 200 inches of travel is now 687 m/s compared to an experimental value of 683 m/s, a difference of +0.6%. Thus, the projectile resistive pressure has an impact on the predicted velocity and the shape of chamber pressure-time curve. While the impact is not surprising, the deviation in projectile resistive pressure must be quantified in order to achieve good predictive results.

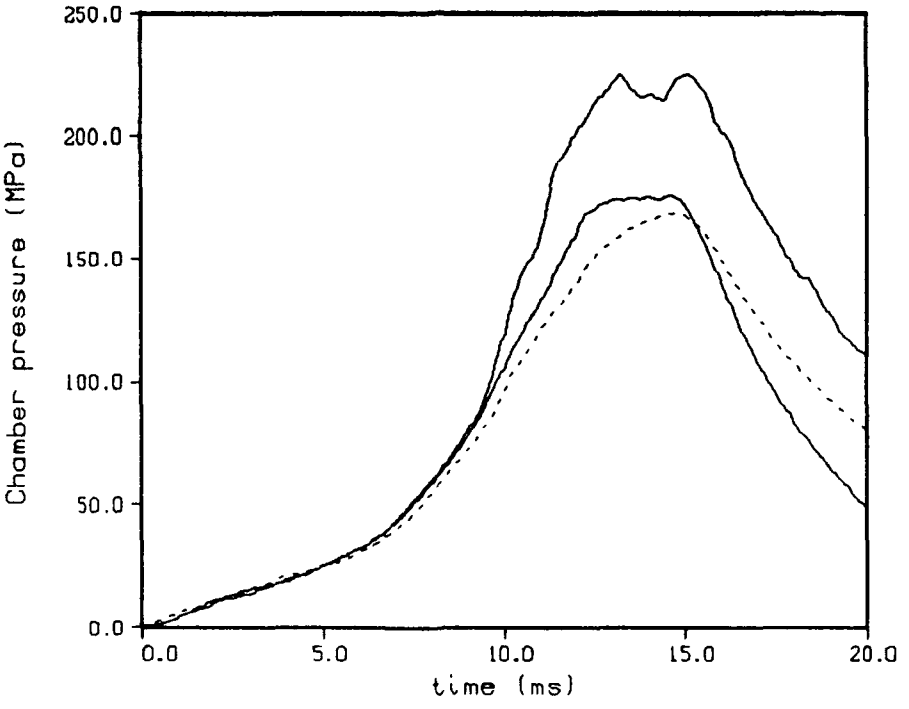

Figure 81. Chamber Pressure - Round 65 (line). Model With Droplet Burning, Shot Start Pressure of 10.0 MPa (dot).

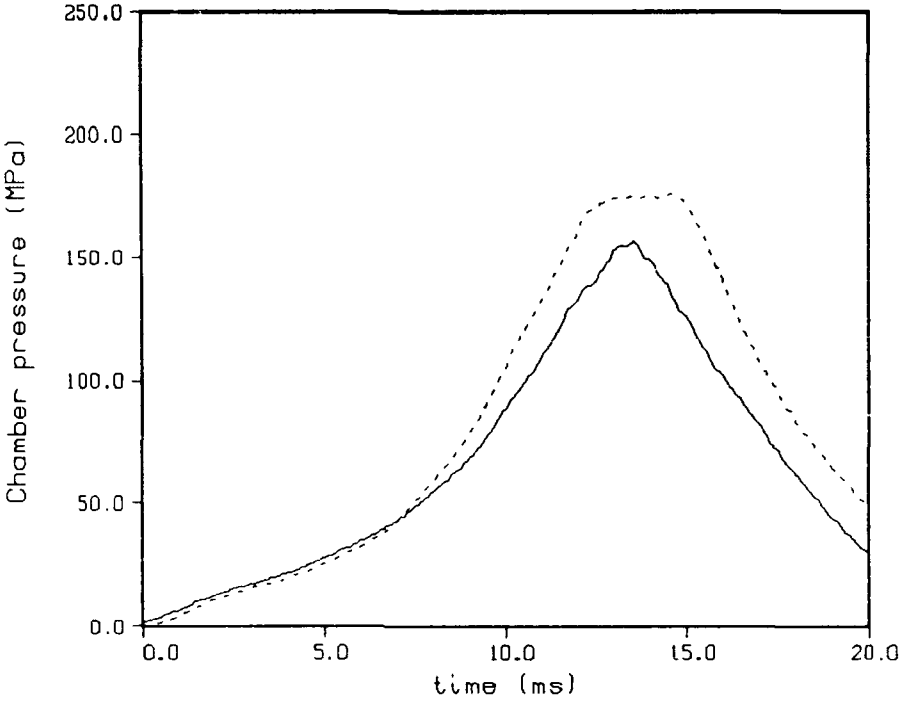

Figure 82. Chamber Pressure - Round 58, Gage D33 (line). Round 65, Gage D33 (dot).

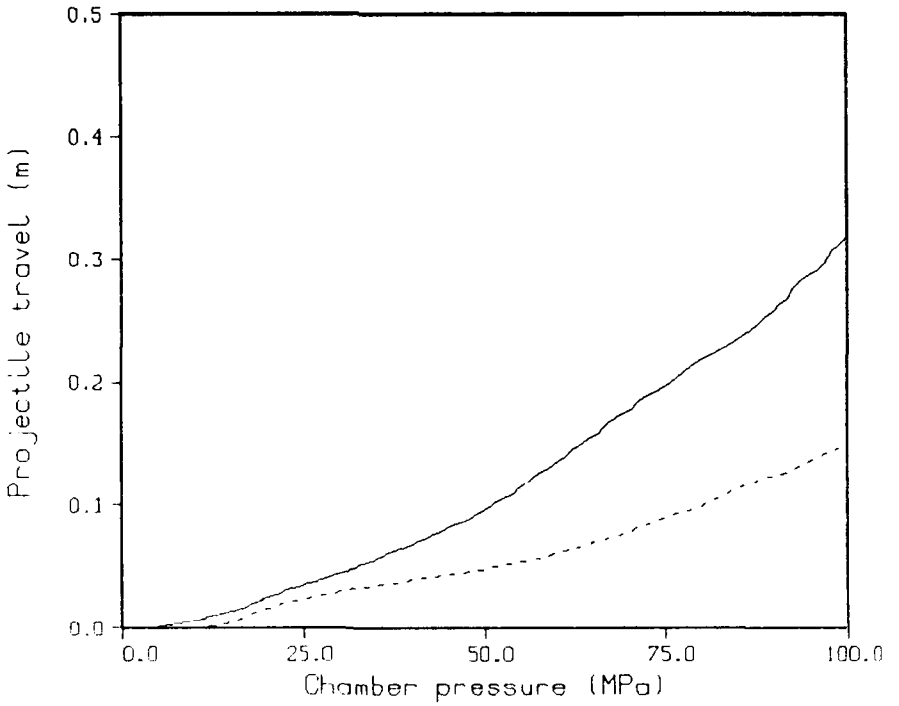

Figure 83. Initial Projectile Travel vs. Chamber Pressure - Round 58 (line). Round 65 (dot).

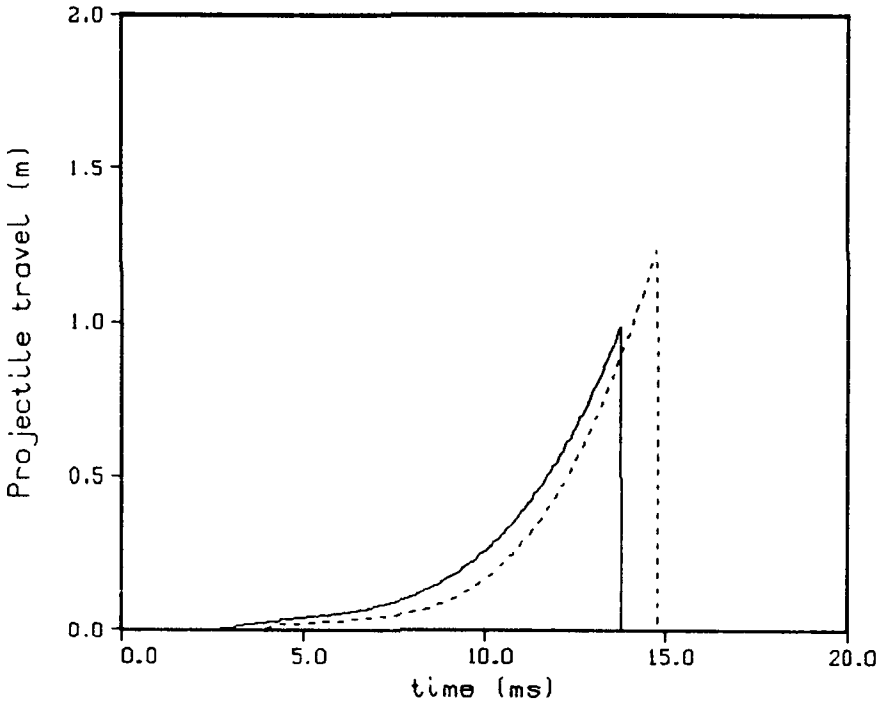

Figure 84. Initial Projectile Travel vs. Time - Round 58 (line). Round 65 (dot).

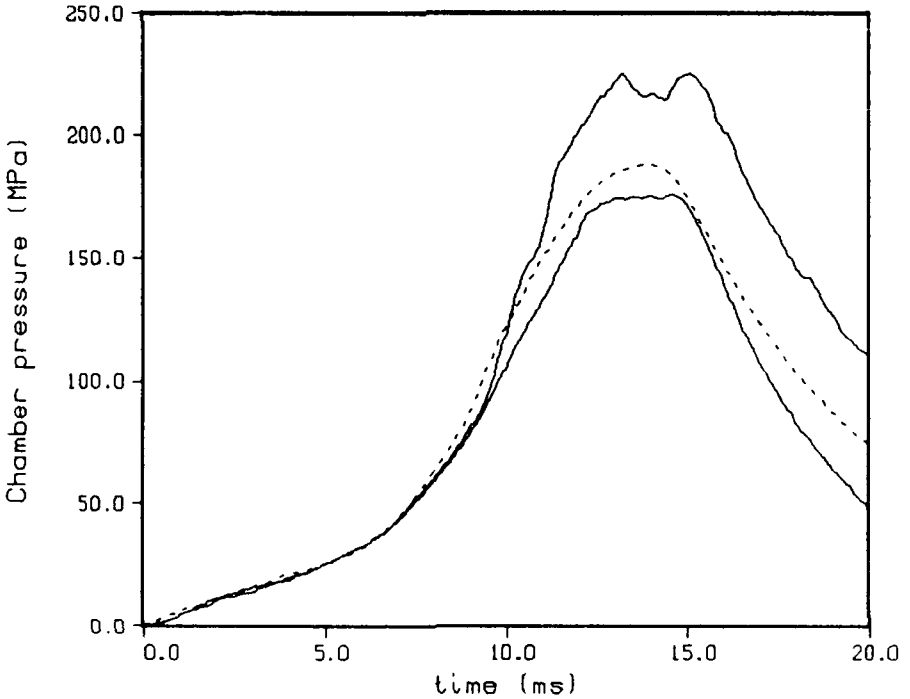

Figure 85. Chamber Pressure - Round 65 (line). Model With Droplet Burning, Shot Start Pressure of 20.0 MPa (dot).

11. CONCLUSIONS

A lumped parameter interior ballistic model has been developed for the Concept VIC regenerative liquid propellant gun, incorporating the major features of this configuration. Most of the required parameters are physical dimensions of the gun and properties of the propellant, which can be chosen without reference to experimental firing data. However, the parameters which must be fixed, based on analyses of gun test data, are the reservoir and damper discharge coefficients and the droplet diameter profile.

A constant reservoir discharge coefficient of 0.95 appears reasonable for all the 30 mm, 105 mm, and 155 mm Concept VIC firings studied thus far. The damper discharge coefficient is chosen to be 0.95 for all 155 mm cases studied and has varied from 0.6 to 0.95 in the 30 mm and 105 mm cases. It has been possible to assume a constant discharge coefficient for all the dampers studied, although the agreement between the model prediction and the experiment is least satisfactory in the comparison of damper pressures. It is suggested that the complicated flow pattern may lead to a variable discharge coefficient. However, the constant discharge coefficient assumption provides good overall agreement between the experiment and the model prediction. The mean droplet diameter also varies for each gun configuration. There are no obvious correlations for the droplet diameter profiles for the various gun configurations, but propellant injection and combustion are strongly influenced by the characteristics of the igniter, the damper, and the regenerative pistons, as well as the chamber pressure.

In general, the model can be used to match experimental data from 155 mm Concept VIC RLPG tests, using reasonable values for the empirical parameters.

In summary, the following observations seem appropriate:

(1) Discrepancies within a given experimental data set, particularly in chamber pressure measurements and even between pressure gages in the same plane, make accurate comparisons between the model predictions and experiment difficult. The source of these discrepancies is unknown; however, many gages show deviation early in the ballistic cycle.

(2) Overall, simulations of the 155 mm Concept VIC are in good agreement with experimental data. However, in order to develop a predictive capability, a more general combustion model is needed. Several approaches are currently under investigation.

(3) The damper submodel remains somewhat unsatisfying as in the earlier 30 mm and 105 mm modeling studies. The performance of the gun is sensitive to small changes in the damper since it directly influences the motion of the control piston, and therefore, propellant injection velocity and rate of propellant flow into the chamber. However, an improved model may require an empirically determined, variable discharge coefficient.

(4) The variations in the projectile resistive pressure profile over the first 4 cm of motion must be understood or controlled in order to accurately predict gun performance.

12. REFERENCES

1. Coffee, T. P., G. P. Wren, and W. F. Morrison. "A Comparison between Experiment and Simulation for Concept VIC Regenerative Liquid Propellant Guns. I. 30 mm." BRL-TR-3072, U.S. Army Ballistic Research Laboratory, Aberdeen Proving Ground, MD, December 1989.

2. Coffee, T. P., G. P. Wren, and W. F. Morrison. "A Comparison between Experiment and Simulation for Concept VIC Regenerative Liquid Propellant Guns. II. 105 mm." BRL-TR-3093, U.S. Army Ballistic Research Laboratory, Aberdeen Proving Ground, MD, March 1990.

3. "Regenerative Liquid Propellant Gun Technology Transition Criteria." Meeting of LP management detailing transition criteria from BRL to ARDEC. Picatinny Arsenal, NJ, November 1988.

4. Coffee, T. P. "A Lumped Parameter Code for Regenerative Liquid Propellant Guns." BRL-TR-2703, U.S. Army Ballistic Research Laboratory, Aberdeen Proving Ground, MD, December 1985.

5. Coffee, T. P. "An Updated Lumped Parameter Code for Regenerative Liquid Propellant In-Line Guns." BRL-TR-2974, U.S. Army Ballistic Research Laboratory, Aberdeen Proving Ground, MD, December 1988.

6. Ballistic Research Laboratory Contract No. DAAK11-84-C-0055, with the General Electric Company, Tactical Systems Department, Aberdeen Proving Ground, MD, 1984.

7. Walter, L. General Electric Company, private communication, April 1989.

8. Corn, R. "Interim Status Report on the M483 Projectile Short Term Sticker Investigation." Ammunition Development and Engineering Directorate, Picatinny Arsenal, NJ, July 1975.

9. Knutelsky, B. Engineering Sciences Division, Picatinny Arsenal, NJ, private report, pp. 5, 6, and 7, April 1989.

10. Baer, P. "Practical Interior Ballistic Analysis of Guns," in Krier, H. and M. Summerfield, Interior Ballistics of Guns, Volume 66, Progress in Astronautics and Aeronautics. New York: New York University, New York, 1979.

11. Magoon, I. General Electric Company, private communication, April 1989.

12. Coffee, T. P. "The Analysis of Experimental Measurements on Liquid Regenerative Guns." BRL-TR-2731, U.S. Army Ballistic Research Laboratory, Aberdeen Proving Ground, MD, May 1986.

13. Coffee, T. P. "Injection Processes in Liquid Regenerative Propellant Guns." BRL-TR-2846, U.S. Army Ballistic Research Laboratory, Aberdeen Proving Ground, MD, August 1987.

14. McBratney, W. F. "Windowed Chamber Investigation of the Burning Rate of Liquid Monopropellants for Guns." BRL-MR-03018, U.S. Army Ballistic Research Laboratory, Aberdeen Proving Ground, MD, April 1980.

15. McBratney, W. F. "Burning Rate Data, LP 1845." ARBRL-MR-03128, Ballistic Research Laboratory, Aberdeen Proving Ground, MD, August, 1981.

16. Luu, Minh. General Electric Company, private communication, April 1989.

APPENDIX A:
INPUT AND OUTPUT FILES - SHOT 17

Below is a listing of the job stream for the 2 liter characterization shot 17. The numbers and labels at the left are read in by the code. The comments at the right are for identification by the user and do not affect the actual code. Following is the summary sheet from the output file. A description of the input and a brief description of the source for the input variables are given first.

The first line is merely a label. It lists the filename of the input job stream and a brief description of the problem.

The initial offset of the projectile and the total distance traveled by the projectile before muzzle exit are given. The diameter of the gun tube is given. The projectile and piston weights are entered (measured by GE).

The initial volume of the liquid reservoir is given. GE reports in Table 2 a volume of 2134 cm^3 and a piston stroke of 1.699 inches = 4.315 cm. To maintain consistency in the code, the liquid volume was taken to be 2166 cm^3, with a piston stroke of 1.7 inches = 4.318 cm. The initial free volume, including the chamber and the tube volume from the offset of the projectile, is derived by GE from a CAD drawing to be 10,057 cc. The initial areas of the reservoir (including control rod) and chamber are derived from the engineering drawings.

The VENT4 option is chosen (VIC gun). The control rod radius vs. relative piston motion is derived from the drawings. The zero point is defined where the outer piston and control rod first fit together. The positive direction is to the left (direction of the piston stroke). In this case only the parts of the control rod to the right (negative direction) are relevent, since the outer piston cannot move to the left with respect to the control rod. The area of the hole in the outer piston is computed from the engineering drawings. There is not a grease dyke on this piston.

The piston resistance is set to zero, since this is not usually large enough to be important. The discharge coefficient into the chamber is set at a constant 0.95 (see discussion in report). The discharge coefficient into the gun tube is set equal to one (no losses).

The flow into the chamber is modeled as steady state Bernoulli flow (FLUX1). There is only one vent hole. The piston thickness is irrelevant for this option. The flow into the gun tube is steady state isentropic flow (FLUX2). The shot start pressure is applied over a distance equal to the 1.5 times the length of the obturating band, a length of 1.5 inches = 3.81 cm (see discussion in report). The value of 4.0 MPa gives very good agreement with the early projectile travel. After shot start, the resistance pressure is quickly lowered to 0.7 MPa (see discussion in report). The 155 mm is a rifled gun.

Next, the physical properties of the propellant HAN1846 are given.

The liquid is pre-pressurized to 3.45 MPa. The initial chamber pressure is one atmosphere.

The droplet diameter is read in as a function of chamber pressure (DROP4). The burning rate is read as a two part function. There is some evidence that there is a break in the slope of the burning rate just under 100 MPa. However, since the rate at higher than 100 MPa is not known, the rate that was measured for lower pressures is used. The droplet diameter table has been chosen to match the chamber pressure.

The primer is injected in the form of hot gas (PRIM3). The actual primer mass is 455 g. From the water shots, the primer presurizes the chamber in about 4.0 ms. A heat loss factor of 0.45 is used. That is, only 45% of the energy of the primer actually pressurizes the combustion chamber. From the GE water shot, chamber pressure reaches about 18 MPa in 4.0 ms. The above value leads to 18.4 MPa at 4 ms.

The default models for the heat loss to the gun tube and the air shock are used. Heat loss to the combustion chamber walls is ignored.

The most complicated Lagrange model (TUBE4) is chosen. The model will take into account the rarefaction wave after burnout of the propellant.

The buffer model is chosen (BUFF2). The areas of the buffer side of the control rod and the hole in the block are from the engineering drawings. The discharge coefficient is set equal to 0.95 (see discussion in report). The initial volume is estimated from the drawings. The buffer is originally pressurized to 3.45 MPa to reduce ullage. The buffer fluid is Brayco 783, which has a density of 0.8885 g/cc. Unfortunately, the bulk modulus for the damper fluid has not been measured. The bulk modulus for a similar fluid, Brayco 756, has been measured up to 21 MPa at 24.4 C. This is fit by a linear function to obtain the derivative of the bulk modulus with respect to pressure. This means that the bulk modulus of the buffer fluid is uncertain, especially at high pressures.

The center bolt radius is given as a function of control rod travel. The bolt on the back of the control rod has been turned to form this vent.

The code will print out results every 0.2 ms (TINC). Because the code must often change the time step, it is more efficient to restrict the maximum time step (HTOP). The error controls EPS and SREC are given typical values.

The integration method flag, MF, is set to 10 (variable step size, variable order Adams method). For the Concept VIC configuration, this ran more rapidly than the backwards differentiation formula previously used. KWRITE is set to zero to eliminate diagnostic messages. A time limit of TMAX is set. If the code takes longer than TMAX seconds to execute, the code will stop gracefully and write the usual summary pages.

The code is only to be integrated once (REP1) and the chamber pressure will be computed normally (CHAM1).

```
dt17 - VIC - 2 liter Charge -    Drop - CD=0.95 - CD5=0.95
 10.16          591.8            offset   proj travel
 15.5                            gun tube diameter
 43200.                          proj weight
109000.                          piston weight
2166.           8140.            v1   v3
 641.19          855.02          a1   a3
vent4                            moving central bolt
   11                            bolt radius versus piston travel
        -3.0620       3.4925
        -2.2873       7.3762
        -0.0521       7.8105
         0.0000       7.8359
         0.7798       8.2169
         1.0820       8.3185
         1.3360       8.3452
         1.5900       8.3185
         1.7170       8.2868
         3.3388       6.6650
        34.2760       6.6650
192.898            0.0           ahole    agres
   61400                         rodwt
no close                         pistons initially meet at point
pis1                             piston resistance
   2
        0.0       0.0
        1.0       0.0
dis1                             dis. coeff. vs. piston travel
   2
        0.0       .95
        1.0       .95
dis1                             dis. coeff. vs. proj travel - tube
   2
        0.0       1.0
        487.17    1.0
```

```
flux1                                   steady state mass flux formulation
  1          1.0                        nvo   pth
flux2                                   isentropic flow into tube
proj1                                   proj resistance
      4
      0.0              4.0
      3.81             4.0
      3.82             0.7
    591.8              0.7
      1.43     5350.0  9.11             rh0   k1   k2
      4035.5     1.2226                 energy   gamma
      66.9       .04988                 surface tension   kinematic viscosity

      22.848     .677                   mol wt gas     covolume
       3.45      0.1   0.0              p1   p3   epsm1
drop4                                   droplets
      0.01    95.2590                   ddr     pbr
      1.64     .103                     adr1    bdr1
      1.64     .103                     adr1    bdr1
      5
      0.0       .0100
      20.0      .0100
      40.0      .0075
      60.0      .0075
    1000.0      .0075
prim3                                   inject hot gas
     455.0  0.004  0.45                 primer mass   injection time   heat
loss
       0.0                              puddle mass
heat1                                   no heat loss to chamber walls
heat2                                   heat loss to gun tube walls
      300.0   1.0                       tube temp   fudge factor
shock2                                  air shock
      0.1   300.                       airp   airt
      1.4    28.84                     airgam airmw
tube4                                   unsteady lagrange distribution
```

```
burn
buff2                                buffer - brayco 783
      139.555  35.04845  0.0        apis   ahole   acir
        .95                         cd5
     898.                           v5
        3.45     3.45               p5     pout5
        0.8885  1600.   11.3        rh0    k1    k2
        0.0  1.4   0.727  0.0       eps5   gam5   cv5   b5
radius                              Read in damper rod radius
        6                           nrat
        0.0000    3.3084
        0.1067    3.3084
        1.0465    3.2576
        1.8288    3.2576
        3.0988    3.2830
        4.3180    3.3269  2.00e-04    1.00e-05      tinc   htop
        1.00e-05  1.00e-08        eps    srec
        10   0                    mf      kwrite
         20.0                     tmax
rep1                                integrate once
cham1                               compute p3

        ***Output***

        muzzle vel (m/sec)        424.10
        max v pis  (m/sec)          4.9
        max p1 (mpa)              105.8
        max p3 (mpa)               70.4
        max p5 (mpa)               87.0
        max pl (mpa)               69.2
        max pr (mpa)               68.6
        max acc (k-g)               3.0
        max mass error              0.03 %
        max energy error            0.02 %
        ballistic efficiency =     31.06 %
        expansion ratio =          10.26
        loss to tube walls =        6.82 %
        run time =       2.1      nstep =     3429
```

APPENDIX B:
INPUT AND OUTPUT FILES - SHOT 28

Below is a listing of the job stream for a 2 liter repeatability shot 28 with droplet burning. Only the parameters that have been changed from Appendix A are described.

The injection and control pistons were modified resulting in an initial liquid propellant volume which is slightly larger. The initial chamber volume is also larger due to the change in contour of the pistons. The damper control rod was redesigned resulting in a change in the damper profile. A new droplet profile has been derived.

```
dt28 - VIC - 2 liter Charge -     Drop - CD=0.95 - CD5=0.95
      10.16       591.8          offset   proj travel
      15.5                       gun tube diameter
      43200.                     proj weight
      109000.                    piston weight
      2233.6      8406.          v1   v3
      641.19      855.02         a1   a3
vent4                            moving central bolt
  17                             bolt radius versus piston travel
     -5.4783      4.8781
     -0.0521      6.8529
      0.0000      6.8783
      1.5286      7.6238
      1.6921      7.6858
      1.9461      7.7203
      2.2001      7.6858
      2.4541      7.5735
      2.5811      7.4778
      2.7567      7.2680
      2.8214      7.1730
      2.9484      7.0279
      3.0754      6.9190
      3.3294      6.7709
      3.5834      6.6906
      3.8374      6.6650
     10.0000      6.6650
148.633      0.0                 ahole    agres
      61400                      rodwt
no close                         pistons initially meet at point
pis1                             piston resistance
  2
      0.0      0.0
      1.0      0.0
```

```
dis1                                    dis. coeff. vs. piston travel
  2
        0.0      .95
        1.0      .95

dis1                                    dis. coeff. vs. proj travel - tube
  2
      0.0        1.0
    487.17       1.0
flux1                                   steady state mass flux formulation
  1              1.0                    nvo   pth
flux2                                   isentropic flow into tube
proj1                                   proj resistance
       4
       0.0              4.0
       3.81             4.0
       3.82             0.7
     591.8              0.7
1.43       5350.0   9.11                rh0   k1   k2
4035.5       1.2226                     energy   gamma
 66.9       .04988                     surface tension   kinematic viscosity
 22.848     .677                       mol wt gas      covolume
  3.45   0.1   0.0                     p1   p3   epsm1
drop4                                   droplets
  0.01  95.2590                         ddr      pbr
  1.64    .103                          adr1     bdr1
  1.64    .103                          adr1     bdr1
       2
     0.0          .0100
  1000.0          .0100
prim3                                   inject hot gas
   450.0  0.004   0.45                  primer mass   injection time   heat loss
     0.0                                puddle mass
heat1                                   no heat loss to chamber walls
```

heat2	heat loss to gun tube walls
300.0 1.0	tube temp fudge factor
shock2	air shock
0.1 300.	airp airt
1.4 28.84	airgam airmw
tube4	unsteady lagrange distribution
burn	
buff2	buffer - brayco 783
139.555 35.04845 0.0	apis ahole acir
.95	cd5
912.	v5
3.45 3.45	p5 pout5
0.8885 1600. 11.3	rh0 k1 k2
0.0 1.4 0.727 0.0	eps5 gam5 cv5 b5
radius	
15	nrat
0.0000 3.3147	
0.4724 3.3147	
0.7264 3.3122	
0.8534 3.3084	
2.1488 3.2652	
2.4028 3.2603	
2.4714 3.2634	
2.7254 3.2680	
2.9794 3.2736	
3.2334 3.2802	
3.4874 3.2878	
3.7414 3.2964	
3.9954 3.3061	
4.2494 3.3170	
4.4527 3.3264	
2.00e-04 1.00e-05	tinc htop

```
        1.00e-05  1.00e-08                    eps   srec
        10            0                      mf    kwrite
        20.0                                 tmax
rep1                                         integrate once
cham1                                        compute p3

        ***Output***

        muzzle vel (m/sec)        411.27
        max v pis  (m/sec)          4.7
        max p1 (mpa)               81.9
        max p3 (mpa)               56.0
        max p5 (mpa)               81.2
        max pl (mpa)               54.6
        max pr (mpa)               54.2
        max acc (k-g)               2.3
        max mass error              0.03 %
        max energy error            0.01 %
        ballistic efficiency =     28.33 %
        expansion ratio =          10.02
        loss to tube walls =        7.07 %
        run time =      2.3        nstep =     3838
```

APPENDIX C:
INPUT AND OUTPUT FILES - SHOT 51

Below is a listing of the job stream for the 5 liter Shot 51 with droplet burning. Only the parameters that have been changed from the Shot 28 model above are described.

The initial liquid propellant volume is larger than the 2 liter case. The volume is also slightly smaller than that reported by GE in Table 2 in order to maintain consistency in the code with the given piston stroke. The damper vent area is changed. A new droplet profile has been derived. The projectile shot start pressure and resistive pressure are changed (see discussion in report).

```
dt51 - VIC - 5 liter Charge -    Drop - CD=0.95 - CD5=0.95
       10.16       591.8         offset proj travel
       15.5                      gun tube diameter
        43200.                   proj weight
       109000.                   piston weight
       5204.86      8406.        v1   v3
        641.19      855.02       a1   a3
vent4                            moving central bolt
  17                             bolt radius versus piston travel
       -5.4783      4.8781
       -0.0521      6.8529
       0.0000       6.8783
       1.5286       7.6238
       1.6921       7.6858
       1.9461       7.7203
       2.2001       7.6858
       2.4541       7.5735
       2.5811       7.4778
       2.7567       7.2680
       2.8214       7.1730
       2.9484       7.0279
       3.0754       6.9190
       3.3294       6.7709
       3.5834       6.6906
       3.8374       6.6650
      10.0000       6.6650
148.633        0.0               ahole    agres
       61400                     rodwt
no close                         pistons initially meet at point
pis1                             piston resistance
  2
       0.0      0.0
       1.0      0.0
```

```
dis1                                    dis. coeff. vs. piston travel
  2
      0.0      .95
      1.0      .95
dis1                                    dis. coeff. vs. proj travel - tube
  2
      0.0     1.0
    487.17    1.0
flux1                                   steady state mass flux formulation
  1           1.0                       nvo   pth
flux2                                   isentropic flow into tube
proj1                                   proj resistance
  4
      0.0          10.0
      3.81         10.0
      4.00          3.0
     591.8          3.0
      1.43    5350.0     9.11          rh0      k1    k2
      4035.5      1.2226               energy   gamma
      66.9      .04988                 surface tension   kinematic viscosity
      22.848     .677                  mol wt gas     covolume
       3.45    0.1   0.0               p1   p3   epsm1
drop4                                   droplets
      0.01     95.2590                 ddr      pbr
      1.64      .103                   adr1     bdr1
      1.64      .103                   adr1     bdr1
       8
       0.0       .0300
      30.0       .0300
      40.0       .0200
      50.0       .0200
      60.0       .0100
      70.0       .0100
     100.0       .0025
    1000.0       .0025
```

```
prim3                                   inject hot gas
        450.0  0.004   0.45             primer mass   injection time   heat loss

         0.0                            puddle mass
heat1                                   no heat loss to chamber walls
heat2                                   heat loss to gun tube walls
        300.0    1.0                    tube temp   fudge factor
shock2                                  air shock
        0.1     300.                    airp   airt
        1.4     28.84                   airgam airmw
tube4                                   unsteady lagrange distribution
burn
buff2                                   buffer - brayco 783
        139.555  35.04845  0.0          apis   ahole   acir
          .95                           cd5
        1532.                           v5
        3.45     3.45                   p5    pout5
        0.8885  1600.   11.3            rh0   k1   k2
        0.0  1.4   0.727  0.0           eps5  gam5  cv5  b5
radius                                  Read in damper rod radius
        24
        0.0000    3.3078
        0.0699    3.3078
        5.1575    3.1661
        5.6274    3.1661
        5.7798    3.1643
        6.0338    3.1605
        6.2878    3.1585
        6.3818    3.1580
        6.6358    3.1593
        6.8898    3.1620
        7.1438    3.1664
        7.3978    3.1725
        7.6518    3.1801
        7.9058    3.1897
```

```
        8.1598     3.1999
        8.4138     3.2111
        8.6678     3.2230
        8.9218     3.2357
        9.1758     3.2492
        9.4298     3.2636
        9.6838     3.2786
        9.9378     3.2946
       10.1918     3.3111
       10.3759     3.3239
     2.00e-04    1.00e-05    tinc  htop
     1.00e-05    1.00e-08    eps   srec
       10   0                mf    kwrite
         20.0                tmax
repl                         integrate once
cham1                        compute p3
```

Output

muzzle vel (m/sec)	612.63
max v pis (m/sec)	18.2
max p1 (mpa)	229.1
max p3 (mpa)	149.2
max p5 (mpa)	272.3
max pl (mpa)	141.2
max pr (mpa)	139.5
max acc (k-g)	5.9
max mass error	0.01 %
max energy error	0.07 %
ballistic efficiency =	26.97 %
expansion ratio =	8.43
loss to tube walls =	5.65 %
run time = 1.9	nstep = 3267

APPENDIX D:
INPUT AND OUTPUT FILES - SHOT 58

Below is a listing of the job stream for the 5 liter Shot 58 with droplet burning. Only the parameters that have been changed from the Shot 51 model in Appendix C are described.

The major difference is in the igniter. The igniter is a hybrid igniter consisting of an externally mounted solid propellant igniter and a liquid prepositioned charge in the chamber. A new droplet profile has been derived.

```
dt58 - VIC - 5 liter Charge -    Drop - CD=0.95 - CD5=0.95
      10.16       591.8          offset   proj travel
      15.5                       gun tube diameter
      43200.                     proj weight
     109000.                     piston weight
      5204.86      8406.         v1   v3
       641.19      855.02        a1   a3
vent4                            moving central bolt
  17                             bolt radius vs. piston travel
     -5.4783      4.8781
     -0.0521      6.8529
      0.0000      6.8783
      1.5286      7.6238
      1.6921      7.6858
      1.9461      7.7203
      2.2001      7.6858
      2.4541      7.5735
      2.5811      7.4778
      2.7567      7.2680
      2.8214      7.1730
      2.9484      7.0279
      3.0754      6.9190
      3.3294      6.7709
      3.5834      6.6906
      3.8374      6.6650
     10.0000      6.6650
148.633      0.0                 ahole    agres
      61400                      rodwt
no close                         pistons initially meet at point
pis1                             piston resistance
  2
      0.0      0.0
      1.0      0.0
dis1                             dis. coeff. vs. piston travel
  2
```

```
        0.0     .95
        1.0     .95
dis1                                    dis. coeff. vs. proj travel - tube
  2
        0.0    1.0
      487.17   1.0
flux1                                   steady state mass flux formulation
  1            1.0                      nvo   pth
flux2                                   isentropic flow into tube
proj1                                   proj resistance
  4
       0.0          10.0
       3.81         10.0
       4.00          3.0
     591.8           3.0
       1.43   5350.0   9.11            rh0   k1   k2
     4035.5     1.2226                 energy   gamma
       66.9     .04988                 surface tension   kinematic viscosity
       22.848    .677                  mol wt gas    covolume
       3.45     0.1   0.0              p1   p3   epsm1
drop4                                   droplets
       0.01    95.2590                 ddr    pbr
       1.64     .103                   adr1   bdr1
       1.64     .103                   adr1   bdr1
       8
        0.0      .0300
       25.0      .0300
       50.0      .0100
       75.0      .0075
      100.0       .0020
      125.0       .0010
      150.0       .0001
     1000.0       .0001
prim3                                   inject hot gas
       280.0  0.004   0.45             primer mass   injection time   heat loss
```

```
        133.0                       puddle mass
heat1                               no heat loss to chamber walls
heat2                               heat loss to gun tube walls
        300.0     1.0               tube temp    fudge factor
shock2                              air shock
        0.1     300.                airp    airt
        1.4     28.84               airgam airmw
tube4                               unsteady lagrange distribution
burn
buff2                               buffer - brayco 783
   139.555     35.04845     0.0     apis    ahole    acir
        .95                         cd5
        1532.                       v5
        3.45     3.45               p5     pout5
        0.8885  1600.   11.3        rh0    k1    k2
        0.0  1.4   0.727  0.0       eps5  gam5  cv5   b5
radius                              Read in damper rod radius
        24
        0.0000     3.3078
        0.0699     3.3078
        5.1575     3.1661
        5.6274     3.1661
        5.7798     3.1643
        6.0338     3.1605
        6.2878     3.1585
        6.3818     3.1580
        6.6358     3.1593
        6.8898     3.1620
        7.1438     3.1664
        7.3978     3.1725
        7.6518     3.1801
        7.9058     3.1897
        8.1598     3.1999
        8.4138     3.2111
        8.6678     3.2230
```

```
        8.9218     3.2357
        9.1758     3.2492
        9.4298     3.2636
        9.6838     3.2786
        9.9378     3.2946
        10.1918    3.3111
        10.3759    3.3239
        2.00e-04   1.00e-05      tinc  htop
        1.00e-05   1.00e-08      eps   srec
        10   0                   mf    kwrite
          20.0                   tmax
repl                             integrate once
cham1                            compute p3

        ***Output***

        muzzle vel (m/sec)       617.16
        max v pis  (m/sec)        18.6
        max p1 (mpa)              233.1
        max p3 (mpa)              151.9
        max p5 (mpa)              285.5
        max pl (mpa)              142.8
        max pr (mpa)              143.2
        max acc (k-g)               6.1
        max mass error              0.01 %
        max energy error            0.07 %
        ballistic efficiency =     27.37 %
        expansion ratio =           8.43
        loss to tube walls =        5.70 %
        run time =      2.4    nstep =    4429
```

APPENDIX E:
INPUT AND OUTPUT FILES - SHOT 65

Below is a listing of the job stream for the 7 liter Shot 65 with droplet burning. Only the parameters that have been changed from the Shot 58 model in Appendix D are described.

The initial liquid propellant volume is larger. The damper vent area is changed to accomodate the longer piston stroke. The pre-positioned charge is smaller. A new droplet profile has been derived. The projectile shot start pressure is changed (see discussion in report).

```
dt65 - VIC - 7 liter Charge -    Drop - CD=0.95 - CD5=0.95
        10.16       591.8        offset   proj travel
        15.5                     gun tube diameter
        43200.                   proj weight
        109000.                  piston weight
        7217.00      8406.       v1   v3
        641.19       855.02      a1   a3
vent4                            moving central bolt
  17                             bolt radius vs. piston travel
       -5.4783       4.8781
       -0.0521       6.8529
        0.0000       6.8783
        1.5286       7.6238
        1.6921       7.6858
        1.9461       7.7203
        2.2001       7.6858
        2.4541       7.5735
        2.5811       7.4778
        2.7567       7.2680
        2.8214       7.1730
        2.9484       7.0279
        3.0754       6.9190
        3.3294       6.7709
        3.5834       6.6906
        3.8374       6.6650
       10.0000       6.6650
148.633        0.0               ahole    agres
       61400                     rodwt
no close                         pistons initially meet at point
pis1                             piston resistance
  2
       0.0      0.0
       1.0      0.0
```

```
dis1                                    dis. coeff. vs. piston travel
  2
0.0     .95
1.0     .95
dis1                                    dis. coeff. vs. proj travel - tube
  2
      0.0       1.0
      487.17    1.0
flux1                                   steady state mass flux formulation
        1           1.0                 nvo   pth
flux2                                   isentropic flow into tube
proj1                                   proj resistance
  4
      0.0         20.0
      3.81        20.0
      4.00         3.0
    591.8          3.0
      1.43   5350.0   9.11             rh0   k1   k2
   4035.5      1.2226                  energy   gamma
     66.9       .04988                 surface tension   kinematic viscosity
     22.848     .677                   mol wt gas     covolume
      3.45      0.1   0.0              p1   p3   epsm1
drop4                                   droplets
      0.01    95.2590                   ddr     pbr
      1.64      .103                    adr1    bdr1
      1.64      .103                    adr1    bdr1
      8
      0.0       .0300
     25.0       .0300
     50.0       .0125
     75.0       .0100
    100.0       .0060
    125.0       .0030
    150.0       .0015
   1000.0       .0015
```

```
prim3                                   inject hot gas
      280.0  0.004   0.45               primer mass   injection time   heat loss
      115.2                             puddle mass
heat1                                   no heat loss to chamber walls
heat2                                   heat loss to gun tube walls
      300.0     1.0                     tube temp   fudge factor
shock2                                  air shock
      0.1     300.                      airp   airt
      1.4      28.84                    airgam airmw
tube4
                                        unsteady lagrange distribution
burn
buff2                                   buffer - brayco 783
      139.555  35.04845  0.0            apis   ahole   acir
      .95                               cd5
      1953.                             v5
      3.45      3.45                    p5    pout5
      0.8885  1600.  11.3               rh0   k1   k2
      0.0  1.4   0.727  0.0             eps5  gam5  cv5  b5
radius                                  Read in damper rod radius
      23
      0.0000    3.3103
      5.1753    3.1661
      9.6203    3.1661
      9.7727    3.1643
     10.0267    3.1605
     10.2807    3.1585
     10.3746    3.1580
     10.6286    3.1593
     10.8826    3.1620
     11.1366    3.1664
     11.3906    3.1725
     11.6446    3.1801
     11.8986    3.1897
     12.1526    3.1999
```

```
        12.4066     3.2111
        12.6606     3.2230
        12.9146     3.2357
        13.1686     3.2492
        13.4226     3.2636
        13.6766     3.2786
        13.9306     3.2946
        14.1846     3.3111
        14.387      3.3251
        2.00e-04    1.00e-05        tinc  htop
        1.00e-05    1.00e-08        eps   srec
        10   0                      mf    kwrite
          20.0                      tmax
rep1                                integrate once
cham1                               compute p3

***Output***

muzzle vel (m/sec)        707.73
max v pis  (m/sec)         22.6
max p1 (mpa)              283.7
max p3 (mpa)              184.9
max p5 (mpa)              364.3
max pl (mpa)              173.8
max pr (mpa)              169.1
max acc (k-g)               7.2
max mass error            0.00 %
max energy error          0.08 %
ballistic efficiency =    25.96 %
expansion ratio =          7.66
loss to tube walls =      5.15 %
run time =      1 5     nstep =    2555
```

No of Copies	Organization
1	Office of the Secretary of Defense OUSD(A) Director, Live Fire Testing ATTN: James F. O'Bryon Washington, DC 20301-3110
2	Administrator Defense Technical Info Center ATTN: DTIC-DDA Cameron Station Alexandria, VA 22304-6145
1	HQDA (SARD-TR) WASH DC 20310-0001
1	Commander US Army Materiel Command ATTN: AMCDRA-ST 5001 Eisenhower Avenue Alexandria, VA 22333-0001
1	Commander US Army Laboratory Command ATTN: AMSLC-DL Adelphi, MD 20783-1145
2	Commander US Army, ARDEC ATTN: SMCAR-IMI-I Picatinny Arsenal, NJ 07806-5000
2	Commander US Army, ARDEC ATTN: SMCAR-TDC Picatinny Arsenal, NJ 07806-5000
1	Director Benet Weapons Laboratory US Army, ARDEC ATTN: SMCAR-CCB-TL Watervliet, NY 12189-4050
1	Commander US Army Armament, Munitions and Chemical Command ATTN: SMCAR-ESP-L Rock Island, IL 61299-5000
1	Commander US Army Aviation Systems Command ATTN: AMSAV-DACL 4300 Goodfellow Blvd. St. Louis, MO 63120-1798

No of Copies	Organization
1	Director US Army Aviation Research and Technology Activity ATTN: SAVRT-R (Library) M/S 219-3 Ames Research Center Moffett Field, CA 94035-1000
1	Commander US Army Missile Command ATTN: AMSMI-RD-CS-R (DOC) Redstone Arsenal, AL 35898-5010
1	Commander US Army Tank-Automotive Command ATTN: AMSTA-TSL (Technical Library) Warren, MI 48397-5000
1	Director US Army TRADOC Analysis Command ATTN: ATAA-SL White Sands Missile Range, NM 88002-5502
(Class. only) 1	Commandant US Army Infantry School ATTN: ATSH-CD (Security Mgr.) Fort Benning, GA 31905-5660
(Unclass. only) 1	Commandant US Army Infantry School ATTN: ATSH-CD-CSO-OR Fort Benning, GA 31905-5660
1	Air Force Armament Laboratory ATTN: AFATL/DLODL Eglin AFB, FL 32542-5000
	Aberdeen Proving Ground
2	Dir, USAMSAA ATTN: AMXSY-D AMXSY-MP, H. Cohen
1	Cdr, USATECOM ATTN: AMSTE-TD
3	Cdr, CRDEC, AMCCOM ATTN: SMCCR-RSP-A SMCCR-MU SMCCR-MSI
1	Dir, VLAMO ATTN: AMSLC-VL-D

No. of Copies	Organization
2	Director Defense Advanced Research Projects Agency ATTN: J. Lupo J. Richardson 1400 Wilson Boulevard Arlington, VA 22209
4	HQDA ATTN: SARD-ZT, G. Singley SARD-TT, I. Szkrybalo SARD-TC, C. Church B. Zimmerman WASH DC 20310
1	HQ, US Army Materiel Command ATTN: AMCICP-AD, B. Dunetz 5001 Eisenhower Avenue Alexandria, VA 22333-0001
13	Commander US Army, ARDEC ATTN: SMCAR-AEE-B, D. Downs SMCAR-AEE-BR, B. Brodman W. Seals A. Beardell SMCAR-AEE-W, N. Slagg SMCAR-AEE, A. Bracuti J. Lannon J. Salo D. Chieu SMCAR-FSS-D, L. Frauen SMCAR-FSA-S, H. Liberman Picatinny Arsenal, NJ 07806-5000
3	Commander US Army, ARDEC ATTN: SMCAR-FSS-DA, Bldg 94 J. Feneck R. Kopman J. Irizarry Picatinny Arsenal, NJ 07806-5000
2	Commandant US Army Field Artillery School ATTN: ATSF-CMW ATSF-TSM-CN, J. Spicer Fort Sill, OK 73503
4	Director Benet Weapons Laboratory US Army, ARDEC ATTN: SMCAR-CCB, L. Johnson SMCAR-CCB-S, F. Heiser SMCAR-CCB-DS, E. Conroy A. Graham Watervliet, NY 12189-4050
1	Commander Materials Technology Laboratory US Army Laboratory Command ATTN: SLCMT-MCM-SB, M. Levy Watertown, MA 02172-0001
1	Commander, USACECOM R&D Technical Library ATTN: ASQNC-ELC-I-T, Myer Center Fort Monmouth, NJ 07703-5301
1	Commander US Army Harry Diamond Laboratories ATTN: SLCHD-TA-L 2800 Powder Mill Road Adelphi, MD 20783-1145
1	Commander US Army Belvoir Research and Development Center ATTN: STRBE-WC Technical Library (Vault) B-315 Fort Belvoir, VA 22060-5606
1	Commander US Army Research Office ATTN: Technical Library P.O. Box 12211 Research Triangle Park, NC 27709-2211
1	Commander US Army, ARDEC ATTN: SMCAR-CCS-C, T. Hung Picatinny Arsenal, NJ 07806-5000
1	Commandant US Army Armor Center ATTN: ATSB-CD-MLD Fort Knox, KY 40121

No. of Copies	Organization
1	Commander Naval Surface Warfare Center ATTN: D.A. Wilson, Code G31 Dahlgren, VA 22448-5000
1	Commander Naval Surface Warfare Center ATTN: Code G33, J. East Dahlgren, VA 22448-5000
2	Commander US Naval Surface Warfare Center ATTN: O. Dengel K. Thorsted Silver Spring, MD 20902-5000
1	Commander (Code 3247) Naval Weapons Center Guns Systems Branch China Lake, CA 93555-6000
1	OSD/SDIO/IST ATTN: Dr. Len Caveny Pentagon Washington, DC 20301-7100
1	Commandant USAFAS ATTN: ATSF-TSM-CN Fort Sill, OK 73503-5600
1	Director Jet Propulsion Laboratory ATTN: Technical Library 4800 Oak Grove Drive Pasadena, CA 91109
1	IITRI ATTN: Library 10 W. 35th Street Chicago, IL 60616
1	Olin Chemicals Research ATTN: David Gavin P.O. Box 586 Chesire, CT 06410-0586
2	Olin Corporation ATTN: Victor A. Corso Dr. Ronald L. Dotson 24 Science Park New Haven, CT 06511

No. of Copies	Organization
2	Director National Aeronautics and Space Administration ATTN: MS-603, Technical Library MS-86, Dr. Povinelli 21000 Brookpark Road Lewis Research Center Cleveland, OH 44135
1	Director National Aeronautics and Space Administration Manned Spacecraft Center Houston, TX 77058
10	Central Intelligence Agency Office of Central Reference Dissemination Branch Room GE-47 HQS Washington, DC 20502
1	Central Intelligence Agency ATTN: Joseph E. Backofen HQ Room 5F22 Washington, DC 20505
1	Calspan Corporation ATTN: Technical Library P.O. Box 400 Buffalo, NY 14225
8	General Electric Ordnance System Division ATTN: J. Mandzy, OP43-220 R.E. Mayer W. Pasko R. Pate I. Magoon J. Scudiere D. Bair L. Walter 100 Plastics Avenue Pittsfield, MA 01201-3698
1	General Electric Company Armament Systems Department ATTN: D. Maher Burlington, VT 05401
1	Honeywell, Inc. ATTN: R.E. Tompkins MN38-3300 10400 Yellow Circle Drive Minnetonka, MN 55343

No. of Copies	Organization
1	Paul Gough Associates, Inc. ATTN: Dr. Paul Gough 1048 South Street Portsmouth, NH 03801-5423
1	Safety Consulting Engineer ATTN: Mr. C. James Dahn 5420 Pearl Street Rosemont, IL 60018
1	Sandia National Laboratories ATTN: R. Rychnovsky, Division 8152 P.O. Box 969 Livermore, CA 94551-0969
1	Sandia National Laboratories ATTN: S. Griffiths, Division 8244 P.O. Box 969 Livermore, CA 94551-0969
1	Sandia National Laboratories ATTN: R. Carling, Division 8357 P.O. Box 969 Livermore, CA 94551-0969
1	Science Applications, Inc. ATTN: R. Edelman 23146 Cumorah Crest Woodland Hills, CA 91364
2	Science Applications International Corporation ATTN: Dr. F.T. Phillips Dr. Fred Su 10210 Campus Point Drive San Diego, CA 92121
1	Science Applications International Corporation ATTN: Norman Banks 4900 Waters Edge Drive Suite 255 Raleigh, NC 27606
1	Sundstrand Aviation Operations ATTN: Mr. Owen Briles P.O. Box 7202 Rockford, IL 61125
1	Veritay Technology, Inc. ATTN: E.B. Fisher 4845 Millersport Highway P.O. Box 305 East Amherst, NY 14051-0305

No. of Copies	Organization
1	Director Applied Physics Laboratory The Johns Hopkins University Johns Hopkins Road Laurel, MD 20707
2	Director CPIA The Johns Hopkins University ATTN: T. Christian Technical Library Johns Hopkins Road Laurel, MD 20707
1	University of Illinois at Chicago ATTN: Professor Sohail Murad Department of Chemical Engineering Box 4348 Chicago, IL 60680
1	University of Maryland at College Park ATTN: Professor Franz Kasler Department of Chemistry College Park, MD 20742
1	University of Missouri at Columbia ATTN: Professor R. Thompson Department of Chemistry Columbia, MO 65211
1	University of Michigan ATTN: Professor Gerard M. Faeth Department of Aerospace Engineering Ann Arbor, MI 48109-3796
1	University of Missouri at Columbia ATTN: Professor F.K. Ross Research Reactor Columbia, MO 65211
1	University of Missouri at Kansas City Department of Physics ATTN: Professor R.D. Murphy 1110 East 48th Street Kansas City, MO 64110-2499
1	Pennsylvania State University Department of Mechanical Engineering ATTN: Professor K. Kuo University Park, PA 16802

No. of Copies	Organization
2	Princeton Combustion Research Laboratories, Inc. ATTN: N.A. Messina M. Summerfield 4275 U.S. Highway One North Monmouth Junction, NJ 08852
1	University of Arkansas Department of Chemical Engineering ATTN: J. Havens 227 Engineering Building Fayetteville, AR 72701
3	University of Delaware Department of Chemistry ATTN: Mr. James Cronin Professor Thomas Brill Mr. Peter Spohn Newark, DE 19711
1	University of Texas at Austin Bureau of Engineering Research ATTN: BRC EME133, Room 1.100 H. Fair 10100 Burnet Road Austin, TX 78758
1	Jet Propulsion Laboratory ATTN: D. P. Maynard Technical Group Supervisor Chemical Processes Group Propulsion Systems Section 4800 Oak Grove Drive Pasadena, CA 91109-8099

No. of Copies	Organization
1	GS2 Division ATTN: Clive Woodley Building R31 RARDE Fort Halstead Sevenoaks, Kent TN14 7BT England

USER EVALUATION SHEET/CHANGE OF ADDRESS

This Laboratory undertakes a continuing effort to improve the quality of the reports it publishes. Your comments/answers to the items/questions below will aid us in our efforts.

1. BRL Report Number BRL-TR-3151 Date of Report SEPTEMBER 1990

2. Date Report Received _____

3. Does this report satisfy a need? (Comment on purpose, related project, or other area of interest for which the report will be used.) _____

4. Specifically, how is the report being used? (Information source, design data, procedure, source of ideas, etc.) _____

5. Has the information in this report led to any quantitative savings as far as man-hours or dollars saved, operating costs avoided, or efficiencies achieved, etc? If so, please elaborate. _____

6. General Comments. What do you think should be changed to improve future reports? (Indicate changes to organization, technical content, format, etc.) _____

CURRENT ADDRESS

_____
Name

_____
Organization

_____
Address

_____
City, State, Zip Code

* If indicating a Change of Address or Address Correction, please provide the New or Correct Address in Block 6 above and the Old or Incorrect address below.

OLD ADDRESS

_____
Name

_____
Organization

_____
Address

_____
City, State, Zip Code

(Remove this sheet, fold as indicated, staple or tape closed, and mail.)